Internal tracheal sensory neuron wiring and function in *Drosophila* larvae

Cheng Qian

Submitted in partial fulfilment of the
requirements for the degree of
Doctor of Philosophy
under the Executive Committee of the Graduate School of Arts and Science

COLUMBIA UNIVERSITY

2018

© 2018

Cheng Qian

All rights reserved

ABSTRACT

Internal tracheal sensory neuron wiring and function in *Drosophila* larvae

Cheng Qian

Organisms possess internal sensory systems to detect changes in physiological state. Despite the importance of these sensory systems for maintaining homeostasis, their development, sensory mechanisms, and circuitry are relatively poorly understood. To help address these gaps in knowledge, I used the tracheal dendrite (td) sensory neurons of *Drosophila* larvae as a model to gain insights into the cellular and molecular organization, developmental regulators, sensory functions and mechanisms, and downstream neural circuitry of internal sensory systems.

In this thesis, I present data to show that td neurons comprise defined classes with distinct gene expression and axon projections to the CNS. The axons of one class project to the subesophageal zone (SEZ) in the brain, whereas the other terminates in the ventral nerve cord (VNC). This work identifies expression and a developmental role of the transcription factor Pdm3 in regulating the axon projections of SEZ-targeting td neurons. I find that ectopic expression of Pdm3 alone is sufficient to switch VNC-targeting td neurons to SEZ targets, and to induce the formation of putative synapses in these ectopic target regions. These results define distinct classes of td neurons and identity a molecular factor that contributes to diversification of central axon targeting.

I present data to show that td neurons express chemosensory receptor genes and have chemosensory functions. Specifically, I show that td neurons express gustatory and ionotropic receptors and that overlapping subsets of td neurons are activated by decrease in O_2 or increase in CO_2 levels. I show that respiratory gas-sensitive td neurons are also activated when animals are submerged for a prolonged duration, demonstrating a natural-like condition in which td

neurons are activated. I assessed the roles of chemosensory receptor genes in mediating the response of td neurons to O_2 and CO_2. As a result, I identify Gr28b as a mediator of td responses to CO_2. Deletion of Gr28 genes or RNAi knockdown of Gr28b transcripts reduce the response of td neurons to CO_2. Thus, these data identify two stimuli that are detected by td neurons, and establish a putative role for Gr28b in internal chemosensation in *Drosophila* larvae.

Finally, I present data to elucidate the neural circuitry downstream of td sensory neurons. I show that td neurons synapse directly and via relays onto neurohormone populations in the central nervous system, providing neuroanatomical basis for internal sensory neuron regulation of hormonal physiology in *Drosophila*. These results pave the way for future work to functionally dissect the td circuitry to understand its function in physiology and behavior.

TABLE OF CONTENTS

LIST OF FIGURES

ACKNOWLEDGEMENTS

I would like to express my gratitude to Wes for his continued mentorship and support. I am especially grateful for his gifting of ideas, encouragements, humor, patience, enthusiasm, and advice.

I would like to thank my thesis committee members, Oliver Hobert, Richard Mann, Rudy Behnia, and Hynek Witcherle, for providing valuable feedback and discussions.

I would like to thank members of the Grueber lab for scientific contributions, helpful advice, and companionship over the years. I received a great deal of advice and assistance from Jenn, Anita, and Sam during my first year in the lab, and for a long while afterwards. I would like to thank Rebecca and Grace for offering sensible advice (and Luke for help with imaging). I am grateful to Margarita and Jennifer for laying some of the early groundwork, and to Shan for the assistance and enthusiasm near the finish line. I am grateful to Rosa, Naureen, Taylor, Katie, Mya, and Nate, for keeping the lab running so smoothly. Thanks to everyeone for making the lab a fun place to work.

Thanks also to our collaborator Albert Cardona, for welcoming me to his lab and training me on electron microscopy reconstruction.

I would like to thank our program directors Carol Mason, Darcy Kelley, and Ken Miller, for their guidance, especially during my early years in the Neurobiology program. I owe thanks to Alla Kerzhner and Rozanna Yakub for always being so helpful.

At Columbia, I would also like to thank the students in the Neurobiology program and our fly floor neighbours for their good company. Finally, I am grateful to my friends in NYC and Canada for providing breaks from science, and my family, for their enthusiasm for me to freely pursue my interests and goals.

Chapter 1: Introduction

"Who knows the countless associations that mingle with his each and every thought? Who can pick apart all the nameless feelings that stream in at every moment from his various internal organs, muscles, heart, glands, lungs, etc., and compose in their totality his sense of bodily life?"

- William James

Introduction

The brain receives sensory information about both the external and the internal world. Across the body, specialized cells are directed outward to face the external environment, tuned to sense and relay the arrival of pressure, light, sound waves, odorants, or tastants. As humans, we consciously experience these sensory phenomena and use them to construct our perception of the external world. In addition, information about the internal environment comprising the chemical and physical state of our internal organs is continuously imparted onto our brains by specialized cells directed inward the body. This stream of internal sensory information, mostly remaining below the level of conscious awareness, regulates physiology and behavior critical to survival.

Information about internal physiology is relayed from visceral organs to the brain by internal sensory neurons. Despite the importance of these neurons in detecting internal state for maintaining homeostasis, their development, sensory mechanisms, and neural circuitry are vastly understudied. The aim of the work described in this dissertation is to help address these gaps in knowledge in a tractable model system. I have focused in particular on the study of internal tracheal sensory neurons in the *Drosophila* larvae. Here, I will first provide a general introduction to the study of internal sensory systems.

Internal sensory neurons in mammals

The mammalian vagus nerve is a long bundle of neurons that serves as the primary link between the brain and internal organs (Figure 1.1). Vagus means wandering in Latin and is named for the meandering trajectory the nerve takes down the body (Clancy et al., 2013). Within this one bundle of nerve are neurons that innervate the airway, lungs, heart, stomach, liver, intestines, pancreas, and kidneys (Berthoud and Neuhuber, 2000). The vagus nerve

mainly conveys sensory information; 80-90% of the abdominal vagus nerve fibers are afferents (Andrews, 1986). The mouse vagus nerve contains ~2,300 sensory neurons (Williams et al., 2016), the cell bodies of which reside in the nodose and jugular ganglion, and the axons primarily target the nucleus of the solitary tract (NTS) in the brainstem (Berthoud and Neuhuber, 2000). The extensive distribution of vagal afferents throughout the body suggests that vagal afferents detect a wide range of physiological stimuli.

Indeed, electrophysiological recording experiments from the mid-to-late 20th century have shown that the vagal nerve fibers can be activated by a wide range of stimuli including glucose, amino acids, warm and cold temperatures, hyperosmolality, acids, irritants, gut hormones (cholecystokinin, CCK; peptide YY, PPY; glucagon-like peptide 1, GLP-1), neurotransmitters (ATP, GABA, 5-HT), cytokines, and mechanical stimulation (Andrews, 1986; Bonaz et al., 2018; Docherty et al., 2005; Paintal, 1973; Pavlov and Tracey, 2012). The vast repertoire of stimuli detected by neurons in the vagus nerve raises a number of important questions at the sensory neuron level alone. What stimuli are vagal nerve fibers at each tissue competent to detect? Are single sensory neurons narrowly or broadly tuned? What are the molecular receptors that mediate sensory detection? What is the relationship between peripheral tissue innervation and central axon projections, and between stimulus tuning and axon projections? What are the molecular and genetic classifications of vagal neurons and their functional relevance? Previous studies have mostly focused on describing the response profiles of vagal sensory neurons, although recent studies have begun to establish a molecular framework for internal sensing (Chang et al., 2015; Williams et al., 2016).

Thermosensory, mechanosensory, and a few chemosensory stimuli activate vagus nerve fibers in multiple tissues. Warm- and cold-sensing neurons have been found along both the respiratory tract and gastrointestinal tract (El Ouazzani and Mei, 1982; Sant'Ambrogio et al., 1988). Similarly, mechanosensitive neurons have been reported in the airway, lungs, and

stomach (Berthoud and Neuhuber, 2000; Mazzone and Undem, 2016). Glucose-sensitive neurons have been reported in both the liver portal vein and the stomach (Grabauskas et al., 2010). Neurons innervating the portal vein are more likely to be inhibited by glucose while neurons innervating the stomach are more likely to be excited by glucose, suggesting there are subtypes glucose-sensing neurons in different tissues. Some studies have reported vagal neurons that are polymodal, responding to a variety of chemicals (Berthoud and Neuhuber, 2000; Mei and Garnier, 1986). Other studies have reported vagal neurons that highly tuned for specific chemical or mechanical stimuli (Jeanningros, 1982; Lal et al., 2001; Mei, 1978). It is possible that different types of neurons vary in their selectivity.

For certain chemosensory stimuli, sensory nerves are likely not the primary sensory receptors. In the circulatory system, arterial O_2 and CO_2 levels are sensed by chemoreceptors in the carotid and aortic body (Prabhakar, 2016). This information is thought to be relayed to the CNS from the carotid body by the glossopharyngeal nerve and from the aortic body by the vagus nerve. In the gastrointestinal system, vagal afferent endings contact the digestive epithelium but do not cross it to directly contact the gut lumen (Bonaz et al., 2018). As a result, ingested nutrients, metabolites, and other chemicals in the gut are thought to be detected by enteroendocrine cells, sparsely distributed cells in the intestinal epithelium. Enteroendocrine cells respond to nutrients by releasing serotonin and gut hormones such as CCK, GLP1, which can activate vagal afferents (Bonaz et al., 2018). Interestingly, taste receptors are expressed in specialized epithelial cells in the respiratory and digestive tracts (Depoortere, 2014; Lee and Cohen, 2014). It is unclear whether taste receptors on these cells detect internal stimuli and relay information to the brain via the vagus nerve (Jang et al., 2007).

Recently, molecularly distinct vagal neuron subtypes with different sensory input and function have been delineated. In the lung, P2ry1-expressing neurons and Npy2r-expressing neurons evoke opposing effects on breathing (Chang et al., 2015). Optogenetic stimulation of

P2ry-1 neurons causes pause in breathing, while stimulation of N2py2r neurons causes rapid shallow breathing. These two subtypes of vagal sensory neuron axons project centrally to different regions of the NTS. Other studies have shown that activation of Mrgprs-expressing vagal sensory neurons innervating the airway causes narrowing of airway, a pathophysiology of asthma (Han et al., 2018). In the digestive system, GPR65-expressing neurons have been found to respond to nutrients, while GLP1R-expressing neurons respond to stretch (Williams et al., 2016). These two subpopulations also project axons to segregated regions in the NTS. Altogether, these results suggest the presence of genetically defined subtypes of vagal neurons with segregated central axon projections and distinct physiological input and function.

More recent studies have also begun to identify the molecules that mediate sensory transduction. Cold sensing in vagal afferents is mediated primarily by TRPA1 (Fajardo et al., 2008), which contrasts cold sensing in somatic afferents, mediated primarily by TRPM8. Stretch sensing in the airway is mediated by Piezo2 (Nonomura et al., 2017), a mechanically activated ion channel which also mediates cutaneous and proprioceptive mechanotransduction. Profiling of vagal afferents has revealed expression of various G protein-coupled receptors for chemosensory stimuli including gut hormones, microbiome-derived metabolites, lipids, inflammation, neurotransmitter signalling, as well as orphan GPCRs with unknown function, in vagal afferents (Egerod et al., 2018). The functional role of these receptors remains to be investigated.

The physiological functions of the vagus nerve have classically been studied by transection of the vagus nerve or whole nerve stimulation. In the airway, activation of afferents by chemical means of inhaled noxious substances elicits defensive reflexes that protects the lungs from damage, including narrowing of airway, secretion of mucus, and cough in some species (Coleridge and Coleridge, 1984; Lee, 2009). These reflexes are mediated by the vagus nerve, as transection of the nerve eliminates these responses (Coleridge et al., 1983). Vagal

reflexes also mediate gastric mobility to promote passage of food in the digestive system, and endocrine and exocrine sections from the pancreas (Chang et al., 2003; Clyne et al., 2000; Takahashi and Owyang, 1997). An important caveat with vagus nerve transection or stimulation experiments is they broadly affect all neurons in the nerve, including efferent neurons. In addition, these methodologies preclude the attribution of functions to specific classes of vagal sensory neurons. However, as mentioned previously, more recent studies have used novel methods that enable imaging and optogenetic manipulation of molecularly-defined subtypes of vagal sensory neurons to study the cellular and molecular logic of sensory encoding.

Vagal sensory neurons have classically been viewed as the sensory arm of a simple reflex arc that detects physiological imbalance and elicits downstream autonomic responses to maintain homeostasis (Rinaman et al., 1989; Sawchenko, 1983). However, neuronal tracing studies have found that vagal sensory input in the NTS is relayed both within the brainstem and also through ascending pathways to a variety of limbic and cortical areas (Craig, 2003; McGovern et al., 2012; McGovern et al., 2015). These data suggest internal sensory information may affect brain function on a level beyond simply inducing purely physiological responses. The idea that the vagus nerve may be an accessible entry way to modulating a wide range of brain functions has not escaped clinical researchers. While our understanding of how internal sensory neuron activity affects downstream neural circuits is in its infancy, electrical stimulation of the vagus nerve is already being used as a medical treatment for epilepsy and depression (Milby et al., 2008; Ogbonnaya and Kaliaperumal, 2013). Some wearable devices are being developed that involve transcutaneous stimulation (e.g. targeted at the ear at points where branches of the vagus nerve travels superficially) and do not require surgery (Kong et al., 2018). In these cases, the clinical experimentations greatly outpace the understanding of the basic neurobiology of internal sensory systems.

A complimentary approach to studying the development and function of internal sensory neurons is to examine these sensory systems in a simpler model organism. *Drosophila* studies of the classical sensory systems have been successful in elucidating sensory processing principles that are informative for homologous mammalian systems (Sanes and Zipursky, 2010; Vosshall, 2001), and the same may hold true for internal sensory neurons.

Internal sensory neurons in invertebrates

Invertebrate such as the nematode *C. elegans* and fruit fly *Drosophila melanogaster* can serve as useful models for studying the development and function of sensory neurons and neurobiology at large (Bellen et al., 2010). Individual neurons are largely invariant, easily identifiable from animal to animal, and can be relatively easily imaged and genetically manipulated. In some cases, specific sensory and behavioral functions can be attributed to a few, or even one neuron.

In *C. elegans*, body cavity neurons (AQR, PQR, and URX neurons) have unique anatomical feature in which their cell bodies and dendrites are positioned within the coelomic fluid, which seems to function analogously to blood. These body cavity neurons function in O_2-sensing and express the soluble guanylate cyclases GCY-35 and GCY-36, which heterodimerizes and binds molecular oxygen to generate cGMP (Cheung et al., 2004; Gray et al., 2004). *C. elegans* prefer 7-14% O_2, presumably because these levels correlate with the presence of bacterial food. Higher O_2 (atmospheric 21%) levels activate these neurons and promote hyperoxia avoidance behaviors. The URX neuron, in addition to sensing O_2, also detects internal fat reserve levels (Witham et al., 2016). URX therefore functions as an integrator of oxygen availability and internal metabolic state. The net activity of URX dictates

the magnitude of fat loss in the periphery and is thought to ensure that fat loss happens only when food is absent (high O_2) and sufficient fat body is present.

In *Drosophila* adult females, internal sensory neurons in the genital tract regulate a post-mating behavioral switch (Hasemeyer et al., 2009; Yang et al., 2009). Virgin female fruit flies readily mate with male flies. After mating, females reject courting males and increase egg production from a few eggs to several dozens a day. This change in receptivity and egg-laying behavior of female flies is triggered by the sex peptide in the male seminal fluid, which is transferred to the female reproductive system during mating. A set of six to eight internal sensory neurons in the female reproductive tract expressing the sex peptide receptor are the main sensory neurons that mediate detection of the peptide. These sensory neurons extend dendrites to the uterus and oviduct, and project axons centrally to target the subesophageal zone (SEZ) and the abdominal ganglion, serving as a direct neural pathway from the reproductive tract to the CNS (Hasemeyer et al., 2009). Studies of this small group of internal sensory neurons have uncovered a few counterintuitive findings. First, the dendrite arborization at the reproductive tract suggest that sex peptide receptor might be localized at the dendrite, where it can interface with the internal body surface to detect the ligand. However, the sex peptide receptor is predominantly localized on the axons and terminals of these sensory neurons (Yang et al., 2009). The sex peptide itself is detected in the hemolymph (insect blood) after mating. Thus, it is possible that sex peptide circulates throughout the body and acts at receptors near the sensory neuron output sites to regulate activity. Second, these sensory neurons are inhibited rather than activated by the ligand, and inhibition of these neurons phenocopies the application of sex peptide (Yang et al., 2009). This suggests that these neurons may be active in virgin females in the absence of sex peptide, and that inhibition of this activity is required for the post-mating behavioral switch.

The *Drosophila* digestive tract is innervated by sensory and efferent neurons and these neurons are largely uncharacterized beyond anatomy. The adult digestive tract can be divided into three segments: the anterior, midgut, and terminal portions. The presence of neurites (labelled by the motor neuron reporter OK371-GAL4) in regions of these segments that contain valves or sphincters suggest that these motor neurons may modulate intestinal smooth muscles to move intestinal contents (Cognigni et al., 2011). Other neurons that innervate the digestive tract are likely sensory. These neurons innervate the esophagus and proventriculus (stomach) in the anterior segment, and a few neurons innervate the posterior portion of the hindgut (Cognigni et al., 2011). A reporter for the fructose-sensing gustatory receptor, $Gr43a^{GAL4}$ labels about four of the proventriulus-innervating neurons (Miyamoto et al., 2012). The cell bodies of these neurons reside in the proventricular ganglion and the dendrites innervate the foregut lumen. Two of the neurons send axons to the subesophageal zone, and the other two send axons to the musculature of the mid gut. Based on the expression of a fructose receptor in a subset of the proventricular neurons, it is tempting to hypothesize that these neurons may detect nutrients in the digestive tract and relay the information to the brain. In *Drosophila* larvae, anatomical studies have described similar intestinal innervations in the proventriculus, anterior and posterior midgut, and the hindgut (Kuraishi et al., 2015). The sensory functions of these neurons are currently unknown.

Aside from sensory neurons innervating the *Drosophila* reproductive and digestive tracts, another population of internal sensory neurons associated with the trachea in the peripheral nervous system has remained largely uncharacterized.

Drosophila larval peripheral nervous system as a model system

The peripheral nervous system of *Drosophila* larva (Figure 1.2A, B) consists of diverse types of external and internal sensory neurons positioned along the body wall. These sensory neurons, and associated end organs, are organized in a segmentally repeated manner and positioned stereotypically from animal to animal.

The larval PNS consists of neurons whose cell bodies are located in each hemisegment of the body, positioned in one of four clusters: the ventral (v), ventral′ (v′), lateral (l), and dorsal (d) clusters (Bodmer and Jan, 1987). The neurons are also divided into classes according to distinct morphologies and functions. Some neurons have a single dendrite (external sensory and chordotonal neurons), while other neurons have more extensively branched dendrites (multidendritic neurons). The multidendritic neurons have been broadly classified into three types: dendritic arborization neurons, bipolar dendrite neurons, and tracheal dendrite neurons (Bodmer and Jan, 1987). These different types of multidendritic neurons differ in the tissue that the dendrites associate with, suggesting they have different sensory functions. The dendritic arborization neurons extend dendrites in roughly two-dimensions across the epidermis and are the most well-characterized type; they are further divided into classes based on morphology (Grueber et al., 2002) and function as proprioceptors (class I), touch receptors (class III and possibly II), and polymodal nociceptive neurons (class IV) (Hughes and Thomas, 2007; Hwang et al., 2007; Yan et al., 2013). Some molecular receptors that mediate sensory transduction have been identified in these neurons. NOMPC mediates mechanotransduction in touch sensing class III neurons (Yan et al., 2013). Piezo mediates noxious mechanical stimuli in nociceptive class IV neurons (Kim et al., 2012b). The bipolar dendrite neurons extend dendrites along connective tissue and function as proprioceptors (Hughes and Thomas, 2007). The mechanosensory channel Piezo mediates mechanotransduction in the bipolar dendrite neurons (Suslak et al., 2015).

The largely unstudied tracheal dendrite (td) neurons are the subject of this dissertation (Figure 1.2C). There are two td neurons in each abdominal hemisegment, named v′td1 and v′td2 for their location in the ventral′ cluster of sensory neurons. Td neurons extend dendrites along internal tracheal branches. Although functions for td neurons are not known, they have been proposed to function as sensors of tracheal status or as proprioceptors based on their association with the tracheal branches (Bodmer and Jan, 1987).

In *Drosophila* larva, PNS neurons project sensory axons to the ventral nerve cord (spinal cord equivalent) of the CNS and terminate in modality-specific regions. Touch sensing and nociceptive neurons project axons to ventromedial regions of the neuropil, proprioceptors to more dorsal neuropil, and vibration sensing chorodotonal axons to intermediate neuropil (Grueber et al., 2007). These somatosensory axons project primarily within the same neuromere in the VNC corresponding to their peripheral segment of origin. In contrast, embryonic td axons from each segment project together in a lateral tract in the VNC, shift to a medial tract at the thoracic neuromere, and extend further anteriorly (Merritt and Whitington, 1995; Merritt and Whitington, 2002). The final targets and mature td axon projections patterns in the third-instar larva are not known. Axon projections can inform studies of sensory function because positions are often modality-specific. However, the lack of knowledge about td axon terminal projections hampers the elucidation of connectivity and function.

Sensory axon targeting in the VNC involve decisions to terminate at specific positions along the mediolateral (M-L), dorsoventral (D-V), and anteroposterior axis (A-P). A Slit gradient is established at the midline and acts through Robo receptors expressed on sensory axons to dictate the position along the M-L axis that the axon terminates (Zlatic et al., 2003). Perpendicular to the Slit gradient, a system of positional cues involving Semaphorins 1a and 2a, as well as Plexin receptors, dictates sensory axon termination along the D-V axis (Zlatic et al., 2009). The Hox genes Ubx and AbdA are expressed in the posterior VNC and define a

repulsive zone that ensures td axons shift to the medial tract only upon reaching more anterior thoracic neuromere (which lack Ubx and AbdA expression) (Merritt and Whitington, 2002). The factors that that position sensory axons along the A-P axis are not known. Td neurons are the only class of sensory neurons that project axons across multiple VNC neuromeres in the A-P axis. Therefore, td neurons can serve as a unique model for understanding sensory axon targeting.

Drosophila neurobiology research is aided by a powerful genetic toolkit that permits labeling and manipulation of neural populations with high specificity (Venken et al., 2011). This cell-specificity is enabled by the GAL4/UAS and related binary expression systems (Brand and Perrimon, 1993). In one construct, expression of the GAL4 transcriptional activator is driven by cell type-specific promoters. In a second construct, a transgene of interest is driven under the control of a promoter sequence called Upstream Activating Sequence (UAS). The GAL4 protein binds to the UAS sequence and potently drives expression of the downstream transgene. GAL4/UAS can be used in combination with a third protein GAL80 to restrict transgene expression. The GAL80 protein binds to and inhibits the activity of GAL4 (Suster et al., 2004). Therefore, a third construct can be introduced in which GAL80 is expressed in a specific population of cells to inhibit UAS transgene expression. Additional binary expression systems that are conceptually similar to GAL4/UAS have also been generated. The LexA/LexAop and QF/QUAS are similar but independent systems that, when used together with GAL4/UAS, enable simultaneous manipulations of multiple populations of cells (Lai and Lee, 2006; Potter et al., 2010). GAL4 lines have been generated by various *Drosophila* laboratories and are often freely shared among researchers or publicly available through stock centres. Recently, 7,000 GAL4 lines were generated as part of the Janelia FlyLight project, in which defined fragments of the genome were fused to the GAL4 sequence and inserted into specific landing sites in the genome (Jenett et al., 2012). Another collection of GAL4 lines was

generated by the InSITE project in which GAL4 sequences are inserted into different locations in the genome to trap enhancer elements (Gohl et al., 2011). Both projects have and continue to generate driver lines in alternate binary expression systems (LexA, QF, split-Gal4, etc.). Many of these GAL4 lines label sparse populations of cells in the *Drosophila* larva and adult nervous system, providing new access to specific neural populations for studying development and function.

Transcriptional control of neuronal diversity

Characterizing the morphology and cellular organization of sensory neurons is an important first step that helps to provide insights into their development and function. Such characterization can reveal subtypes of neurons which provide the basis for investigations into mechanisms underlying subtype-specific morphology or function. Transcription factors are important regulators of neuronal (and cellular) diversity across vertebrates and invertebrates (Hobert, 2008; Jan and Jan, 1994; Spitz and Furlong, 2012). Transcription factor proteins contain DNA-binding domains, enabling them to attach to specific sequences of DNA and regulate gene expression. In the nervous system, transcriptional regulation leads differential expression of genes in neurons that confer them with diverse morphological, biophysical, and functional properties (Hobert et al., 2010).

The *Drosophila* larval PNS multidendritic sensory neurons have been a useful model for identifying factors that control diversification of neuronal morphology. Larval touch-sensing and nociceptive neurons have complex dendrite morphology and project axons to a ventral region the VNC neuropil, while proprioceptive neurons have simple dendrite morphology and project axons to a dorsal region of the VNC neuropil (Grueber et al., 2007). The transcription factor Cut is expressed in touch-sensing and nociceptive neurons (in a graded

fashion that correlate with the neuron's dendrite complexity) and is not expressed in proprioceptive neurons (Grueber et al., 2003). Cut plays a causal role in conferring touch/nociceptive and proprioceptive neurons with aspects of their class-specific dendrite morphology and axon projections (Corty et al., 2016; Grueber et al., 2003). Specifically, touch neurons mutant for Cut convert from neurons with complex dendritic fields and ventral axon projections to neurons with stunted dendrites and dorsal axon projections. Conversely, proprioceptive neurons that ectopically express Cut convert from neurons with simple dendrites to neurons with over-branched dendrites. Recently, Cut has been shown to function in a hierarchical manner with other downstream transcription factors to sculpt dendrite morphology. Specifically, Cut represses two dendrite "simplicity-promoting" transcription factors, POU domain transcription factors Pdm1 and Pdm2 (Corty et al., 2016). In the absence of Cut, Pdm1 and Pdm2 are relieved from repression and function to produce simplified and stunted dendrites. Therefore, morphological features of *Drosophila* larval PNS multidendritic neuron classes can be specified by the differential expression of transcription factors, including the POU domain proteins.

POU domain transcription factors are regulators of neural development in both vertebrate and invertebrate sensory systems (Corty et al., 2016; Erkman et al., 1996; Komiyama et al., 2003; McEvilly et al., 1996). The POU domain is a bipartite domain composed of two conserved subdomains that are both required for DNA-binding but are held together by a non-conserved flexible linker (Sturm and Herr, 1988). The *Drosophila* genome encodes five POU proteins, POU domain motif 1 (Pdm1), Pdm2, Pdm3, Drifter, and Acj6. Each of these factors shows specific expression in sensory circuits and corresponding roles in sensory system development. As mentioned above, Pdm1 and Pdm2 function in dendritic diversification in the somatosensory system (Corty et al., 2016). Drifter and Acj6 regulate olfactory wiring (Komiyama et al., 2003). The POU domain motif 3 (Pdm3) has been shown to regulate odor

receptor expression, axon targeting in olfactory neurons and ellipsoid body ring neurons, and glial development (Bauke et al., 2015; Chen et al., 2012; Tichy et al., 2008). In the olfactory and ellipsoid body ring neurons, loss of Pdm3 function causes imprecise targeting defect at the axon terminal. In summary, due to their specific expression patterns and broad roles in nervous system development, POU transcription factors are a good candidate gene family for specifying unique aspects of sensory projections, perhaps including the development of internal sensory neurons.

Molecular chemosensory receptors in *Drosophila*

How animals such as *Drosophila* sense their external chemical environment is relatively well understood in terms of peripheral neuroanatomy and sensory encoding logic (Vosshall and Stocker, 2007). In particular, the identification of chemoreceptor gene families in rodents (Adler et al., 2000; Buck and Axel, 1991), *Drosophila* (Certel et al., 2000; Clyne et al., 1999b; Vosshall et al., 1999), and *C. elegans* (Sengupta et al., 1996) was a major breakthrough in chemosensory research that revolutionized our understanding of the molecular organization of olfactory and gustatory systems. In addition to expression in gustatory and olfactory receptor neurons, chemosensory receptor genes have been reported to be expressed in cells not associated with canonical gustatory and olfactory system in vertebrates and invertebrates. The function of these chemosensory receptor genes in other tissues, whether they function to detect internal ligands or are used in non-chemosensory roles, is a major outstanding question.

In *Drosophila*, the detection of most tastants are thought to be accomplished through members of the Gustatory Receptor (GR) family, which encodes 68 proteins (Montell, 2009). *Drosophila* GRs are seven-transmembrane (non-GPCR) chemoreceptors that are expressed in

gustatory sensilla receptor neurons. Each GR gene is named after its numbered cytological location on the chromosomal map followed by a lowercase letter – "a" for single genes (e.g. Gr5a) or "a", "b", "c" and so on for the clustered genes (e.g. Gr64a, Gr64b, Gr64c) (Chyb, 2004). Different isoforms are distinguished by the suffixed letter after a period (e.g. Gr28b.a, Gr28b.b, Gr28b.c, etc.). The expression of GRs in the gustatory system has been comprehensively characterized, primarily based on GR-GAL4 drivers, since success in analysing GR expression with *in situ* hybridization has been extremely limited (Delventhal and Carlson, 2016).

In contrast to mammalian gustation or olfaction, which are detected by receptors composed of dimers of one or two receptor types, most functional *Drosophila* GR complexes are composed of three or more subunits (Montell, 2009). The specific ligand detected by a neuron is determined by the specific combination of GR subunits that are expressed. As an example, Gr8a, Gr66a, and Gr98b comprise a functional heteromultimeric receptor that is necessary and sufficient to detect the plant-derived aversive compound L-canavanine (Shim et al., 2015). However, for most aversive compounds, the composition of functional receptor complexes is not known. Detection of caffeine, for example, requires Gr33a, Gr66a, and Gr93a. However, misexpression of all three GRs in sweet-sensing gustatory neurons is not sufficient to confer sensitivity to caffeine (Lee et al., 2009). Currently, a number of studies have identified GRs that are necessary for detection of a variety of bitter or toxic compounds (Lee et al., 2009; Moon et al., 2006; Moon et al., 2009), but the minimal GR composition sufficient for detection have yet to be elucidated. In addition to bitter compounds, a number of GRs (Gr5a, Gr43a, and Gr64 genes) have been suggested to be sugar receptors (Dahanukar et al., 2007; Mishra et al., 2013). GRs are also involved in the detection of non-volatile pheromones (Bray and Amrein, 2003; Miyamoto and Amrein, 2008). The majority of GRs are expressed in small subsets of

gustatory neurons (1-4% of cells) (Chyb, 2004). However, a few genes show broader expression patterns, suggesting they may be more broadly tuned receptor subunits.

GRs have been implicated in diverse sensory contexts beyond gustation. Gr21a and Gr63a are expressed in a limited number of olfactory receptor neurons (which in general express Olfactory Receptors (ORs)), where they detect carbon dioxide (Jones et al., 2007). Gr43a has been suggested to function as a hemolymph fructose receptor in neurons in the brain (Miyamoto et al., 2012). In the adult, GRs are expressed in the wing margin, ovipositor (Montell, 2009), enteroendocrine cells in the gut (Park and Kwon, 2011a), and in multidendritic sensory neurons on the body (Park and Kwon, 2011b), where their functions are unknown. Gr28b.d has been shown to have atypical role in temperature sensing (Ni et al., 2013). In the larva, Gr28b is expressed in polymodal nociceptive class IV neurons where they mediate detection of blue, violet and UV light (although the isoform responsible is not known) (Xiang et al., 2010).

The *Drosophila* genome contains about 60 Ionotropic Receptors (IRs) genes, which are predicted to encode ligand-gated ion channels with three transmembrane domains (Joseph and Carlson, 2015). IRs have been found to be expressed in gustatory and olfactory receptor neurons. Some IRs have been shown to detect salt, amino acids, and acids. Unlike most GRs, single IRs or co-expression of two IRs is sufficient to confer response to ligands. For example, Ir76b is thought to function as a low salt sensor (Zhang et al., 2013). However, co-expression of Ir76b with Ir20a confers responsiveness to amino acids, while blocking the salt response of Ir76b (Ganguly et al., 2017). The expression of the IR20a clade members in the larva has been examined using IR-GAL4 drivers. One member, Ir56a-GAL4, has been reported to label sensory neurons associated with the trachea.

In *Drosophila*, volatile chemicals in the environment are primarily detected by members of the Olfactory Receptor (OR) family, which is predicted to encode over 62 seven-

transmembrane-domain (non-GPCR) proteins (Joseph and Carlson, 2015). Most olfactory receptor neurons express one member of the OR family and an obligate co-receptor, Or83b, also known as Orco. While mammalian olfactory receptors (GPCRs unrelated to *Drosophila* ORs) are expressed in various non-chemosensory tissues (Kang and Koo, 2012), *Drosophila* ORs show restricted expression in olfactory receptor neurons.

The *Drosophila* genome also contains three genes that encode atypical soluble guanylyl cyclases: Gyc-88E, Gyc89-Da, and Gyc89-Db. These guanylyl cyclases have been suggested to function as molecular oxygen sensors and are activated under hypoxic or anoxic conditions. Gyc-88E is active as a homodimer and can confer responsiveness to anoxia when expressed in COS-7 cells, although a higher level of activity is seen when it is co-expressed with Gyc89-Da or Gyc89-Db (Morton, 2004). These guanylyl cyclases have been found to be co-expressed in certain larval sensory neurons, including a subset of td neurons and terminal sensory cone neurons (Vermehren-Schmaedick et al., 2010). RNAi knockdown of these guanylyl cyclases causes a delay in the hypoxia escape response in which larvae withdraw from food in hypoxic conditions. The hypoxia response behavior has been attributed to the terminal sensory cones neurons, which due to their position on the tail would allow animals to still detect environmental gas levels while most of their anterior torso is buried in food. However, it is unclear whether changes in oxygen levels are detected by the more internally situated td neurons.

Overall, *Drosophila* chemosensory receptor gene functions are best characterized in the olfactory and gustatory systems. However, a lack of understanding of their functions in other cells, including td neurons, presents an opportunity to discover atypical chemosensory receptor functions.

Figure 1.1: Anatomy of the mammalian vagus nerve

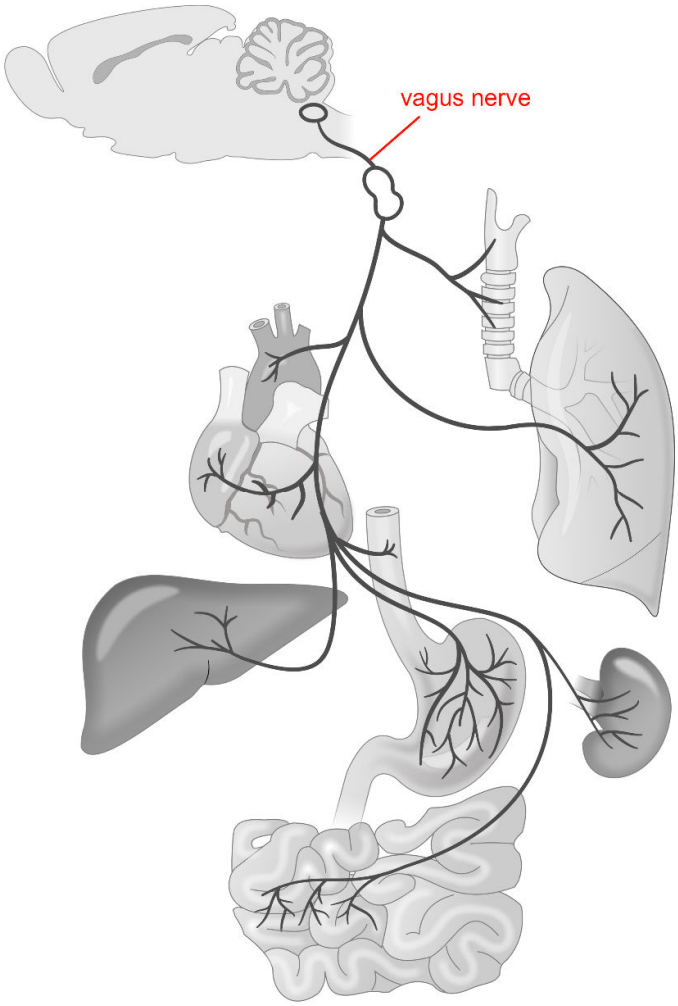

Adapted from dissertation (Strochlic, 2015) with permission.

Figure 1.2: The *Drosophila* larval PNS

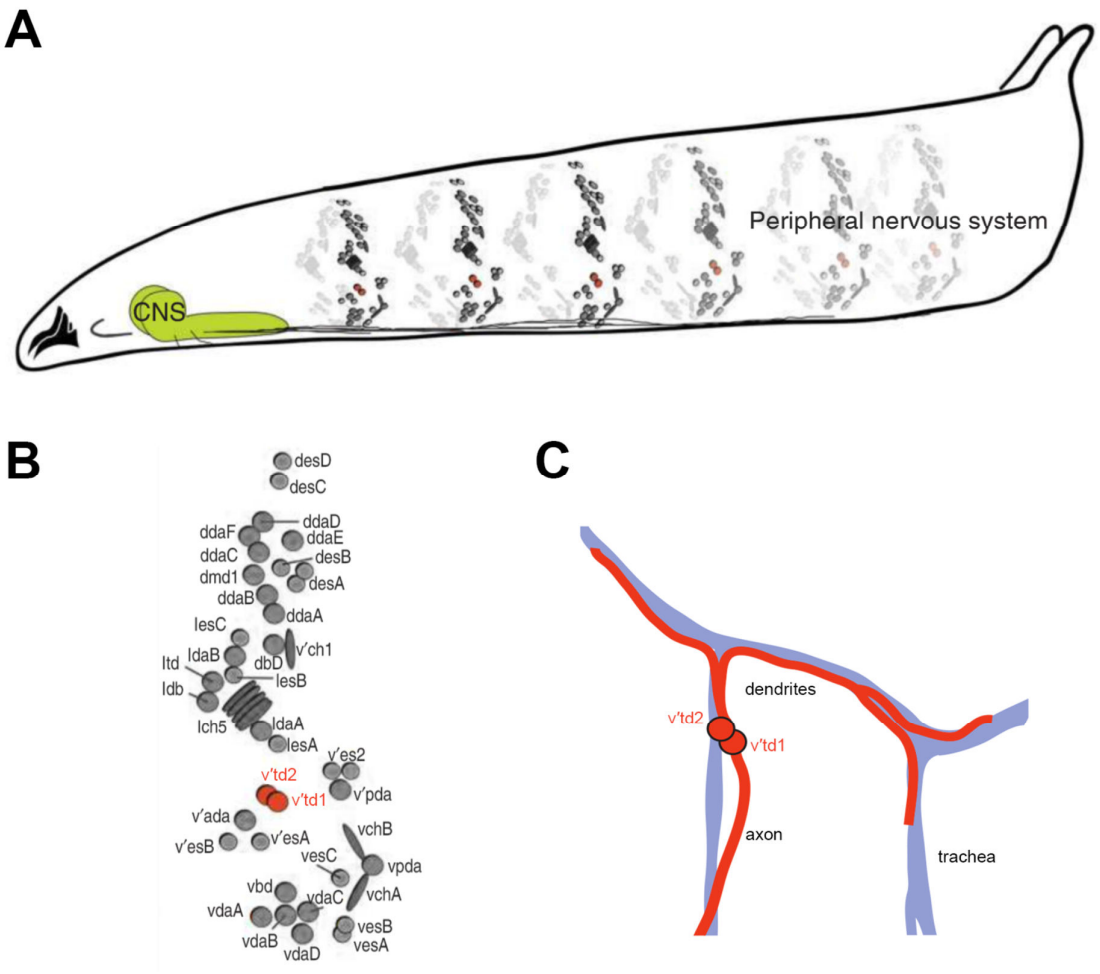

A) Schematic of a third-instar *Drosophila* showing sensory neuron elements that comprise the peripheral nervous system. For simplicity, only sensory neurons from a subset of the abdominal segments are shown. Sensory axons bundle and project to the central nervous system (CNS).
B) Schematic of the arrangement of sensory neurons in a single abdominal hemisegment.
C) Schematic of tracheal dendrite (td) neurons. A pair of td neurons (in red) extend dendrites that associate with tracheal branches.
Adapted from published work (Singhania and Grueber, 2014) with permission.

Chapter 2: Diversity of tracheal sensory neuron axon projections is controlled by Pdm3

Abstract

Despite their conservation across species, the organization and development of internal sensory systems are still relatively poorly understood. A largely unstudied population of larval *Drosophila* sensory neurons, termed tracheal dendrite (td) neurons, innervate internal respiratory organs and may serve as a model for understanding the sensing of internal states. Here, we characterize the peripheral anatomy, central axon projection, and diversity of td sensory neurons. We provide evidence for prominent expression of specific gustatory receptor genes in distinct populations of td neurons, suggesting novel chemosensory functions. We identify two anatomically distinct classes of td neurons. The axons of one class project to the subesophageal zone (SEZ) in the brain, whereas the other terminates in the ventral nerve cord (VNC). We identify expression and a developmental role of the POU-homeodomain transcription factor Pdm3 in regulating the axon extension and terminal targeting of SEZ-projecting td neurons. Remarkably, ectopic Pdm3 expression is alone sufficient to switch VNC-targeting axons to SEZ targets, and to induce the formation of putative synapses in these ectopic target zones. Our data thus define distinct classes of td neurons and identify a molecular factor that contributes to diversification of axon targeting.

---

[*] This chapter is adapted from a published manuscript (Qian et al., 2018). I am grateful to Margarita Kaplow, Jennifer Lee, and Wes Grueber for their valuable contributions to the data and text of this chapter.

Qian, C.S., Kaplow, M., Lee, J.K., and Grueber, W.B. (2018). Diversity of Internal Sensory Neuron Axon Projection Patterns Is Controlled by the POU-Domain Protein Pdm3 in Drosophila Larvae. J Neurosci 38, 2081-2093.

Introduction

Internal influences on the brain control many aspects of behavior and physiology, including feeding, metabolism, osmoregulation, mood, and cognition. For example, internally detected nutrient signals regulate feeding behavior (Coll et al., 2007; Minokoshi et al., 2004). Internally detected sex peptide alters post-mating reproductive behavior (Yang et al., 2009). Across species, these so-called interoceptive signals are conveyed centrally by internal sensory neurons and in some cases, by direct sampling of chemicals in the blood within specialized brain cells (Craig, 2003; Critchley and Harrison, 2013). Relative to the classical senses (vision, hearing, smell, taste, touch), much less is known about the development and function of sensory systems that monitor internal state.

The simpler neuroanatomy of the invertebrate nervous system may provide an entry point for understanding interoceptive circuitry. The *Drosophila* larval peripheral nervous system is comprised of both surface neurons that detect external stimuli such as touch and heat, and internal sensory neurons with largely unknown functions. Tracheal dendrite (td) neurons are one class of internal sensory neurons. These cells extend sensory terminals along the trachea (the fly respiratory organ), and axons target as yet uncharacterized regions of the CNS (Bodmer and Jan, 1987; Merritt and Whitington, 1995). Axon projection patterns can inform studies of sensory function because positions are often modality-specific (Murphey et al., 1989; Pfluger et al., 1988). However, lack of knowledge about td axon terminal projections hampers the elucidation of connectivity and function.

Transcription factors control neuronal diversification and endow neurons with subtype-specific morphologies, functions and connectivity. Studies of *Drosophila* multidendritic sensory neurons have helped identify factors that control diversification of neuronal morphology (Corty et al., 2009). POU domain transcription factors are regulators of neural development in both vertebrate and invertebrate sensory systems (Corty et al., 2016; Erkman

et al., 1996; Komiyama et al., 2003; McEvilly et al., 1996). The *Drosophila* genome encodes five POU factors, POU domain motif 1 (Pdm1), Pdm2, Pdm3, Drifter, and Acj6. Each of these factors shows specific expression in sensory circuits and corresponding roles in sensory system development. Pdm1 and Pdm2 function in dendritic diversification in the somatosensory system (Corty et al., 2016) and Drifter and Acj6 in olfactory wiring (Komiyama et al., 2003). The POU domain motif 3 (Pdm3) has been shown to regulate odor receptor expression, axon targeting in olfactory neurons and ellipsoid body ring neurons, and glial development (Bauke et al., 2015; Chen et al., 2012; Tichy et al., 2008). Thus, due to their specific expression patterns and broad roles in nervous system development, POU transcription factors are a good candidate gene family for specifying unique aspects of sensory projections, perhaps including the development of interoceptive circuits.

Here, we characterize the peripheral anatomy, central axon projection, and molecular diversity of *Drosophila* td sensory neurons. Through single cell labeling, we constructed a map of td central axon projections, revealing diverse targets. We identify two subtypes of tracheal sensory neurons that project to different regions in the CNS. These axon trajectories are unusually complex among peripheral sensory receptors and project to regions of the brain not previously associated with processing of sensory information from abdominal receptors. Using a candidate gene approach revealed by enhancer trap expression, we show that the development of tracheal sensory axon trajectory is regulated by the POU-homeodomain (HD) transcription factor Pdm3. Together with earlier studies, these data support prominent roles for POU-HD transcription factors in the development of somatosensory circuitry. This work introduces a model for studying molecular, developmental, and circuit mechanisms that underlie the sensing of internal body state.

Td neuron dendrites project along specific tracheal branches

There are two adjacent tracheal dendrite (td) neurons in each abdominal hemisegment from A1-A6, named v′td1 and v′td2 for their location in the ventral′ cluster of sensory neurons, and one td neuron in A7 (Figure 2.1A,B). Fitting with the naming of individual sensory neurons according to their ventral to dorsal position, v′td1 is the more ventral of the two neurons. We screened GAL4 and LexA lines from the InSITE (Gohl et al., 2011), Janelia (Jenett et al., 2012), and OK (courtesy of Dr. Brian McCabe, unpublished) collections for drivers for peripheral sensory neurons, and identified several lines that labeled td neurons (Figure 2.2). GAL4 and LexA lines typically showed expression in characteristic subsets of td neurons, suggesting that td neurons may have diverse identities and functions.

To characterize v′td1 and v′td2 dendrite morphologies, we used GAL4/LexA dual-color labeling. We resolved peripheral arbors with single cell resolution and characterized their relationship to each other and to tracheal branches (Figure 2.1C-E). We used antibody against Coracle, a septate junction resident protein, to visualize tracheal cell structure. td cell bodies reside next to the ganglionic branch (GB) of the larval tracheal system (nomenclature following (Manning and Krasnow, 1993)) and extend dendrites along the GB and dorsally (Figure 2.1C). Major dendrites bifurcate and extend along the lateral trunk (LT). Branching along the LT tubules was sparse; however, there were local areas of branching and dendrite enlargements, most consistently at tracheal fusion cells (Figure 2.1E, arrow), which are located along LT where tracheal tubes fuse during development. Dendrites terminate either on the LT or lateral group (LG) branch, sometimes with enlargements near or at the termination (Figure 2.1E"). We did not observe differences between the trajectories of v′td1 and v′td2 in abdominal segments A3 and A4, although v′td2 was relatively simplified in segment A2 (Figure 2.1D). v′td1 and v′td2 dendrites were often fasciculated along the lateral tracheal branches. Dendrites were also tightly associated with tracheal branches along most of their length (Figure 2.1E). Using

electron microscopy, we identified fasciculated processes on the basal surface of tracheal cells, within a thin basement membrane (Figure 2.1F). Thus, td neurons have mostly similar dendritic morphologies, although GAL4 expression patterns suggested distinct classes of td neurons. We therefore examined td neuron diversity as manifest in axon projection patterns.

Td neuron axons project to the VNC and the SEZ

Sensory neuron diversity is reflected in axon projection patterns (Grueber et al., 2007; Kwon et al., 2014; Merritt and Whitington, 1995; Vosshall et al., 2000), so we examined td axons in greater detail using the collection of GAL4 and LexA lines. Although functions for td neurons are not known, they have been proposed to function as sensors of tracheal status or as proprioceptors based on the location of their dendrites (Bodmer and Jan, 1987). In the fly CNS, the terminal location of axon projections correlates with sensory modality. Within the ventral nerve cord (VNC), nociceptive and touch sensing axons project to ventromedial regions of the neuropil, proprioceptors to more dorsal neuropil, and vibration sensing chordotonal axons to intermediate neuropil (Grueber et al., 2007; Merritt and Whitington, 1995; Zlatic et al., 2009). These somatosensory axons also project primarily within the same VNC neuromere after they enter the CNS (Figure 2.3A) (Merritt and Whitington, 1995). By contrast, in embryonic stages, td axons from each segment project together along a far-lateral VNC tract, shift to a medial tract when they reach the thoracic neuromere, and extend further anteriorly (Merritt and Whitington, 1995), although the final targets and mature td axon patterns in the third instar larva have not been described. We labeled a subset of td neurons using *R31D10-LexA>13XLexAop2-mCD8-GFP*, and visualized their axon projections in the third instar CNS with major Fasciclin 2 (Fas2)-positive axonal tracts as landmarks (Grueber et al., 2007; Landgraf et al., 2003). After entering the VNC, td axons project anteriorly along the

ventrolateral (VL) tract to the T3 neuromere (Figure 2.3A', B). At T3, axons turned medially and dorsally to the dorsomedial (DM) fascicle. Thus, td axons make a series of shifts along both the mediolateral and dorsoventral axes as they project to anterior parts of the CNS. Based on these patterns, td axon projections are different from all other characterized types of sensory neurons that innervate the body of the larva (Figure 2.3A,A').

Prior studies on embryos showed that some td axons extended anteriorly beyond the T3 medial turn (Merritt and Whitington, 1995), but axon terminal locations were not known. To determine their ultimate targets, we examined td axon projections using GAL4 and LexA drivers that labeled subsets of td neurons. The subset of td neurons labeled by *R31D10-LexA* extended axons beyond the VNC to target the subesophageal zone (SEZ) in the brain (Figure 2.3B,C). By contrast, a different subset of td neurons labeled by *R22C07-Gal4* extended axons only to the T3 neuromere in the VNC (Figure 2.3C'). Colabeling of both populations revealed that despite their different targets, VNC and SEZ targeting td axons project along the same initial path in the VNC (Figure 2.3C"). Thus, td sensory neurons can be segregated into at least two classes based on axon projections that remain entirely within the VNC or project anteriorly to the SEZ.

We asked whether SEZ and VNC td axons have different patterns of association or fasciculation as they project through the VNC to their targets, which could help to explain distinct targeting. Notably, although SEZ-targeting and VNC-targeting td axons fasciculate as they enter the VNC from the periphery, once they arrive in the VL tract axons segregate according to their final targets, such that SEZ-targeting td axons group together and VNC-targeting td axons similarly group together (Figure 2.3D). These data suggest that td axons show hierarchical axon-axon associations as they target to the SEZ and VNC. Initial associations between axons from the same segment may be suppressed as axons encounter

other “like-type” axons, which segregates cohorts into distinct subtype-specific bundles en route to their terminal targets.

Given the projection of td axons to the SEZ, we asked how their terminal targeting relates to gustatory receptor neuron axons, which strongly innervate the SEZ. Colabeling of td neurons (with *R31D10-LexA*) and gustatory sensory neurons (with *Gr32a-Gal4*) showed that SEZ-targeting td axons terminate in a similar location as gustatory sensory axons (Figure 2.3E). Compartmentalization of the SEZ is still poorly understood so we cannot eliminate modality-specific fine scale axon organization; nevertheless, the terminal location of these projections raise the possibility of chemosensory roles for td neurons.

Td neurons could conceivably make synaptic contacts with targets in an *en passant* fashion along their entire length, or only in axon terminal regions. To determine whether SEZ and VNC td neurons might have entirely distinct or potentially similar synaptic targets, we expressed the active zone marker Brp.short in different td neuron classes. VNC td neurons labeled by *R22C07-Gal4* showed presynaptic zones in VNC neuropil along the VL tract and near the DM fascicle (Figure 2.3F). Notably, SEZ td neurons labeled by *R31D10-LexA* showed Brp.short labeling at the axon terminals in the SEZ, and also along the length of the axons in the VNC (Figure 2.3G). These data are consistent with presence of *en passant* synapses along the length of td axons.

Based on these axon projections and putative presynaptic sites, we identify at least two distinct projection patterns, patterns of axon-axon association, and output sites, for td neurons to the VNC and SEZ. td neuron circuitry appears to be distinct from other known classes of mechanoreceptors, proprioceptors, and nociceptors, but may share neuropil targets with other chemosensory neurons.

Td neurons express GAL4 drivers for chemosensory receptors

Given that td axons project to chemosensory recipient regions of the SEZ, we examined whether td neurons express chemosensory receptor genes. A large battery of gustatory receptor (GR) genes have been identified and the expression patterns of many of them can be assessed using available GAL4 lines. A previous analysis of the expression patterns of 68 gustatory receptors using *Gr-Gal4* drivers identified 7 GRs that were expressed outside of larval head taste organs (Kwon et al., 2011). We found that 4 of these *Gr-Gal4s* are expressed in td neuron subsets (Figure 2.4, Figure 2.2). In *Drosophila*, functional GR complexes require the expression of multiple GR subunits. Almost all GR-expressing td neurons show expression of multiple GR drivers, suggesting GR expression in td neurons could be functionally relevant. We considered the caveat that *Gr-Gal4* promoter fusions may not reflect GR expression in td neurons. Arguing against this possibility, a $Gr33a^{Gal4}$ knock-in line (Moon et al., 2009) showed expression in td neurons in the same pattern as the promoter fusion. In addition to GRs, the IR20a clade of Ionotropic Receptors (IR) are proposed to be gustatory and pheromone receptors (Bray and Amrein, 2003; Joseph and Carlson, 2015; Koh et al., 2014). A previous analysis of the expression patterns of these IR drivers identified *IR56a-Gal4* expression in neurons associated with the trachea (Stewart et al., 2015). We confirmed the expression of IR56a in a specific subset of td neurons (Figure 2.2). We also identified another IR driver, *Ir76b-Gal4*, that is expressed in a subset of td neurons. Overall, these data suggest that chemosensory receptor genes are expressed in td neurons.

A cellular and molecular map of larval td neurons

The GAL4 lines we identified label cohorts of fasciculated td axons, obscuring single axon projection patterns. To determine the axonal morphologies of all individual td neurons,

we generated Flybow and MultiColor FlpOut (MCFO) clones (Hadjieconomou et al., 2011; Nern et al., 2015)(Figure 2.5A-M). We examined multiple clones from each of the 13 v′td neurons in the larva (two neurons per hemisegment from A1 to A6, and one neuron per hemisegment in A7). Clonal analysis revealed two main subtypes of v′td neurons with different axon projections in the CNS. All axons project along the canonical td tract described above (Figure 2.3B), but terminated at different positions along this tract. Among v′td2 neurons, axon projections were heterogeneous. Neurons in the more anterior abdominal segments A1-A3 projected to the SEZ (Figure 2.5A-C), neurons in A4 and A5 projected just short of the DM fascicle (Figure 2.5D,E; see also Figure 2.3C'), and neurons in A6 projected only along the VL fascicle (Figure 2.5F). Segment A7 contains only one td neuron and its axon terminated along the VL fascicle, supporting a v′td2 identity (Figure 2.5G). We also noted that the A7 td axon often sprouted collateral branches that projected medially (Figure 2.5G). By contrast, all v′td1 neurons extend axons along the td tract to the DM fascicle and then anteriorly to the SEZ (Figure 2.5H-M). At the SEZ, the axons turn slightly laterally, defasciculate, and terminate as a tuft of processes (Figure 2.3B). Td identity (i.e. v′td1 or v′td2) and axon projections correlated with GR and IR driver expression patterns (Figure 2.2). v′td1 neurons generally expressed IR drivers (Ir56a and Ir76b), but did not express GR drivers with the exception of the A1 v′td1, which expressed *Gr28a-Gal4*. v′td2 neurons that project to the SEZ and VNC shared expression of *Gr28b.c-Gal4* and *Gr89a-Gal4*, but showed divergent expression of *Gr28a-Gal4* (in SEZ-projecting v′td2s) and *Gr33a-Gal4* (in VNC-projecting v′td2s).

In summary, these data reveal distinctions between v′td1 and v′td2 axon targets and gene expression patterns. In addition, we find distinctions in the projections of v′td2 depending on segment of origin. Our results reveal diversity of v′td neurons and support the possibility of multiple functions.

Pdm3 is expressed in SEZ-targeting td neurons

Given our identification of distinct morphologies and gene expression patterns among td neurons, we next examined factors that diversify subtypes. As a starting point, we examined enhancer trap GAL4 lines that showed td neuron expression. Lines in our GAL4 collection rarely labeled all td neurons and instead showed cell specific and segment specific expression. We examined one line, *OK282-Gal4*, in more detail. *OK282-Gal4* drove expression of *UAS-mCD8::GFP* in v′td2 in A1, both td neurons in A2 segments, and v′td1 in segments A3-A6 (Figure 2.6A, E). Other than these td neurons, the only other body sensory neuron labeled was a nearby external sensory neuron. Thus, most, but not all, SEZ-projecting td neurons showed *OK282-Gal4* expression, but no VNC-projecting td neurons showed expression. We performed splinkerette PCR (Potter and Luo, 2010) to identify the location of the GAL4 insertion. Molecular mapping placed the insertion 27 bp upstream of the first exon of the *pdm3* gene (Figure 2.6B). Pdm3 is a POU-homeodomain transcription factor that is important for sensory axon targeting and olfactory receptor gene expression in the olfactory system, and targeting of ring neuron axons in the ellipsoid body (Chen et al.; Tichy et al., 2008). The expression pattern of *OK282-Gal4* was highly specific, and appeared to faithfully report the expression pattern of Pdm3 in both the PNS and CNS based on anti-Pdm3 labeling of *OK282-Gal4, UAS-mCD8::GFP* larvae (Figure 2.6C,D). Importantly, anti-Pdm3 labeled each td neuron marked by *OK282-Gal4* driven reporter expression (Figure 2.6C). We therefore refer to *OK282-Gal4* as $pdm3^{OK282}$*-Gal4*. Based on expression and known roles in axon targeting, we considered Pdm3 as a strong candidate regulator of td neuron morphogenesis.

Pdm3 regulates terminal targeting of td neurons

The expression pattern of Pdm3 within td neurons correlates well with axon targeting. Specifically, Pdm3 is expressed in most SEZ-targeting td neurons but not in VNC-targeting td neurons (Figure 2.6E). We performed gain- and loss-of-function experiments to test the sufficiency and necessity of Pdm3 in td axon targeting. First, we asked whether ectopic Pdm3 expression in VNC-targeting td neurons alters axon targeting. *R22C07-Gal4* labels v′td2 neurons in A4-A6, which are Pdm3-negative and target the VNC (Figure 2.7B). Misexpression of Pdm3 under the control of *R22C07-Gal4* promoted ectopic extension of bundled td axons anteriorly beyond the VNC and into the SEZ (Figure 2.7C). The maximum distance of extension of the axons was not significantly different from $Pdm3^{+}$ SEZ targeting v′td1 neurons in A4-A6 (labeled by *R31D10-LexA*, Figure 2.7A,D). We observed thinning at the anterior parts of the retargeted axon bundle, suggesting that some, but not all, overextended td axons project all the way to the SEZ. These data suggest that Pdm3 expression is sufficient to switch td axon targeting from the VNC toward the SEZ. In addition, we wondered whether this switch is accompanied by changes in synaptic connectivity. Because VNC axons do not normally make synapses with targets in the SEZ, coexpression of Brp.short and *UAS-pdm3* provided a simple assay for altered synapse distribution. We observed Brp signal in the SEZ and in the thoracic neuromeres of the nerve cord in overextended axons, suggesting that VNC neurons that have been retargeted are competent to form synapses in anterior regions of the VNC and in the SEZ (Figure 2.7E). Thus, Pdm3 is sufficient for formation of long-range axon projections in td neurons, and for establishing sensory connectivity in the upper VNC and SEZ.

To determine whether Pdm3 expression was sufficient to promote SEZ projections in non-td axons, we drove expression in nociceptive Class IV (cIV) dendritic arborization neurons, where Pdm3 is not normally expressed, using *ppk-Gal4*. cIV sensory axons normally project directly to ventromedial neuropil and remain largely within their segment of origin

(Gerhard et al., 2017; Grueber et al., 2007). Misexpression of Pdm3 did not disrupt expression of the *ppk-Gal4* reporter. However, we observed extensive axon targeting defects in cIV neurons, most prominently defasciculation, axon wandering away from the ventral neuropil, and thinning of the axon scaffold near the midline (Figure 2.7F,G). cIV axon terminals still targeted the medial neuropil and did not make an initial "td-like" anterior turn at the lateral part of the neuropil, suggesting that Pdm3 does not on its own determine initial td-like axon trajectories (Figure 2.7F,G). This conclusion is also consistent with expression of Pdm3 in only a subset of td neurons, although all td neurons take the same initial trajectory. Some stray cIV axons projected anteriorly beyond the T1 neuropil and towards the SEZ (Figure 2.7F,G). Thus, Pdm3 promotes projection toward the SEZ most robustly in td neurons, suggesting context dependence of axon guidance activity rather than a strict sufficiency of Pdm3 for SEZ projection.

We next examined the necessity of Pdm3 for td axon targeting. We used *R31D10-LexA* to label three Pdm3^{+} td neurons that project to the SEZ (Figure 2.8A). In *pdm3*^{f00828} mutants, td axons took apparently normal projections along the lateral tract, made a normal dorsomedial turn at T3 and projected anteriorly (Figure 2.8B), but axon terminals collapsed around the midline (Figure 2.8B). This result suggests that Pdm3 is not necessary for projection to the SEZ but is required for correct axon targeting within the SEZ.

In addition to expression in td neurons, Pdm3 is also expressed in CNS glial cells and neurons and, consistent with prior results (Chen et al., 2012), the VNC showed an elongation phenotype in *pdm3*^{f00828} mutants. To reduce Pdm3 function more selectively in neurons, we expressed *UAS-pdm3RNAi* using a pan-neuronal *elav-Gal4* driver, and used *R31D10-LexA* to label SEZ td axons. We reasoned that *elav-Gal4* would allow early enough expression in postmitotic neurons to assess roles in axon guidance or targeting. Consistent with this, we confirmed knock down of Pdm3 expression in larval td neurons (Figure 2.8E). In addition,

neuronal knockdown using *elav-Gal4* did not lead to the elongated VNC phenotype (Figure 2.8F). In *elav-Gal4>pdm3RNAi* animals, td axons in the SEZ collapsed around the midline (Figure 2.8C). Thus, in both *pdm3* mutants and pan-neuronal RNAi knockdown animals, td axon terminals exhibited mistargeting, as seen by incorrect contact of the midline by axons (Figure 2.8D). We did not observe defects in the morphogenesis of td dendrites in $pdm3^{f00828}$ null mutants (Figure 2.8G), suggesting that Pdm3 is dispensable for td dendritogenesis. Overall, our results suggest that Pdm3 expression in td neurons is sufficient to promote SEZ axon targeting but might normally function in a redundant fashion.

We wondered whether other POU domain proteins have redundant roles in td neurons. We used *Pdm1-Gal4* (Thompson and Cohen, 2006), anti-Pdm2 (Grosskortenhaus et al., 2006), anti-Acj6 (Clyne et al., 1999a), and a knock-in *Drifter-Gal4* (Hasegawa et al., 2011) and examined expression of these POU proteins in third instar larva. We did not observe expression in td neurons (Figure 9). Moreover, studies of these four POU proteins in select embryonic stages have not shown expression in cells in a location that corresponds to the td neurons (Certel et al., 2000; Sotillos et al., 2010). Overall, based on new and existing expression data collected at several stages of development, we suspect additional regulators beyond the POU proteins may be regulating td axon targeting.

Pdm3 misexpression suppresses *Gr33a-QF* reporter expression

Pdm3 could be regulating axon projection identity or neuronal fate in general. We therefore asked whether Pdm3 regulates broader aspects of td neuronal identity. Given that SEZ-projecting and VNC-projecting td neurons differentially express some GRs and IRs, we manipulated Pdm3 expression and asked whether chemosensory receptor expression in td neurons was altered. We focused on the expression of *Ir76b*, *Gr28a* (both expressed within

SEZ-td population), and *Gr33a* (expressed within VNC-td population). We did not observe a change in the expression of *Ir76 b-Gal4*, *Gr28a-Gal4*, or *Gr33a^{Gal4}* reporter lines in *pdm3* mutants, indicating that Pdm3 is not necessary for GR/IR reporter expression (Figure 2.10A). We next used *R22C07-Gal4* to drive ectopic Pdm3 expression in VNC-projecting A4-A6 v′td2 neurons, and used QF reporters (Choi et al., 2016; Zhang et al., 2013) to assess GR/IR expression. In control background, *Ir76b-QF* expression matched *Ir76b-Gal4* expression; *Gr28a-QF2* and *Gr33a-QF* expression largely matched their respective GAL4 reporter expression, although expression differed slightly (Figure 2.10A,B). We found that ectopic Pdm3 expression in VNC-td neurons using *R22C07-Gal4>UAS-pdm3* decreased the frequency with which *Gr33a-QF* reporter labeled A4-A6 v′td2 neurons from 100% to 31% (Figure 2.10B,C). Ectopic Pdm3 expression did not affect *Ir76b-QF* or *Gr28a-QF2* expression (Figure 2.10B). Thus, Pdm3 expression is sufficient to suppress VNC-td GR reporter expression, although other inductive factors may be necessary to induce SEZ-td GR/IR expression. Together, these results suggest that Pdm3 regulates both axon targeting and GR expression aspects of td neuronal identity.

Discussion

Td neurons project to the VNC and SEZ

High-resolution studies of sensory axon morphology in embryos identified unusual axon projections of td neurons beyond their segment of origin to a common target in thoracic neuromeres (Merritt and Whitington, 1995). Whether this neuromere represented an intermediate or terminal axon target was unknown because mature td axon projections in the third instar larva were not described. Here we show that all td neurons make long-range projections but have dichotomous terminal zones anteriorly in the SEZ and in the VNC. The

SEZ receives chemosensory inputs and contains numerous peptidergic fibers (Kwon et al., 2011; Schlegel et al., 2016). Based on their location along trachea, td neurons were proposed to function as proprioceptors or gas sensors (Bodmer and Jan, 1987; Morton et al., 2008), although the function of td neurons is as yet unknown. Our anatomical data are more consistent with roles for td neurons as internal chemosensors. We note that axons that project to the SEZ form *en passant* synapses throughout the VNC, suggesting distributed input to central circuits. SEZ- and VNC- targeting axons could conceivably share postsynaptic partners in the VNC, with SEZ-targeting axons connecting with an additional population of targets in the SEZ, although precise connectivity remains to be determined. A recent electron microscopic study of the SEZ identified ascending sensory projections that form synapses with a subset of peptidergic Hugin neurons (Schlegel et al., 2016). These sensory projections likely correspond to a subset of td neurons. Functional interrogation of this Hugin circuit, and reconstruction of additional downstream targets (Schneider-Mizell et al., 2016) of SEZ- and VNC-projecting td neurons will provide insights into possible roles for the td system in behavior and physiology.

Td neurons express GRs and IRs

We identified expression of multiple GR and IR reporters in td neurons. This finding, together with our anatomical data, suggests that td neurons may function to sense internal chemical stimuli. In *Drosophila*, the combinatorial coexpression of specific GRs determines the tuning of gustatory neurons to specific ligands (Lee et al., 2009; Shim et al., 2015; Sung et al., 2017). The patterns of coexpressed GRs that we observed in td neurons have not been observed in other gustatory neurons (Choi et al., 2016; Kwon et al., 2011), suggesting possible tuning to novel ligands. Two GRs that appear to be expressed in td neurons, Gr33a and Gr89a, are expressed in all adult bitter neurons (Weiss et al., 2011), and Gr33a is broadly required for responses to aversive cues in the context of feeding (Moon et al., 2009). These GRs have been

proposed to function as “core bitter coreceptors” (Moon et al., 2009). It is possible that at least a subset of td neurons may detect aversive chemical stimuli. Given that td dendrites appear to be bathed in hemolymph and associated with the trachea, td neurons may detect both dissolved circulating stimuli (e.g. ingested toxins, metabolites, electrolytes) and gaseous stimuli (e.g. CO_2, O_2). The expression of a reporter for Ir76b, a detector of low salt (Zhang et al., 2013), and oxygen-sensitive guanylyl cyclase (Langlais et al., 2004; Morton et al., 2008) in different subsets of td neurons is consistent with this idea. We speculate that td neurons may detect chemical imbalances and relay signals to the SEZ and VNC to elicit behavioral or physiological responses to restore homeostasis. Neurons in the SEZ could regulate feeding (Huckesfeld et al., 2016), and neurons in the VNC could regulate locomotion (Kohsaka et al., 2017; Schoofs et al., 2014) or fluid balance (Cognigni et al., 2011; Santos et al., 2007). In mammals, lung-innervating sensory neurons comprise molecularly distinct subtypes with different anatomical projections and functions (Chang et al., 2015). Here, we show that larval *Drosophila* trachea-innervating sensory neurons similarly comprise molecularly distinct subtypes with distinct axon projections. Future studies to image and manipulate td activity, and disrupt chemosensory receptor gene function, should clarify the sensory functions of td neurons and the underlying molecular mechanisms.

Td dendrites associate with tracheal branches

We uncover multiple levels of specificity of td neuron dendrite-substrate relationships, including strict association with a tracheal substrate, arborization across specific tracheal branches, and dendritic specializations at tracheal fusion cells. The factors that specify sensory dendrite organization of td neurons are unknown and do not appear to include Pdm3. Whether dendrite specializations are important for detection of chemicals in the tracheal lumen or whether trachea merely serve as an attachment site to allow sensing of abdominal hemolymph

status is not clear (Bodmer and Jan, 1987; Merritt and Whitington, 1995). The positioning of td dendrites may place them out of direct contact with the tracheal interior; however, association across tracheal cells could still permit sensing of tracheal physiology. Future studies to monitor tracheal system and td dendrite development will help to sort out mechanisms of dendrite-substrate interactions and the importance of this association for td neuron function.

Td as a model for studying complex axon guidance

Many of the guidance decisions made by sensory axons involve decisions to terminate at specific mediolateral and dorsoventral positions or in specific neuropil layers (Clandinin and Zipursky, 2002; Zlatic et al., 2003; Zlatic et al., 2009). For td axons, the guidance decisions are complex. Single td axons switch between medial and lateral positions, and dorsal and ventral positions and do so at specific locations along their length. Moreover, the terminal position of td axons varies according to cell identity and segment of origin. We predict that studies of td neurons may be especially useful for understanding sequential and regionally-restricted guidance switches in axons, a model more akin to long-range projections, such as vertebrate corticospinal tract axons that navigate multiple choice points (Finger et al., 2002), than other locally-projecting *Drosophila* sensory axons.

Pdm3 regulates td axon projection identity

We provide initial insight into one major choice of td axons: the choice to project, or not, to far anterior regions of the CNS (SEZ). We find that the Pdm3 transcription factor is expressed in most, but not all, td neurons that project to the SEZ and is expressed in none of the td neurons that terminate in the VNC. Ectopic Pdm3 expression promoted anterior axon growth along the canonical td axon path, indicating that Pdm3 expression is sufficient for SEZ projections. This effect depends on sensory context because misexpression of Pdm3 in cIV

dendritic arborization neurons did not convert axons to a td-like projection, but rather led to axon defasciculation, overgrowth, and axon straying, occasionally into the SEZ. Loss of Pdm3 led to modest disruptions of terminal targeting in SEZ-projecting tds, suggesting sufficiency, but redundancy with other factors, in SEZ targeting. We noted specific patterns of axon-axon segregation among axons that project to the SEZ and those that project to the VNC. Thus, in addition to the possibility that Pdm3 functions as a growth-promoting factor, other explanations could account for Pdm3 misexpression phenotypes, such as promoting specific patterns of axon-axon interactions that underlie pathfinding to anterior CNS.

With respect to fine terminal targeting, one potential role for Pdm3 may be to inhibit midline contact of sensory axon terminals, which could account for the Pdm3 loss-of-function phenotype in td neurons and part of the Pdm3 misexpression phenotype in cIV neurons. The normal functions of Pdm3 in different cell types suggest context-dependent roles to promote terminal targeting. Identifying whether conserved transcriptional targets are shared between these different systems will be an important future step. Studies of Pdm3 might reveal how axon initial growth, pathfinding, terminal targeting, and maintenance are regulated in a modular fashion across different neurons, which could be important not only for axon wiring during development but also for regeneration.

Pdm3 regulates td chemosensory receptor identity

Our results extend the roles for Pdm3 in axon targeting and chemosensory receptor expression. Prior studies identified roles for Pdm3 in targeting of olfactory sensory neurons, in olfactory receptor expression (Tichy et al., 2008), and in ellipsoid ring (R) neuron axon targeting (Chen et al., 2012). In R neurons, Pdm3 controls axon terminal targeting, without impacting dendritic arborization, cell fate determination, or initial axon outgrowth. Our results for td neurons support a role in axon terminal growth and targeting, or maintenance, and in

regulation of GR expression. Thus, consistent with prior findings in the olfactory system (Tichy et al., 2008), we demonstrate Pdm3 regulates multiple aspects of neuronal identity.

Figure 2.1: Td sensory dendrites associate with tracheal branches

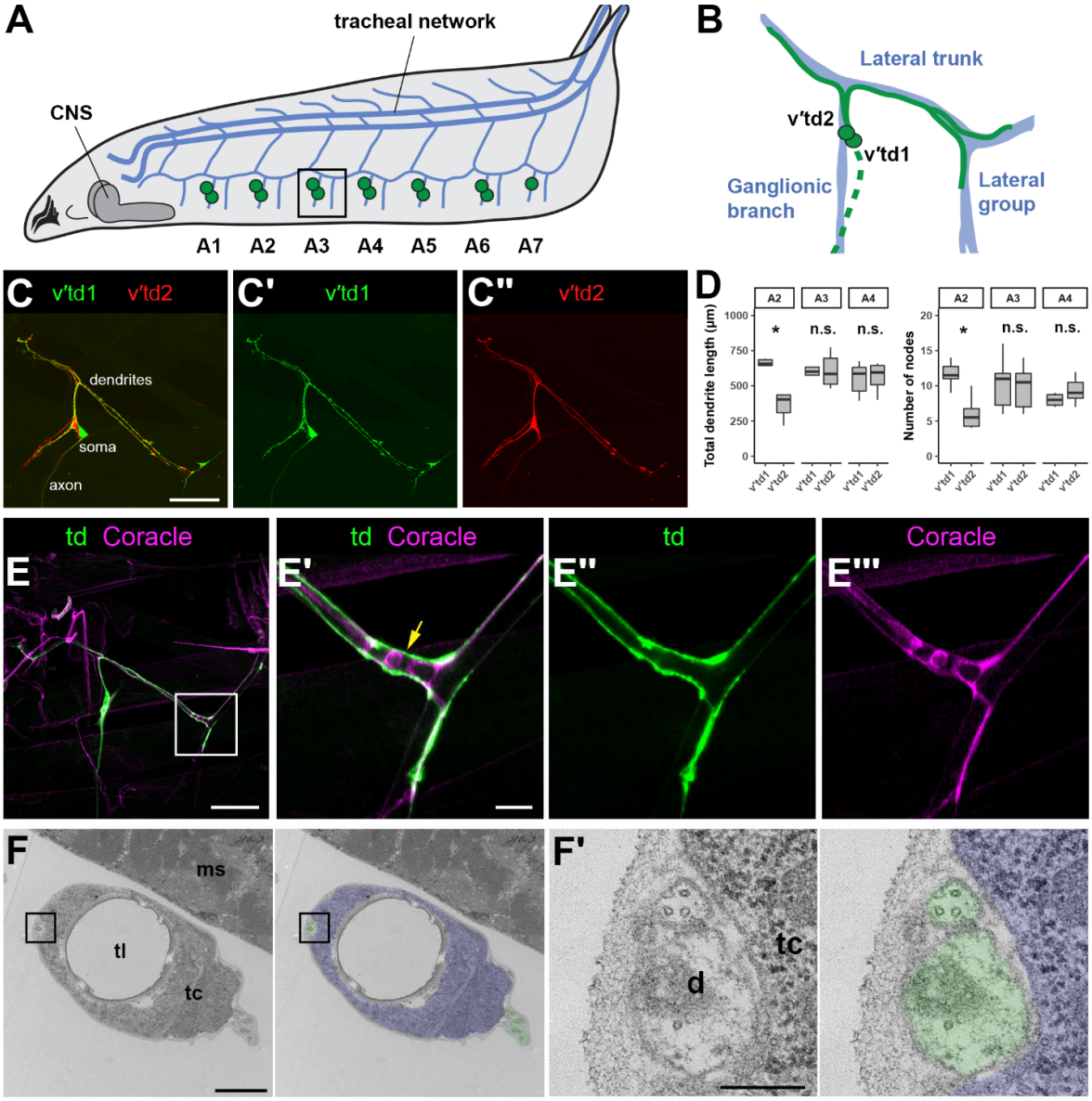

A, Schematic of larva showing segmentally-repeated td cell bodies (green) relative to the tracheal network (blue; only major tracheal branches are shown).

B, Schematic of v′td1 and v′td2 neurons in one hemisegment, showing cell bodies (green circles), dendrites (solid green lines), and axons (dashed green line), and association with specific tracheal branches (blue).

C, Dual-color labeling of v′td1 (**C'**; labeled by *R35B01-LexA>mCD8::GFP*) and v′td2 (**C''**; labeled by *260-Gal4>mCherry*) neurons in segment A3.

D, Dendrite lengths and node count quantifications for v′td1 (labeled by *R35B01-LexA*) and v′td2 (labeled by *260-Gal4*) neurons in segments A2-A4. Dendrite length was reduced in v′td2 relative to v′td1 in segment A2 (Bonferroni adjusted *p = 0.012, Mann-Whitney *U*-test, $U < 0.0001$), but not in segments A3 or A4. Similarly, dendrite nodes were reduced in v′td2 relative to v′td1 in segment A2 (Bonferroni adjusted *p = 0.018, Mann-Whitney *U*-test, $U = 1$), but not in segments A3 (Bonferroni adjusted p = 1, $U = 16.5$) or A4 (Bonferroni adjusted p = 0.558, $U = 10$). n = 6 animals.

E, Td dendrites project along tracheal branches. Coracle labeling shows septate junctions of tracheal epithelial cells. **E'-E'''**, Enlarged image of area boxed in E showing enlargements of td dendrites near tracheal fusion cell (yellow arrow).

F, Electron micrographs of tracheal tube cross section showing tracheal cell (tc; shaded blue), putative td dendrites (d; shaded green), tracheal lumen (tl), muscle (ms). **F'**, Higher magnification image of boxed area in F, showing two neuronal processes closely associated with the tracheal cell, enclosed by basement membrane.

Boxplots show median (middle line) and 25th to 75th percentile, with whiskers extending to the most extreme data point within 1.5 times the interquartile range of the hinge.

Scale bars = 50 μm (C-C'', E), 10 μm (E'-E'''), 2 μm (F), 250 nm (F')

Figure 2.2: GAL4/LexA driver expression patterns in td sensory neurons

	v'td1 neurons						v'td2 neurons						
	A1	A2	A3	A4	A5	A6	A1	A2	A3	A4	A5	A6	A7
OK282-Gal4		+	+	+	+	+	+	+					
Gr28a-Gal4	+						+	+	+				
Gr28b.c-Gal4							+	+	+	+	+	+	+
Gr33a-Gal4[a]										+	+	+	
Gr89a-Gal4							+	+	+	+	+	+	
Ir56a-Gal4					+	+							+
Ir76b-Gal4		+	+	+	+	+							
R22C07-Gal4										+	+	+	
R31D10-LexA				+	+	+							
R35B01-Gal4	+	+	+	+	+		+						
R35B01-LexA		+	+	+									
R73B01-Gal4							+	+	+	+	+	+	+
260-Gal4								+	+	+	+	+	+

Green and red cells indicate SEZ and VNC targeting td neurons, respectively.

[a]*Gr33a*^{Gal4} knock-in line shows expression in the same td neurons.

Figure 2.3: Td axons project to the VNC and the SEZ

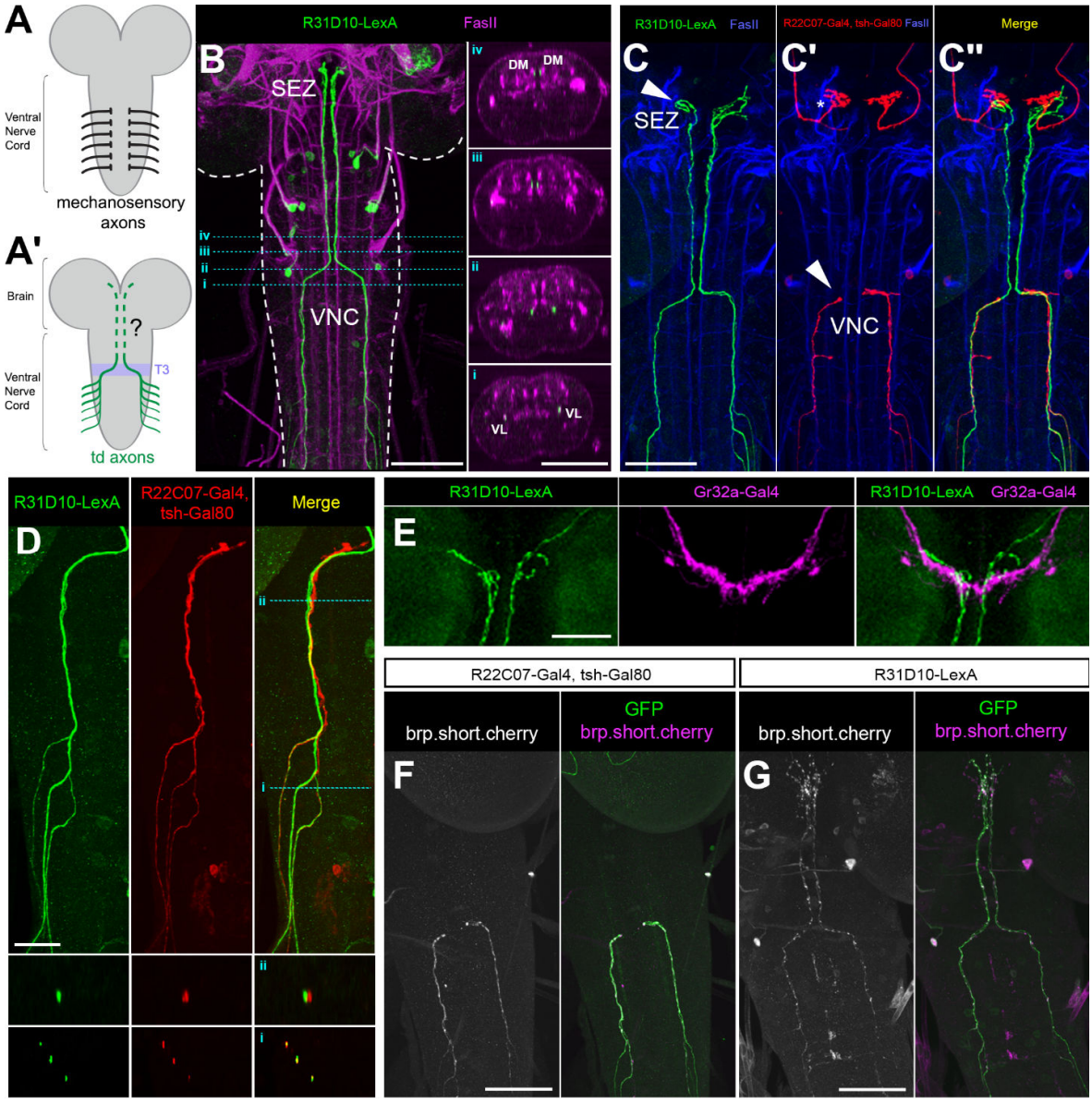

A, Schematic of CNS showing axon trajectories of typical abdominal mechanosensory neurons (**A**), and td neurons (**A'**). Dashed line and question mark in A' indicates unresolved terminal trajectory of td axons; purple band indicates T3 neuromere.

B, Td axons labeled by *R31D10-LexA>GFP* fasciculate and project anteriorly in the CNS (outlined in white). Roman numerals and dotted cyan lines indicate position of cross sections on the right, showing that td axons initially travel anteriorly along the ventrolateral (VL) fascicle (section i), then shift to the dorsomedial (DM) fascicle (section iv).

C, Two subtypes of td axon projections to the VNC and the SEZ. A subset of td neurons labeled by *R31D10-LexA>mCD8::GFP* targets the SEZ (**C**). Another subset of td neurons labeled by *R22C07-Gal4>mCherry* targets the VNC (**C'**). *Tsh-Gal80* was used to suppress VNC expression in the *R22C07-Gal4* driver. *R22C07-Gal4* also labels other sensory neurons from the head that project axons to the SEZ (asterisk).

D, VNC-targeting and SEZ-targeting axons from the same segment initially fasciculate with each other as they enter the VNC (section i), but segregate into separate bundles in the VL tract (section ii). Roman numerals and dotted cyan lines indicate position of cross sections on bottom.

E, SEZ-targeting td axons (green) terminate in close proximity to axon terminals of gustatory sensory neurons (magenta).

F,G, Presynaptic sites of VNC-targeting td axons (**F**) and SEZ-targeting td axons (**G**) labelled by brp.short.cherry reveal *en passant* synapses along the td axon bundle tract (labelled by GFP in green).

Scale bars = 50 μm (B, C-C'', F, G), 20 μm (D, E)

Figure 2.4: GR and IR GAL4 reporters label td neurons

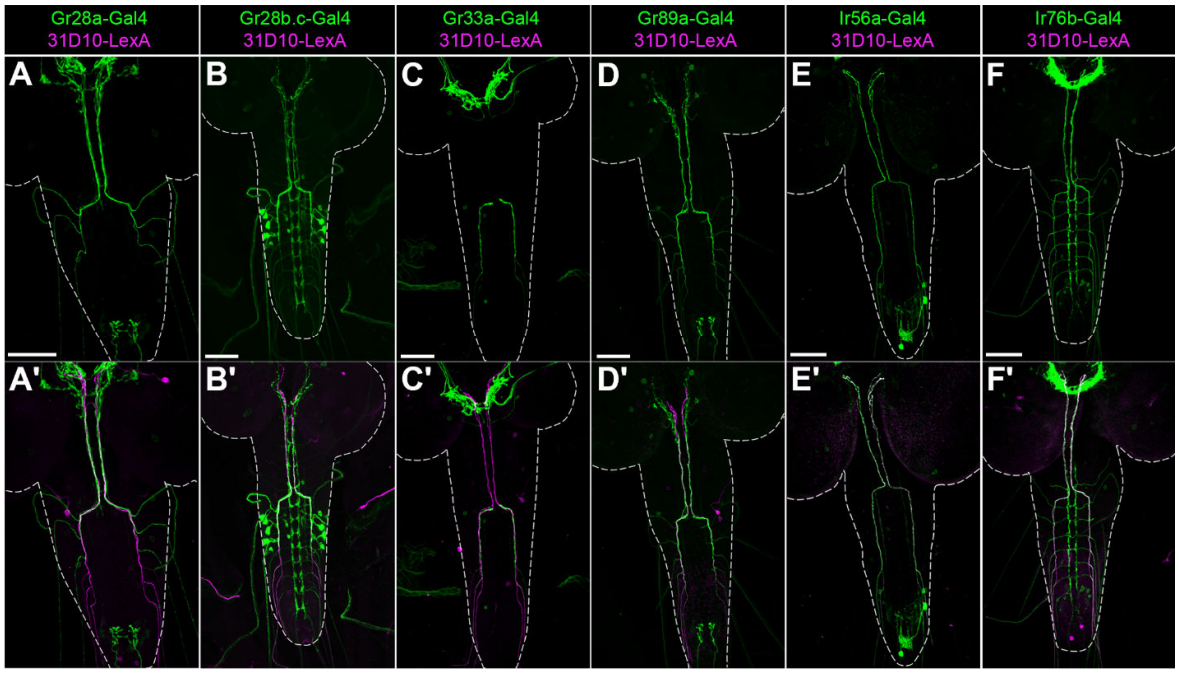

A-F, CNS images showing expression of *Gr-Gal4* and *Ir-Gal4* lines that label td neurons. **A'-F'**, Same images dual-labeled with *R31D10-LexA* which labels a subset of td neurons. In addition to td neurons, most of the GAL4 lines labeled gustatory neurons from the head (**A-D**, **F**), and a few lines labeled terminal sensory neurons (**A**, **D**), class IV sensory neurons (**B**), external sensory neurons (**F**), or CNS neurons (**B**, **E**).

All scale bars = 50 μm

Figure 2.5: Td axon projections correlate with cell identity and segment of origin

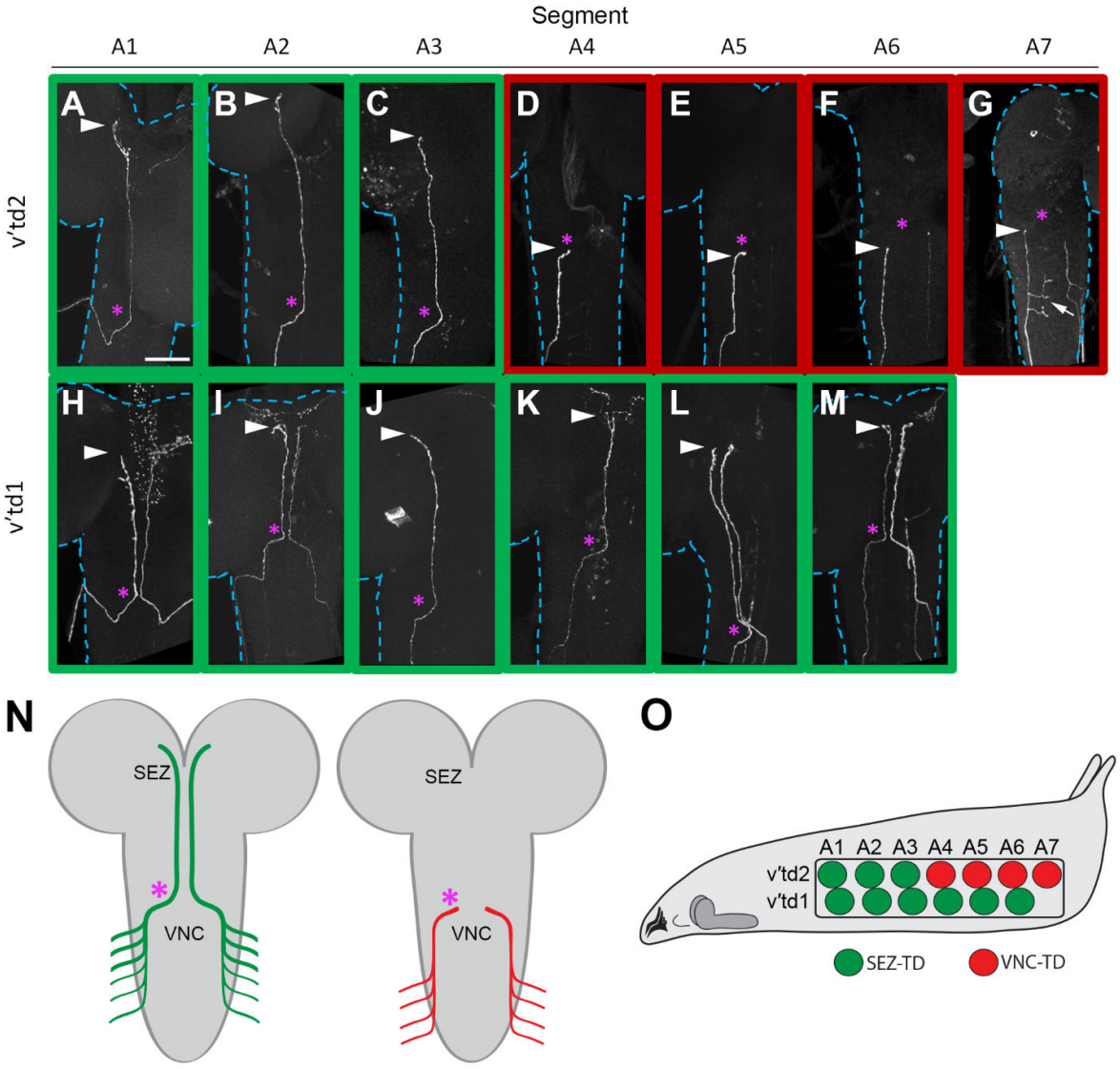

A-M, Individual central axon projections of all 13 td sensory neurons. Labeled single td neurons were generated using the MCFO technique. Magenta asterisks indicate the approximate location of the T3 neuromere. Arrowhead indicates axon termination. For all image panels, axon of interest is shown on the left side of the CNS. Blue dashed lines outline the CNS. White arrow in (**G**) indicates collateral branches from the A7 v′td2.

N,O, Schematic summarizing the axon projections (**N**) of SEZ-targeting td neurons (green; SEZ-TDs) and VNC-targeting td neurons (red; VNC-TDs), and the segment of origin and identity of these neurons in the larva body (**O**). Magenta asterisks indicate the approximate location of the T3 neuromere, as in Figure 4A-M.

Scale bar = 50 μm (A-M)

Figure 2.6: Pdm3 is expressed in SEZ-targeting td neurons

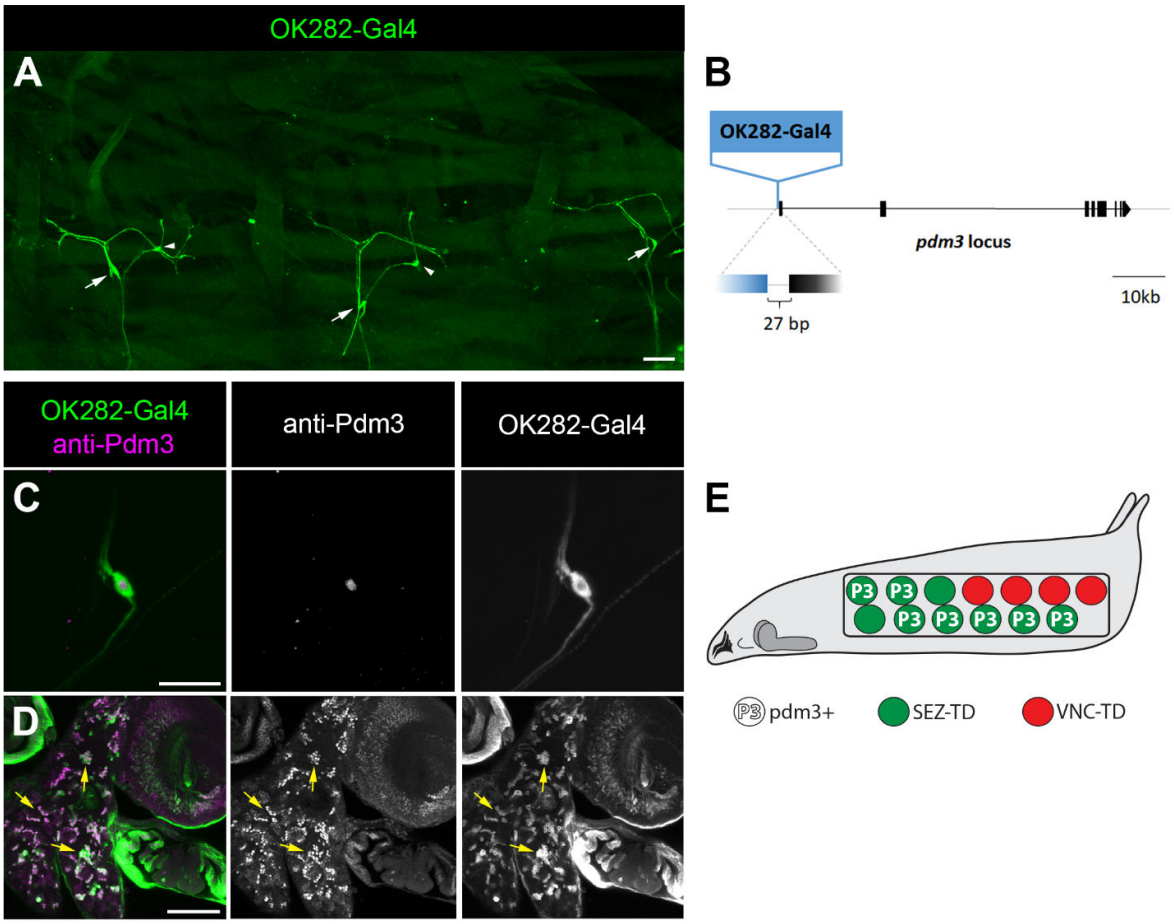

A, Expression of *OK282-Gal4>UAS-mCD8::GFP* in td neurons (arrow) and a nearby external sensory neuron in the periphery (arrowhead). Image spans three abdominal hemisegments.

B, *OK282-Gal4* is inserted upstream of the *pdm3* locus.

C,D, *OK282-Gal4* expression pattern matches anti-Pdm3 labeling in td neurons (**C**), and in CNS (**D**). Yellow arrows indicate some areas of the CNS with high overlap between the two expression patterns.

E, Schematic summarizing expression pattern of Pdm3 in td neurons, as determined by $pdm3^{OK282}$*-Gal4* expression pattern and anti-Pdm3 labeling. Pdm3 (P3) is expressed in most of the SEZ-targeting td neurons (green circles), but not in the VNC-targeting td neurons (red circles).

Scale bars = 50 μm (A, D), 20 μm (C)

Figure 2.7: Misexpression of Pdm3 in VNC-targeting td neurons promotes SEZ targeting

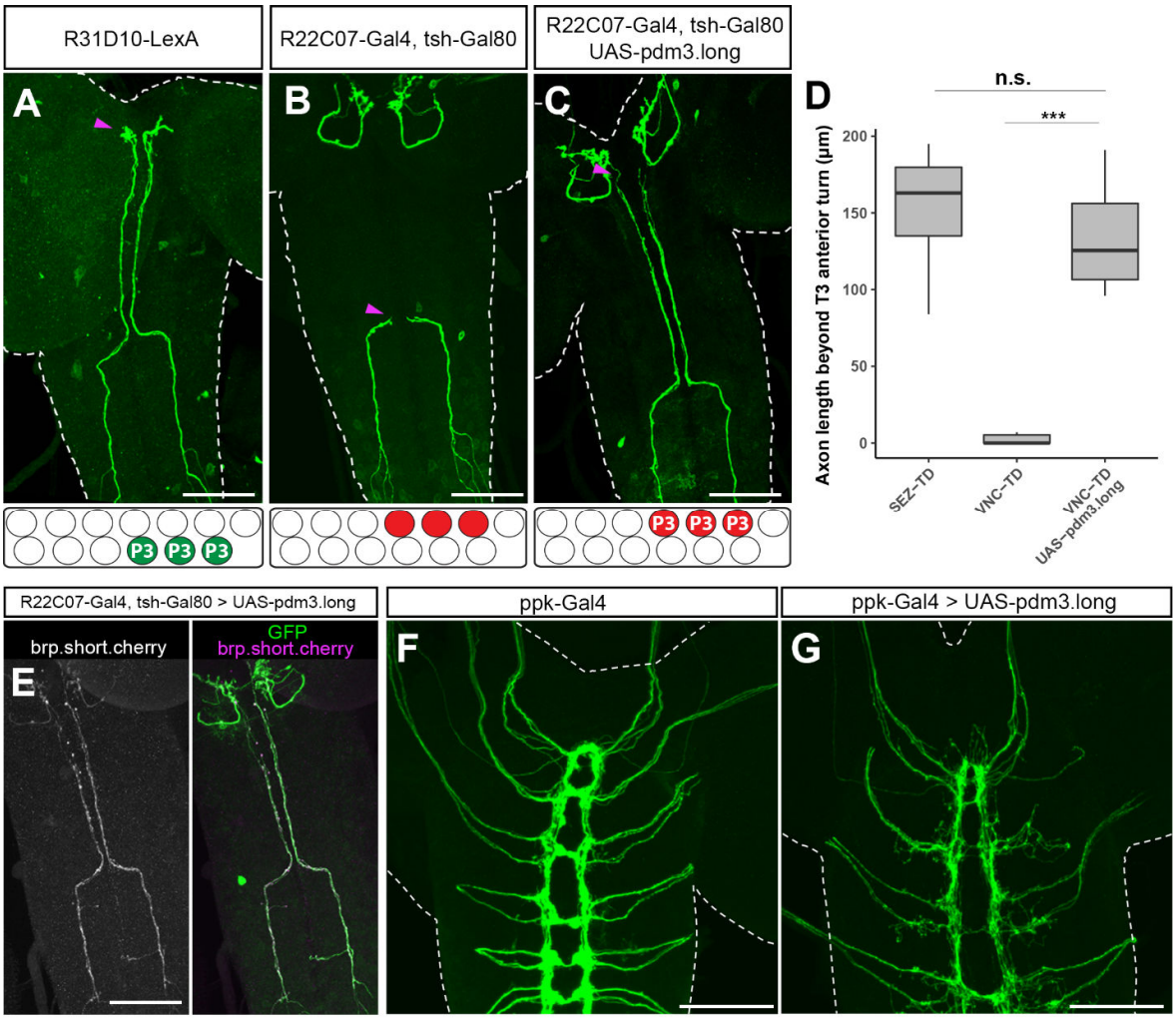

A-C, Td axons in control (A,B) and upon ectopic Pdm3 expression (C) conditions. Arrowhead indicates termination of td axons. Below each confocal image are keys showing SEZ-targeting td neurons labeled by *R31D10-LexA* (**A**; green) or VNC-targeting td neurons labeled by *R22C07-Gal4* (**B**; red), P3 indicates Pdm3 expression. Ectopic Pdm3 expression using *R22C07-Gal4* switches td axon targeting from the VNC to the SEZ (**C**).

D, Quantification of the length of the axon bundle beyond the axons' anterior turn at T3. Kruskal-Wallis test showed a significant difference of means ($H(2) = 24.40$, $p < 0.0001$). Post hoc pairwise comparisons showed that VNC-targeting td neurons ectopically expressing Pdm3 have increased axon lengths (***$p < 0.0001$, Mann-Whitney *U*-test, $U < 0.0001$), which did not differ significantly from the length of SEZ-targeting td neurons ($p = 0.332$, Mann-Whitney *U*-test, $U = 48$). n = 12 animals per condition.

E, Ectopic expression of Pdm3 in *R22C07-Gal4* neurons promotes presynaptic structures in the overextended axon segments.

F,G, Ectopic expression of Pdm3 in non-td sensory neurons (cIV nociceptive neurons) causes defasciculation and axon wandering.

Boxplots show median (middle line) and 25th to 75th percentile, with whiskers extending to the most extreme data point within 1.5 times the interquartile range of the hinge.

All scale bars = 50 μm

Figure 2.8: Pdm3 is required for correct axon targeting within the SEZ

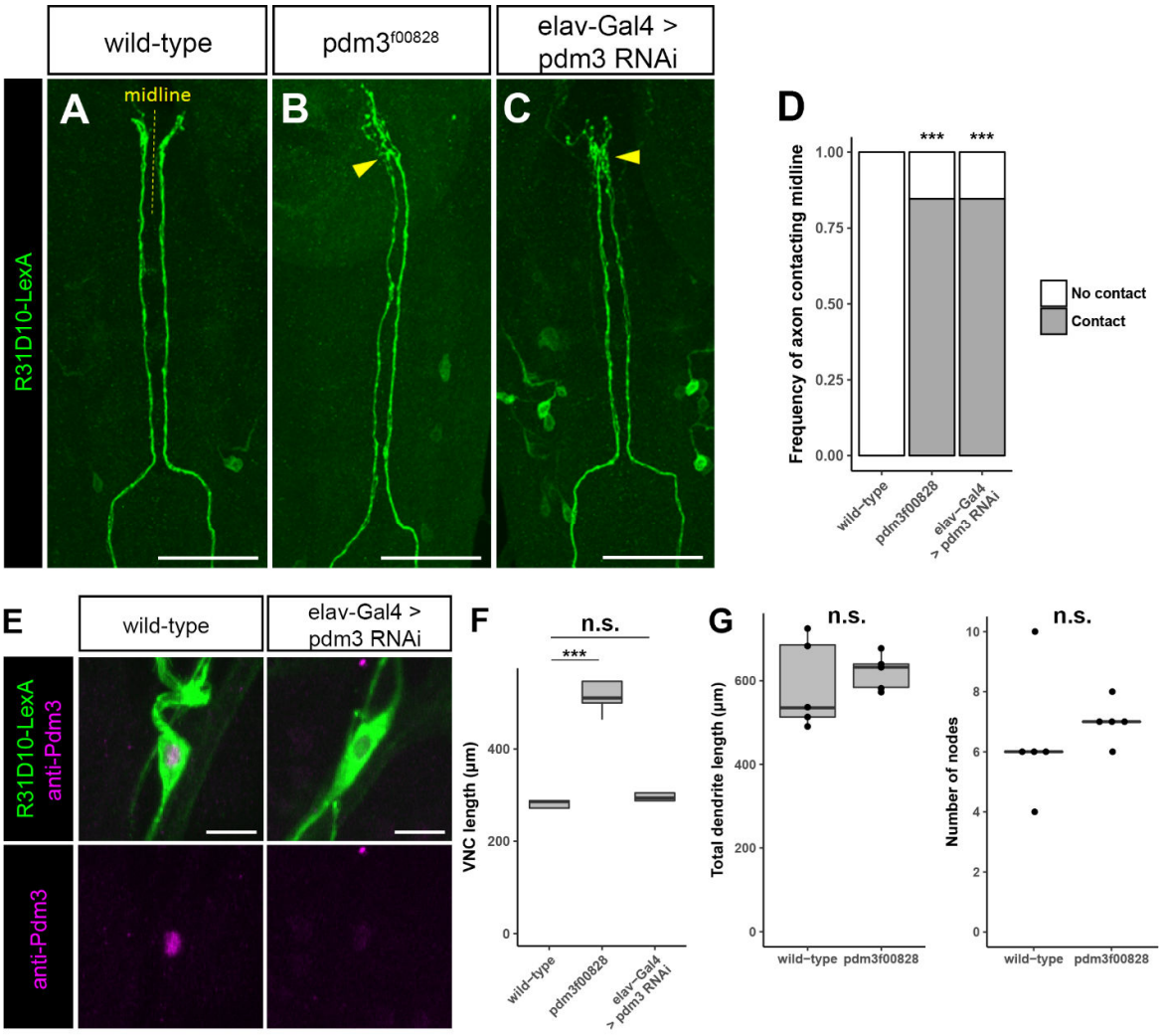

A-C, Td axons in control and Pdm3 loss-of-function conditions. In control condition (**A**), td neurons labeled by *R31D10-LexA* project axons to the SEZ, where the axons turn slightly laterally away from the midline. In *pdm3* mutant (**B**) and pan-neuronal Pdm3 RNAi knockdown conditions (**C**), td axon terminals extend toward the SEZ but incorrectly contact the midline (yellow arrowheads).

D, Quantification of midline contacts by td axon terminals. Increased axon midline contacts were observed in *pdm3* mutant (χ^2 (1, N = 26) = 19.07, ***p < 0.0001) and pan-neuronal Pdm3 RNAi knockdown (χ^2 (1, N = 26) = 19.07, ***p < 0.0001) conditions. n = 13 animals per condition.

E, Confirmation of Pdm3 knockdown in td neurons.

F, The VNC is abnormally elongated in *pdm3* mutant larvae, but not upon pan-neuronal knockdown of Pdm3. Kruskal-Wallis test showed significant difference of means (H(2) = 9.89, p = 0.007). Post hoc pairwise comparisons showed increased VNC lengths in *pdm3* mutants (***p < 0.0001, Mann-Whitney *U*-test, U < 0.0001), but not pan-neuronal Pdm3 RNAi knockdown animals (p = 0.590, Mann-Whitney *U*-test, U = 7.5). n = 5 animals per condition.

G, Loss of Pdm3 does not lead to morphological defects in td dendrites as measured by total dendrite lengths (p = 0.602, Mann-Whitney *U*-test, U = 10) and node counts (p = 0.190, Mann-Whitney *U*-test, U = 6.5). Analysis of A5 v′td1. n = 5 animals per condition.

Boxplots show median (middle line) and 25th to 75th percentile, with whiskers extending to the most extreme data point within 1.5 times the interquartile range of the hinge.

Scale bars = 50 μm (A-C), 10 μm (E)

Figure 2.9: Other POU domain proteins are not expressed in td neurons

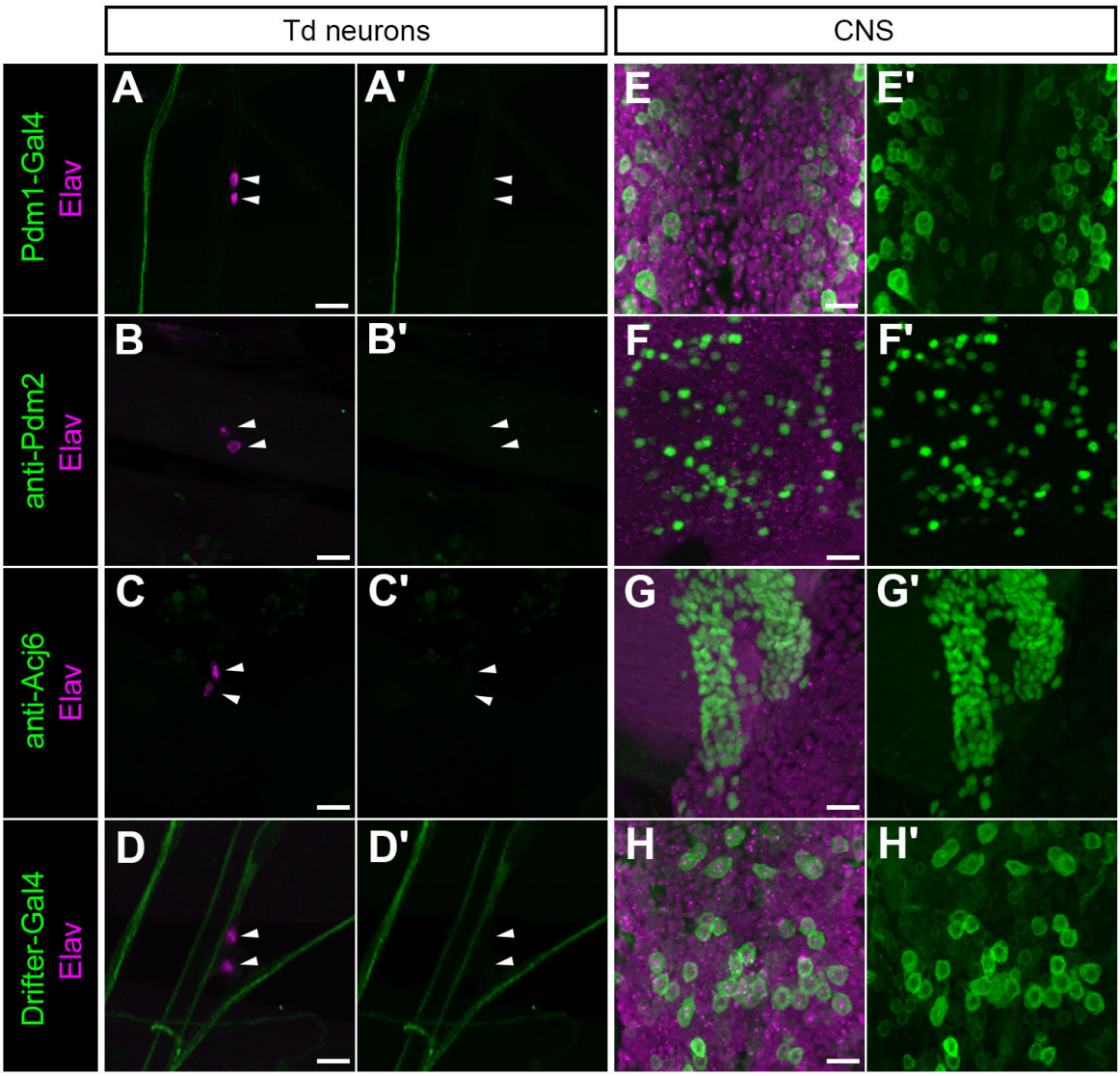

Co-labeling of td nuclei (magenta) and POU protein antibodies or Gal4 reporters (green) in third instar larvae. **A**, *Pdm1-Gal4* labels axons from dorsal cluster neurons, which bypass magenta td neurons. **D**, *Drifter-Gal4* labels tracheal cells, which are the labeled structures adjacent to td nuclei, but not td neurons. **E-H**, Positive control labeling of each marker in CNS. **A'-H'**, Green channel only. Scale bars = 10uM.

Figure 2.10: Misexpression of Pdm3 in VNC-tds suppresses *Gr33a-QF* reporter expression

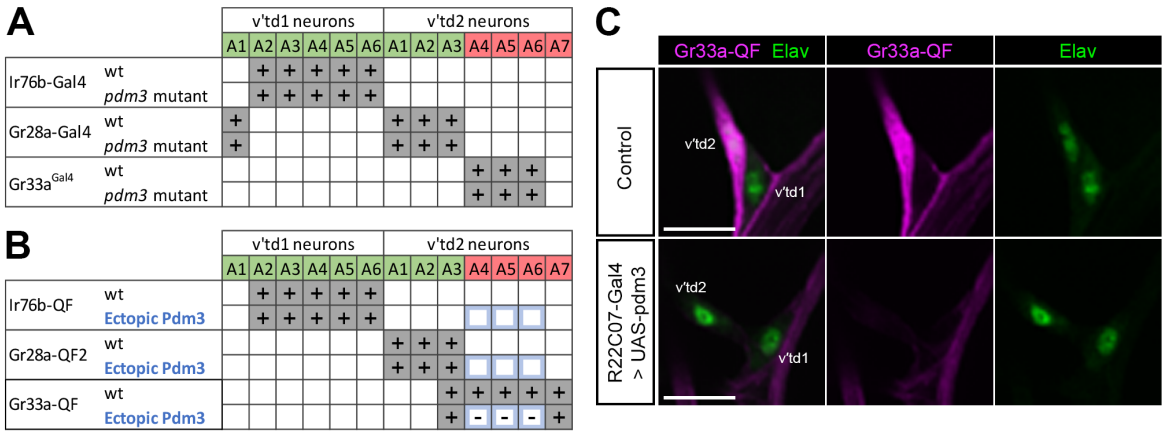

A,B, Summary of GR/IR reporter expression in wild-type, *pdm3* mutant (**A**), and ectopic Pdm3 expression (**B**) conditions. Green and red cells indicate SEZ- and VNC- targeting td neurons, respectively. Cells with expression (100% of cell labeled, n>=3 animals) are indicated by '+'; cells with reduced expression are indicated by '-' (n>=3 animals). **B**, Cells with blue outline indicate td neurons misexpressing Pdm3 through *R22C07-Gal4>UAS-pdm3*. *Gr33a-QF* labeled v′td2 in A4-A6 with 100% frequency (n=7 animals, 42 total cells examined) in control condition and only 31% frequency (n=7 animals, 42 total cells examined) in ectopic Pdm3 condition.

C, Expression of *Gr33a-QF>QUAS-mtdTomato* in td neurons in control and ectopic Pdm3 expression conditions. *Gr33a-QF* also labels glial cells, near td and adjacent nerves. Anti-Elav labels td nuclei. Images show td neurons in A5.

Scale bars = 10 μm

Chapter 3: Tracheal sensory neurons detect changes in O_2 and CO_2 levels

Abstract

Internal sensory neurons monitor the chemical and physical state of internal body organs, providing critical information to the nervous system for maintaining homeostasis and survival. A population of larval *Drosophila* sensory neurons, tracheal dendrite (td) neurons, innervate internal respiratory organs and may serve as a model of elucidating the cellular and molecular basis of internal chemosensation. Here, we report that subsets of *Drosophila* larval td neurons are activated by decrease in O_2 and increase in CO_2 levels. We show that these respiratory gas-sensitive td neurons are also activated when larvae are submerged for a prolonged duration, demonstrating a natural-like condition in which td neurons are activated. We assessed the roles of chemosensory receptor genes in mediating the response of td neurons to O_2 and CO_2. As a result, we identify Gr28b as a mediator of td responses to CO_2. Deletion of Gr28 genes or RNAi knockdown of Gr28b transcripts reduce the response of td neurons to CO_2. Together, our work identifies two stimuli that are detected by overlapping subsets of td neurons, and establish a putative role for Gr28b in internal chemosensation in *Drosophila* larvae.

---

[*] I am grateful to Shan Lu for her valuable contribution to the submersion assay data of this chapter.

Introduction

Internal sensory neurons play an important role in detecting internal state for maintaining homeostasis and survival. Across species, such neurons innervate visceral organs to detect and relay information about the chemical and physical state of target organs to the CNS. In mammals, internal sensory neurons relay information about internal stimuli such as nutrients, temperature, stretch, irritants and hormones (Fajardo et al., 2008; Hillsley and Grundy, 1998; Paintal, 1973; Williams et al., 2016). Although electrophysiology experiments over decades have revealed a wide of range of stimuli that can activate internal sensory neurons, how most of these stimuli are detected at the cellular and molecular level is largely unknown. The simpler nervous system in *Drosophila* larvae may serve as a genetically tractable model for elucidating how sensory neurons encode information about internal state.

To investigate the cellular and molecular basis of internal chemosensation, we use the larval *Drosophila* tracheal dendrite (td) neurons as a model. Td neurons extend dendrites that innervate internal tracheal branches (respiratory system) and have unknown sensory functions. We previously characterized the anatomy of the 13 bilateral td neurons in larva and found that 9 td neurons projected axons to the SEZ, a chemosensory recipient region in the brain, hinting that perhaps a subset of td neurons have chemosensory functions (Qian et al., 2018). The segmentally repeated td neurons associate with specific tracheal tubules of each segment. These tracheal tubules are connected as part of an extensive and branched respiratory system. In 2nd and 3rd instar stage larva, air enters the tracheal system through functional spiracle openings, located near the head and tail (Hu and Castelli-Gair, 1999). The association of td dendrites with tracheal tubules hint that td neurons may sense tracheal status. However, the specific stimuli that are sensed by td neurons are not known.

The three major chemoreceptor families in *Drosophila* are the Gustatory Receptor (GR), Ionotropic Receptor (IR), and Olfactory Receptor (OR) families. Chemoreceptors from

these gene families are expressed and function in the gustatory and olfactory systems to allow animals to sample their external chemical environment (Joseph and Carlson, 2015). A number of genes in these families have been reported to be expressed in cells outside of the olfactory or gustatory systems, where their functions are not known (Montell, 2009; Park and Kwon, 2011a, b). We previously showed that td neurons express members of the GR and IR families. In addition, td neurons express two atypical soluble guanylyl cyclases, Gyc88E and Gyc89Db, which function as molecular O_2 sensors that respond to decreases in O_2 levels (Langlais et al., 2004; Morton, 2004). Altogether, these findings led us to hypothesize that td neurons may detect respiratory gas levels in the trachea.

The cellular and molecular basis of CO_2-sensing have been previously investigated in the olfactory system of adult and larval *Drosophila* (Faucher et al., 2006; Kwon et al., 2007). In the olfactory system, CO_2 is sensed by two receptors, Gr21a and Gr63a, which are co-expressed in specific external sensory neurons in both larva and adult. In addition, a population of gustatory neurons respond to aqueous and gaseous CO_2, but do not express or require Gr21a/63a (Fischler et al., 2007). Thus, additional unidentified molecules mediate CO_2 detection in *Drosophila*. Across mammalian taste, olfactory, and internal chemoreceptor systems, a common theme in the sensing of CO_2 is the involvement of carbonic anhydrase enzymes, which catalyse the conversion of CO_2 into bicarbonate ions and free protons (Black et al., 1971; Chandrashekar et al., 2009; Sun et al., 2009). Carbonic anhydrase enzymes in *Drosophila* have only recently been characterized (Syrjanen et al., 2013; Syrjanen et al., 2015) and it is not known if they are expressed in neurons or play a role in CO_2 sensing. Whether additional GRs, carbonic anhydrases, other molecules, or some combination of the above mediate CO_2 detection in *Drosophila* is not known.

Here, we used a recently developed calcium integrator tool CaMPARI2 (Fosque et al., 2015) to functionally image the response of all 13 td neurons to changes in O_2 and CO_2 levels.

Our results show that specific and partially overlapping subsets of td neurons are activated by changes in O_2 and CO_2 levels, as well as in conditions when gas exchange is impaired. Furthermore, we provide evidence that Gr28b mediates the response of td neurons to CO_2.

Td neurons detect decreases in O_2 level

The expression of molecular O_2 sensors Gyc-88E and Gyc-89Db in a subset of td neurons hint that they may detect O_2 levels. To assess td neuron activity *in vivo* in response to gaseous stimuli, we used CaMPARI2, a calcium integrator that undergoes permanent green-to-red photoconversion in the presence of high intracellular calcium and UV light. We used *elav-Gal4* to drive expression of *UAS-CaMPARI2LT* pan-neuronally. To measure neural responses to hypoxia, we placed third-instar larvae in a customized chamber and exposed the animals either to ingoing streams of air (21% O_2, 79% N_2, 0.04% CO_2) or 0% O_2 (100% inert N_2). During gas delivery (for 30 s or 1 min), we simultaneously applied UV light to enable CaMPARI2 photoconversion, ensuring that CaMPARI2 only captured neural activity during this time window (Figure 3.1A). We then dissected the larvae and imaged red and green fluorescence in all 13 td neurons for post hoc assessment of neural activity. When larvae were exposed to air, td neurons showed virtually no green-to-red photoconversion (Figure 3.1C), suggesting that td neurons are largely inactive in normoxic conditions. However, when larvae were exposed to 0% O_2, the A1 and A2 v′td2 neurons showed significantly higher red/green fluorescence ratio compared to controls, suggesting that these two specific td neurons were activated by hypoxia (Figure 3.1C-E).

Td neurons detect increases in CO_2 level

Given that a subset of td neurons detects decreases in O_2 level, we next tested whether td neurons also respond to changes in CO_2, the complementary product gas in cellular respiration. We exposed larvae to air and different concentrations of CO_2 for 30 s and quantified CaMPARI2 responses. While 10% CO_2 did not elicit responses in td neurons, 79% CO_2 (with O_2 held constant at atmospheric 21% levels) elicited responses in A1, A2, and A3 v′td2 neurons, and 100% CO_2 elicited the strongest responses in the same three neurons (Figure 3.2). Of these neurons, A1 and A2 v′td2 neurons also responded to decreases in O_2 (Figure 3.1), demonstrating an overlap in the neurons that detect decreases in O_2 and increase in CO_2. By contrast, the A3 v′td2 neuron was insensitive to low O_2 and responded specifically to high CO_2 level.

Td neurons are activated by prolonged submersion

Given that td neurons were activated by low O_2 and high CO_2 levels, we wondered whether td neurons may be activated in conditions where there is impaired gas exchange. In natural conditions, *Drosophila* larvae dig and dive into their surrounding substrate to search for food. However, if the substrate is too liquid, the low friction hampers their movement and prevents them from returning to the surface, resulting in asphyxiation and lethality (Kim et al., 2017). More generally, submersion in any liquid medium (e.g. rainwater) naturally inhibits gas exchange, resulting in low O_2 and accumulation of emitted CO_2 inside the animal over time. We hypothesized that submersion in liquid may be a natural stimulus that activates the gas-sensitive td neurons.

Here, we used CaMPARI2 to assess whether td neurons are activated when larvae are submerged underwater for a prolonged period of time. Previous studies have shown that when

oxygen is completely removed, *Drosophila* larvae survive and move for at least the first 40 min (Callier et al., 2015). To capture neural activity following prolonged (but non-fatal) submersion, we placed larvae underwater for up to 30 min and applied UV during the last 1 min to enable CaMPARI2 photoconversion (Figure 3.3A,B). As a control, we applied 1 min of UV to larvae during a short 1 min submersion. After 30 min of submersion, v′td2 neurons in segments A1-A3 showed significantly higher responses than controls (Figure 3.3C,D). Therefore, the same set of O_2- and CO_2-sensitive td neurons were also activated by prolonged submersion, suggesting that these td neurons may be activated when gas exchange becomes impaired in natural-like conditions.

We considered the possibility that CaMPARI2 responses may reflect calcium signals resulting from cell death (Zhivotovsky and Orrenius, 2011). However, the CaMPARI2 responses we observed for both gas stimuli and submersion were specific to a subset of td neurons and were absent from other td neurons. For example, A1-A3 v′td1 neurons, which are are directly adjacent to v′td2 neurons and likely exposed to similar internal gas levels, did not show CaMPARI2 responses to gaseous stimuli or prolonged submersion (Figure 3.3C,D). In summary, our results suggest prolonged submersion activates specific gas-sensitive td neurons.

Gas-sensitive td neurons express distinct chemosensory receptors

Previous embryonic *in situ* hybridization studies reported that the molecular oxygen sensors Gyc88E and Gyc89Db are expressed in A1 and A2 v′td2 neurons (Langlais et al., 2004). Here, we note that these same two td neurons respond to decreases in O_2 levels in third instar larvae (Figure 3.4). In addition, we previously showed that a number GR-GAL4 and IR-GAL4 reporters labelled td neurons (Qian et al., 2018). The functions of the specific combination of GRs and IRs that are expressed in td neurons are not known. Three td neurons

appear to detect CO_2 and also express a unique combination of three GRs (Gr28a, Gr28b.c, and Gr89a; Figure 3.4). Thus, the gas-sensitive td neuron cohort correlates with expression of specific chemosensory receptor genes, providing some initial candidates for assessing the molecular basis of O_2 and CO_2 detection in td neurons.

Evidence that Gr28b mediates responses to CO_2 in td neurons

As an initial effort to identify molecules that mediate the response of the td neurons to high CO_2, we focused on the three GRs (Gr28a, Gr28b.c, and Gr89a) that are co-expressed in all three CO_2-sensitive td neurons (Figure 3.4). To determine whether any of these GRs are necessary for td response to high CO_2, we measured the response of A1-A3 v′td2 neurons to 100% CO_2 in larvae with reduction or loss of Gr28a, Gr28b, or Gr89a function. Specifically, we crossed *elav-Gal4, UAS-CaMPARI2* flies to *UAS-RNAi* fly lines, or where available, examined CaMPARI2 responses in mutant backgrounds. We found that $Gr28a^1$ mutants and Gr89a RNAi knockdown animals showed largely normal responses to 100% CO_2. However, Gr28b RNAi knockdown (via 2 different RNAi lines) significantly reduced A1-A3 v′td2 neurons' response to 100% CO_2 (Figure 3.5). The A3 v′td2 showed the strongest reduction while A1 and A2 v′td2 showed more moderate reductions. The residual responses in A1 and A2 likely reflect their ability to still sense the hypoxia component of the 100% CO_2 treatment (i.e. decrease of O_2 from 21% to 0%). We observed a similar phenotype in *ΔGr28* deletion mutants lacking both Gr28a and Gr28b. Altogether, our results suggest that Gr28b mediates CO_2-induced responses in a subset of td neurons.

The Gr28b locus is complex and encodes five isoforms (a,b,c,d,e), each of which has a unique transcriptional start site and exon, joined to two common exons (Montell, 2013). Both of the Gr28b RNAi lines (TRiP and KK) that we used targets the common exons. A previous

study created GAL4 lines in which the promoter region immediately upstream of each isoform is fused to GAL4, then examined the expression pattern of all five Gr28b isoforms in larva (Thorne and Amrein, 2008). Consistent with our analyses, only the Gr28b.c-Gal4 reporter labels neurons that can now be identified as td neurons. Thus, the Gr28b reporter expressions suggest that the Gr28b.c isoform may mediate a response to high CO_2 levels.

Gr28b.c-Gal4 also labels td neurons that did not respond to CO_2 (Figure 3.2 and 2.4), suggesting Gr28b.c expression alone may not be sufficient for CO_2-sensitivity. We wondered whether co-expression of all three GRs that are expressed in CO_2-sensitive neurons are required to confer CO_2-sensitivity. To test this, we ectopically expressed Gr28a pan-neuronally, such that three additional td neurons (A4-A6 v′td2) now co-express Gr28a, Gr28b.c, and Gr89a. The resultant A4-A6 v′td2 neurons did not acquire responsiveness to CO_2, suggesting that additional factors beyond Gr28a and Gr89a are likely involved (Figure 3.6). Note that our ectopic expression experiments do not simply render the cells equal. A4-A6 v′td neurons express the three receptors plus their endogenous receptor Gr33a. Thus we cannot eliminate the possibility that Gr33a interferes with the effect of other receptors (Figure 3.4) (Delventhal and Carlson, 2016; Sung et al., 2017). Altogether, our results show that the Gr28b gene (possibly the C isoform) mediates response to CO_2 in td neurons. In addition, based on Gr28b.c-Gal4 reporter expression patterns, CO_2-sensitivity may also require the co-expression of additional unidentified factors.

We assessed whether GRs are involved in the detection of low O_2 levels. We did not observe any reduced response of A1 and A2 v′td2 neurons to hypoxia in Gr28a mutant, Gr28b and Gr89a RNAi knockdown conditions (Figure 3.7). We also performed preliminary studies to test the involvement of Gyc88E and Gyc89Db. We did not observe a significant decrease in CaMPARI2 response in Gyc88E and Gyc89Db RNAi knockdown conditions (n = 5; Figure 3.7). This was surprising given that Gyc88E and Gyc89Db are known to be oxygen sensors,

however these preliminary studies relied on a small sample size and reliance on single RNAi lines, so are not definitive with regard to the role of Gyc88E and Gyc89Db. Follow-up experiments in the future should be able to clarify whether Gyc88E and Gyc89Db mediate oxygen-sensing in td neurons.

Discussion

The sensory functions of td neurons were completely unknown. Here, we explored the responses of td neurons to gaseous stimuli and found that partially overlapping subsets of td neurons respond to a decrease in O_2 and increase in CO_2 levels. We also provide evidence that these neurons are activated by prolonged submersion underwater. Furthermore, we identified a possible role for Gr28b in mediating the response to increased CO_2.

We provide evidence of internal sensory neurons that respond to gaseous stimuli. Gas-sensing neurons in *Drosophila* had previously only been studied in the context of external sensory neurons with sensilla directed to the external environment. In *Drosophila* larvae, a pair of chemosensory neurons in the head terminal organ express Gr21a and Gr63a which together functions as CO_2 receptors. Ablation of these neurons abolish behavioral avoidance to 1% CO_2 (Faucher et al., 2006). While this pair of chemosensory neurons appear to account for the behavioral avoidance to CO_2, it was unclear whether other neurons in the larva also responded to gaseous stimuli. Here we show that three specific td neurons are activated by high CO_2 levels (79-100%). Surprisingly, we did not observe activation of td neurons with 10% CO_2, which is several orders of magnitude higher than the atmospheric CO_2 concentration of 0.04% (by way of comparison, exhaled breath of humans contains 5% CO_2 (Hibbard and Killard, 2011)). We consider three possibilities for why td neurons did not respond to 10% CO_2. First, our assay with CaMPARI2LT may not be sensitive enough to detect weaker activation of td neurons at

lower CO_2 concentrations. Second, the actual CO_2 concentrations in the fine tracheal branches associated with td neurons are not known both in natural conditions. It is possible that actual CO_2 concentrations in these tracheal branches can reach relatively high levels in the absence of efficient gas exchange. Third, carbon dioxide in water can undergo interconversion (catalysed by carbonic anhydrases) to form bicarbonate and a free proton (Guyenet and Bayliss, 2015). Thus, high CO_2 may be detected inside the body as increases in H^+ concentration (i.e. low pH). While td neurons respond to high CO_2, the precise mechanism of stimulus detection is unclear and it remains an open possibility that td neurons detect H^+ concentrations in equilibrium with CO_2 levels.

We provide initial evidence that Gr28b mediates the response of td neurons to high CO_2. Previous studies have identified CO_2-sensitive olfactory neurons in larva and adult, where detection is mediated by Gr21a/Gr63a (Faucher et al., 2006; Kwon et al., 2007). In addition, a population of gustatory neurons in the adult responded to aqueous and gas phase (10%-100%) CO_2 (Fischler et al., 2007). Unlike the olfactory neurons, these gustatory neurons lack Gr21a/63a expression and therefore must detect CO_2 through as yet unidentified receptors. Here, we report a population of CO_2-sensitive td neurons in larva that similarly lack Gr21a/63a expression, providing a new opportunity to investigate the molecular basis of CO_2 detection. We find that of the three GRs that are expressed in CO_2-sensitive td neurons, only loss of Gr28b function resulted in a decrease in the CO_2 response. The functions of most Gr28b isoforms - including Gr28b.c that is expressed in td neurons - are not known. A few studies have shown that Gr28b proteins appear have non-canonical roles as gustatory receptors. For example, the Gr28b.d isoform functions as a warmth sensor (Ni et al., 2013), and an unidentified Gr28b isoform functions as a photoreceptor (Xiang et al., 2010). Our results suggest that Gr28b.c mediates CO_2-detection, however it is unclear if Gr28b.c alone is sufficient to function as a receptor or whether CO_2-detection requires other factors to be co-expressed. Future studies that

ectopically express Gr28b.c and potential co-factors in other sensory neurons will be important for clarifying the full repertoire of GRs for CO_2-detection (Shim et al., 2015).

Out of the three td neurons that responded to increases in CO_2, two neurons also responded to decreases in O_2. The two O_2-sensing td neurons express molecular oxygen sensors soluble guanylyl cyclases Gyc88E and Gyc89Db. Previous studies have found that hypoxia induces a withdrawal behavior in which larva stop feeding and back out of the food, and that this behavior is mediated by soluble guanylyl cyclase expressing neurons (Vermehren-Schmaedick et al., 2010). It is not known if td neurons contribute to this escape behavior. Here, we identify sensory neurons associated with internal tracheal branches that respond to decreases in O_2. Since these tracheal neurons are situated more internally, they could be well-positioned to detect and elicit responses to dangerously low internal O_2 levels during prolonged diving into food (Kim et al., 2017), as compared to tail sensory neurons which could be more affected by ambient O_2 levels. Our demonstration that gas-sensitive td neurons are activated by prolonged submersion underwater provides one environmental context in which these neurons may normally be active. Another possibility is that td neurons may sense transient fluid-filling of trachea that occur during developmental transitions (e.g. moulting). Therefore, it would be interesting to investigate whether activity of td neurons modulate escape or surfacing behaviors, as well as molting progression.

Our imaging and anatomical results together show that CO_2- and O_2-sensitive td neurons project axons to the SEZ. Previous studies showed that olfactory CO_2-sensing neurons in the larva target the larval antennal lobe (Python and Stocker, 2002). Thus, internal and external CO_2-sensitive neurons may have different downstream functions. The brain regions that receive O_2 sensory input have not been identified in *Drosophila*. Our studies show that O_2-sensing td neurons (which are also sensitive to CO_2) target the SEZ. Both td neuron axons and gustatory sensory axons target the SEZ, raising the possibility that internal chemosensation and

gustation may have similar downstream effects. However, emerging connectomics data suggest that td neurons and gustatory sensory neurons are likely to primarily target distinct downstream populations in the SEZ (Schlegel et al., 2016). Furthermore, td neurons that project axons to the SEZ have additional postsynaptic targets in the VNC through *en passant* synapses (Chapter 4). Future studies that manipulate td neuron activity or that of their downstream CNS targets should provide insights into their behavioral or physiological functions.

Figure 3.1: A subset of td neurons detect decreases in O_2 level

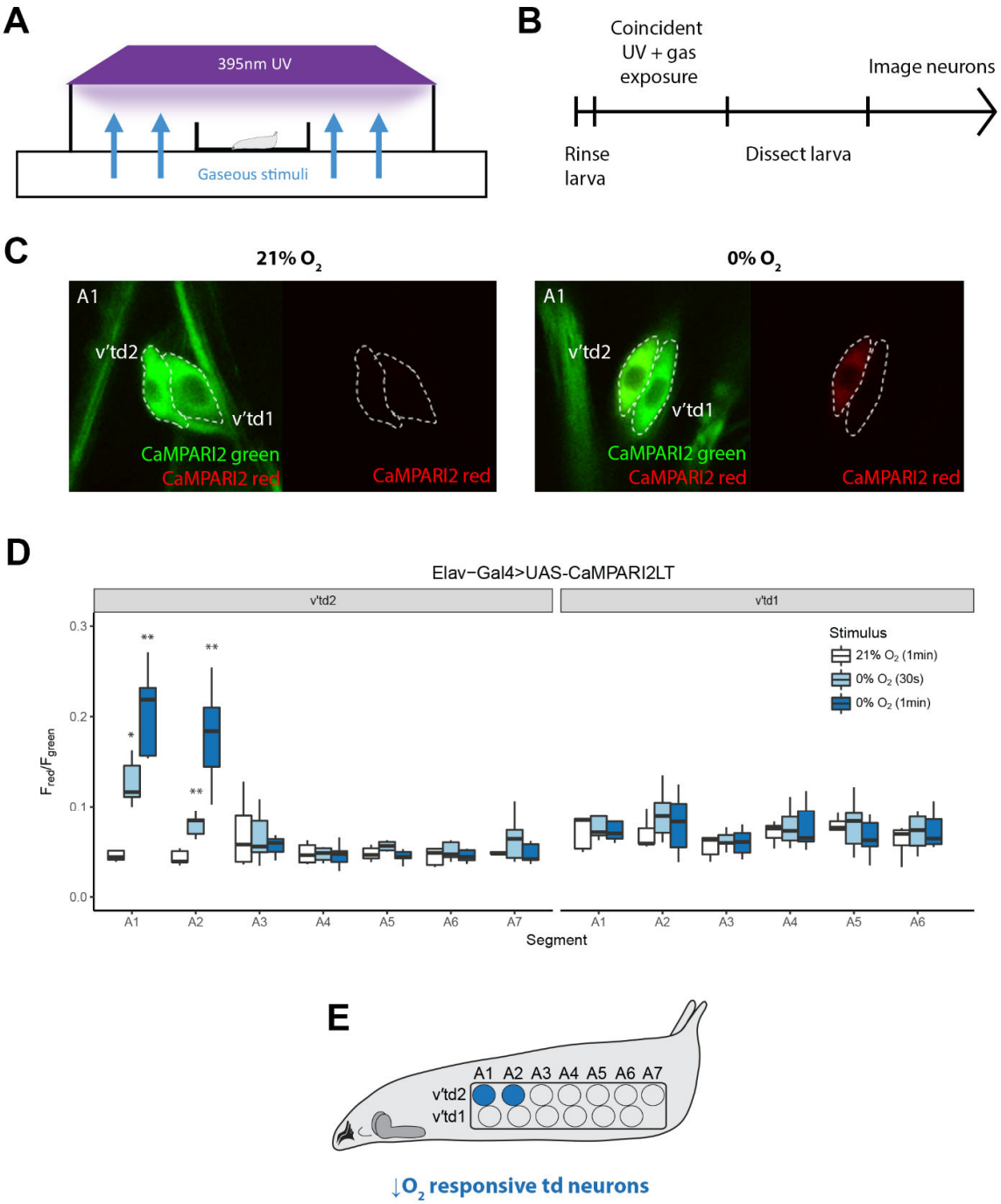

A, Schematic of gas-delivery apparatus. An individual larva is placed in the apparatus and simultaneously exposed to gaseous stimuli (from a FlyPad below) and UV for CaMPARI2 photoconversion (from above) for a set duration.

B, Protocol for post-hoc neural imaging of CaMPARI2 responses to gaseous stimuli.

C, Green and red CaMPARI2 fluorescence in A1 td neurons in response to hypoxia. Larvae that were exposed to 1 min of air (21% O_2) and UV showed little to no red CaMPARI2 fluorescence in this pair of td neurons. Larvae that were exposed to 1 min of hypoxia (0% O_2) and UV showed increased red CaMPARI2 fluorescence in the v′td2 neuron. CaMPARI2 was expressed pan-neuronally (*elav-Gal4>UAS-CaMPARI2LT*).

D, Quantification of red/green CaMPARI2 fluorescence in all 13 td neurons across segments A1-A7 in response to hypoxia. Two specific td neurons (v′td2 in A1 and A2) responded to 30 s and 1 min of hypoxia. n = 5-8 animals per condition.

E, Schematic showing the relative positions of the two oxygen-sensitive td neurons on the larva.

Figure 3.2: A subset of td neurons detect high CO_2 level

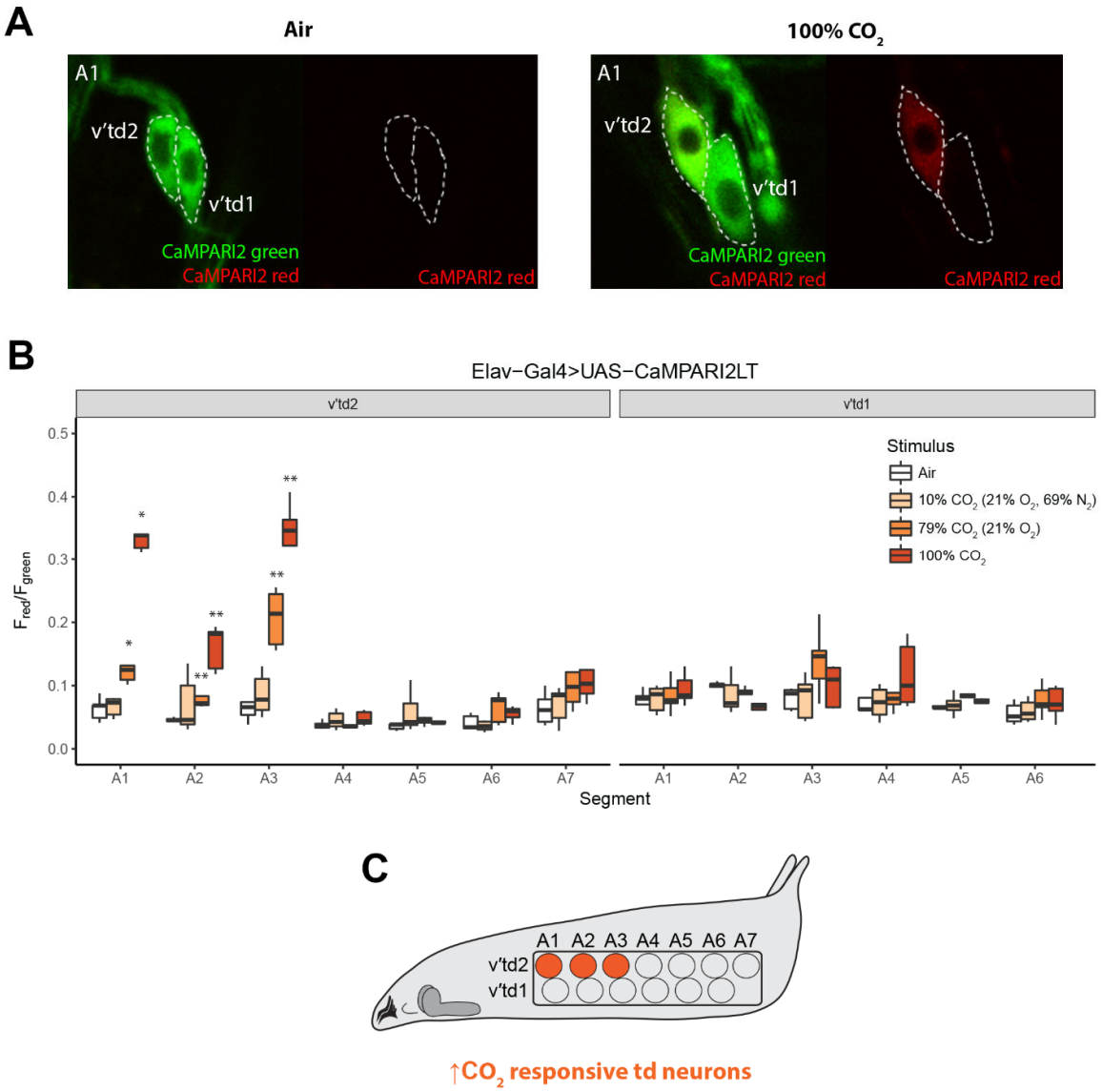

A, Green and red CaMPARI2 fluorescence in A1 td neurons in response to high CO_2. Larvae that were exposed to 30 s of air (~0.04% CO_2) and UV showed virtually no red CaMPARI2 fluorescence in this pair of td neurons. Larvae that were exposed to 30 s of 100% CO_2 and UV showed red CaMPARI2 fluorescence in the v′td2 neuron.

B, Quantification of red/green CaMPARI2 fluorescence in all 13 td neurons across segments A1-A7 in response to high CO_2. Three specific td neurons (v′td2 in A1, A2, and A3) responded to high CO_2 levels. n = 5-8 animals per condition.

C, Schematic showing the relative positions of the three carbon dioxide-sensitive td neurons on the larva.

Figure 3.3: Gas-sensitive td neurons are activated by prolonged submersion

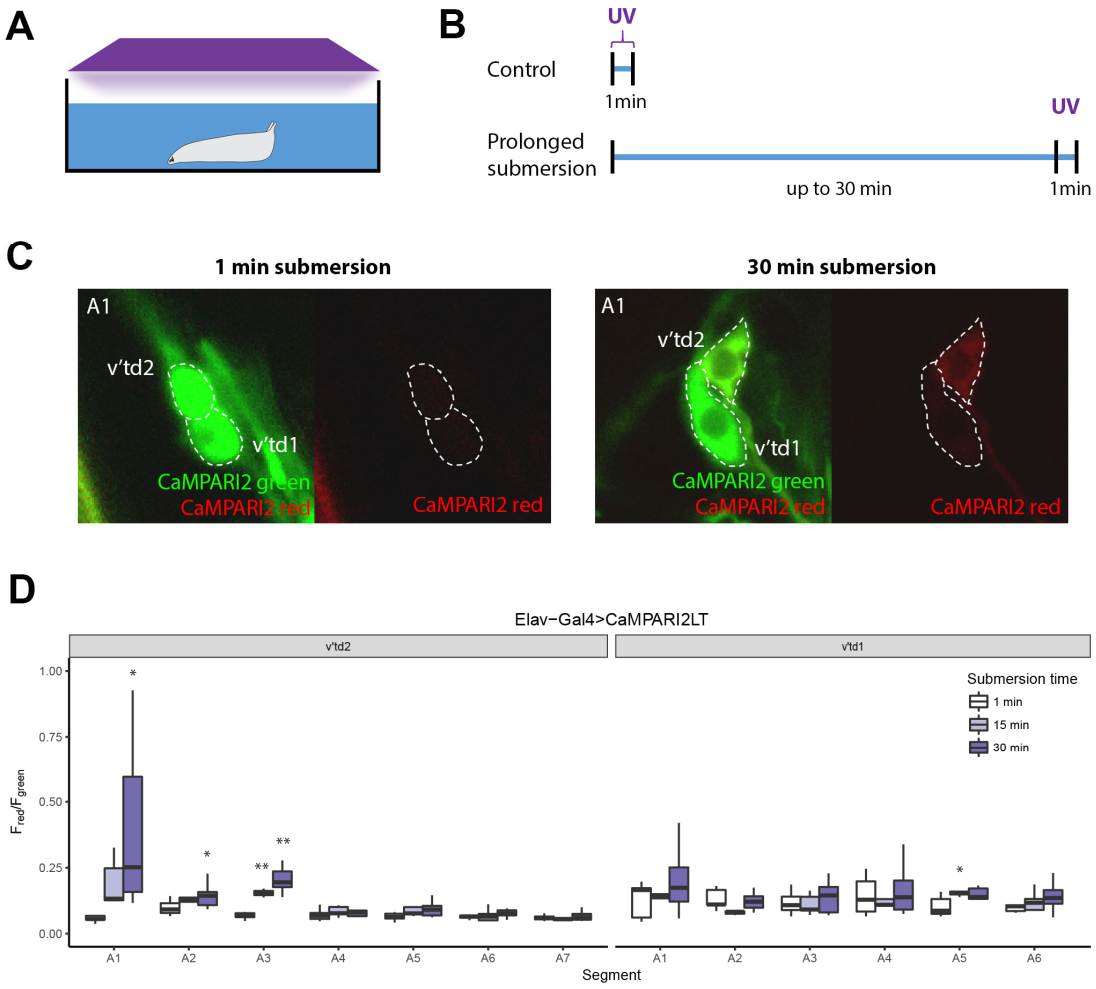

A, B, Schematic (**A**) and timeline (**B**) of submersion CaMPARI2 assay. UV light was applied to the larva for 1 min during a brief submersion (control) or at the end of a prolonged submersion (experimental).

C, Green and red CaMPARI2 fluorescence in A1 td neurons in response to prolonged submersion. Larvae that were submerged for a prolonged period of 30 min showed red CaMPARI2 fluorescence in the v′td2 neuron. n = 5-11 animals per condition.

D, Quantification of red/green CaMPARI2 fluorescence in all 13 td neurons across segments A1-A7 in response to submersion. The three gas-sensitive td neurons (v′td2 in A1, A2 and A3) were activated by 30 min of submersion underwater.

Figure 3.4: Gas-sensitive td neurons express distinct chemosensory receptors

	v'td2 neurons							v'td1 neurons					
	A1	A2	A3	A4	A5	A6	A7	A1	A2	A3	A4	A5	A6
Stimulus	O_2 CO_2	O_2 CO_2	CO_2										
Gyc88E *in situ**	+	+											
Gyc89Db *in situ**	+	+											
Gr28a-Gal4	+	+	+					+					
Gr28b.c-Gal4	+	+	+	+	+	+	+						
Gr33a-Gal4				+	+	+							
Gr89a-Gal4	+	+	+	+	+	+							
Ir56a-Gal4							+					+	+
Ir76b-Gal4									+	+	+	+	+

Top two rows: stimulus detected by td neurons. Remaining rows: expression of chemosensory receptors. Blue cells highlight expression that match O_2-sensitive td neurons. Orange cells highlight expression that partially match CO_2-sensitive td neurons. The combined expression of Gr28a, Gr28b.c, and Gr89a are unique to CO_2-sensitive td neurons.

*determined in embryo stage animals.

Figure 3.5: Td response to high CO_2 is mediated by Gr28b

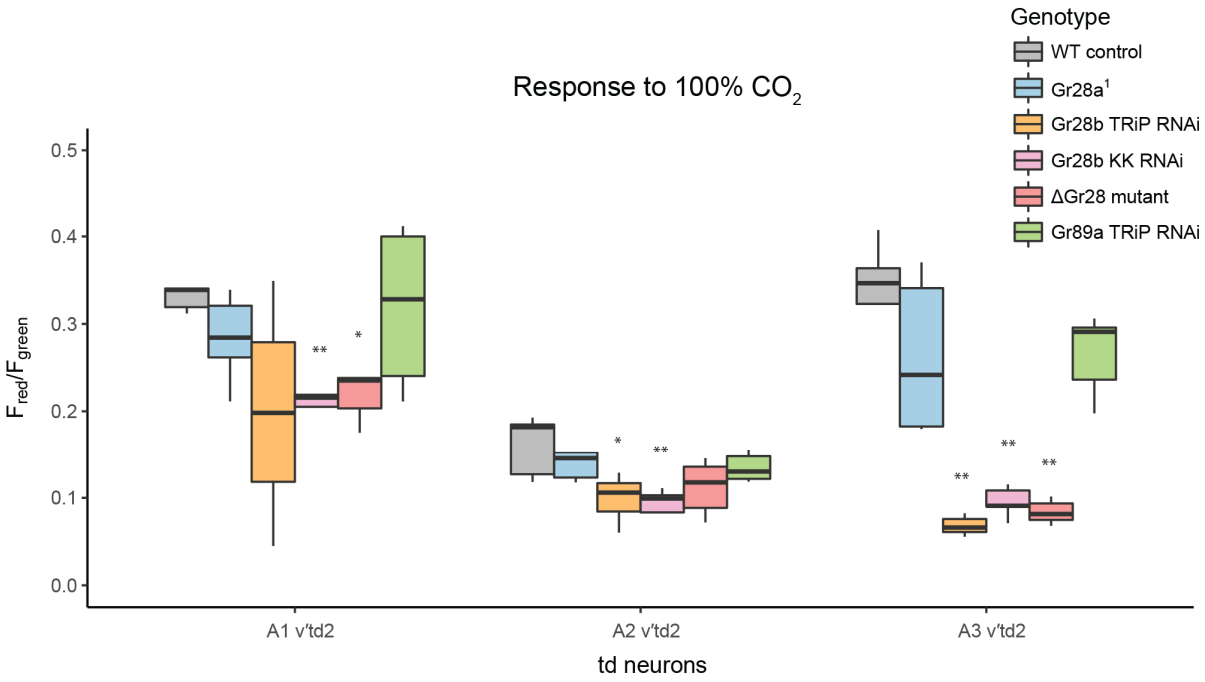

Quantification of red/green CaMPARI2 fluorescence in the three CO_2-sensitive td neurons in control and loss-of-function conditions in response to 30 s of 100% CO_2. RNAi knockdown of Gr28b decreased the response to high CO_2. n = 5 animals per condition.

Figure 3.6: Ectopic expression of Gr28a expression in Gr28b.c^{+}, Gr89a^{+} td neurons do not confer responsiveness to CO_2

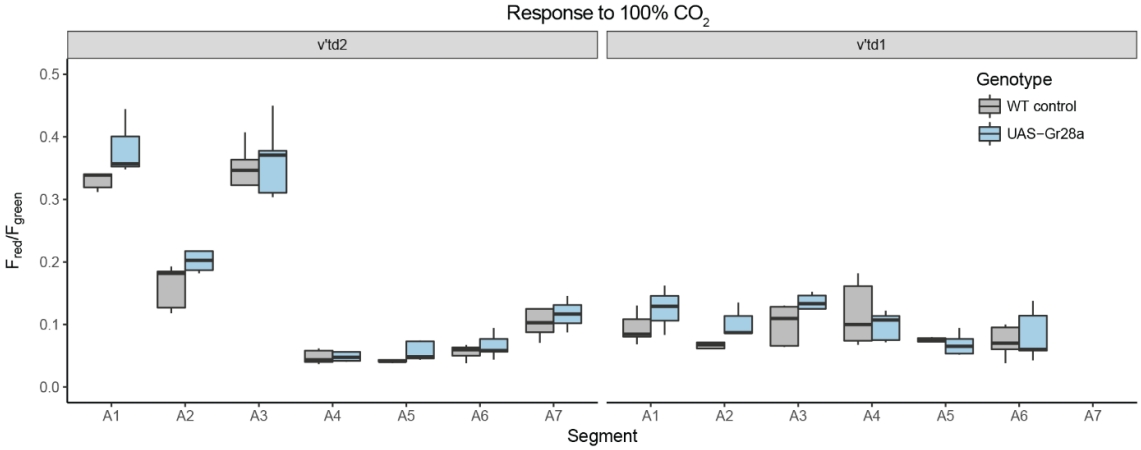

Quantification of red/green CaMPARI2 fluorescence all 13 td neurons in response to 30s of 100% CO_2 in control and pan-neuronal ectopic Gr28a expression conditions. v′td2 neurons in A4-A6 that acquire co-expression of $Gr28a^+$, $Gr28b.c^+$, $Gr89a^+$ do not show ectopic response to high CO_2. n = 5 animals for A2-A6, n = 3 for A1, n = 2 for A7.

Figure 3.7: Preliminary results of td response to low O_2 in chemosensory receptor loss-of-function conditions

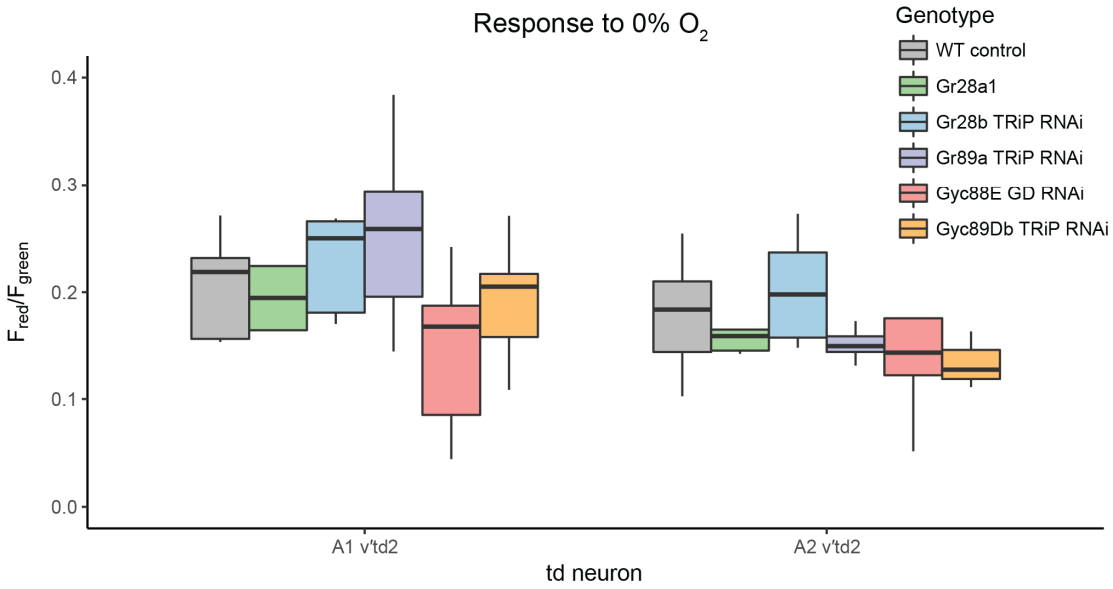

Quantification of red/green CaMPARI2 fluorescence in the two O_2-sensitive td neurons in control and loss-of-function conditions in response to 1 min of 0% O_2. Reduction in Gyc88E, Gyc89Db, and GR function did not significantly decrease response to low O_2. n = 5-6 animals per condition.

Chapter 4: Neural circuits downstream of tracheal sensory neurons

Abstract

The identity of CNS neural populations that receive and process information about internal physiological state is largely unknown in *Drosophila*. In *Drosophila* larvae, tracheal dendrite (td) sensory neurons innervate internal tracheal branches and have chemosensory functions. Td neurons project axons to the CNS to target the subesophageal zone (SEZ) and along a unique tract in the ventral nerve cord (VNC), but their postsynaptic partners are not known. Here, we used complementary confocal microscopy and electron microscopy (EM) methods to identify neurons downstream of the td neurons. We identify two populations of hormone-producing neurons as direct and indirect downstream targets of td neurons. We show that GPA2/GPB5 neurons in the VNC are postsynaptic partners of td neurons, and that DH44 neurons receive relayed td input in the SEZ. Our results are consistent with regulation of hormonal physiology by internal sensory neurons.

---

[*] I am grateful to Anita Burgos for her valuable contribution to the MCFO labelling data of this chapter. I would also like to thank the following people for EM neuron reconstructions: Philipp Schlegel, Ingrid Andrade, Julie Tran, Nusreen Imambocus, Anita Burgos, Maartin Zwart, Haluk Lacin, Akira Fushiki, Albert Cardona, Waleed Osman, Sebastian Huckesfeld, Nadia Riebli, Casey Schneider-Mizell, Atit Patel, Javier Valdes Aleman, Aref Arzan Zarin, Suguru Takagi, Laura Herren, Jim Truman, Anton Miroschnikow, Alex MacLachlan, and Hanbo Chen.

Introduction

Internal physiological state influences central nervous system function and behavior. Information about internal state is conveyed centrally by internal sensory neurons. Downstream, the central brain circuits through which visceral input affects specific behaviors and physiological responses are largely unclear. In mammals, internal sensory inputs are conveyed by vagal sensory neurons centrally to the nucleus of the solitary tract (NTS). The NTS is a heterogenous brain region with many neuronal types (Roman et al., 2016). Vagal input is relayed from the NTS to other brainstem nuclei and also through ascending pathways to a variety of limbic and cortical areas (Craig, 2003; McGovern et al., 2012; McGovern et al., 2015). The heterogeneity and complexity of mammalian nervous system presents a challenge to studying the specific neural circuits downstream of internal sensory input. Here, we use the simpler nervous system of *Drosophila* larva as a model for understanding the central circuitry downstream of internal sensing.

We previously showed that *Drosophila* internal tracheal dendrite (td) sensory axons project along a unique trajectory in the ventral nerve cord (VNC) separate from other sensory neurons (Qian et al., 2018). A majority of td neurons project axons beyond the VNC to target the subesophageal zone (SEZ), the brain region that receives gustatory sensory input. The postsynaptic targets of td neurons are almost completely unknown. Hugin is a neuropeptide that regulates feeding and locomotion (Schoofs et al., 2014). A recent electron microscopy (EM) study of the SEZ identified ascending sensory projections that synapse on a subset of Hugin neurons (Schlegel et al., 2016). These sensory projections likely arise from a subset of td neurons and converge on a different population of Hugin neurons in the SEZ compared to gustatory sensory axons. These results hinted that the td downstream circuitry in the SEZ diverges at least partially from the downstream circuitry of gustatory sensory neurons. Additional td downstream targets in the SEZ and VNC have not been identified.

Here, we used complementary confocal microscopy and EM methods to identify the neural circuitry downstream of td neurons. We show that td neurons, through direct and relayed pathways, connect to neurons that produce glycoprotein A2 and glycoprotein B5 (GPA2/GPB5) dimer hormone and Diuretic Hormone 44 (DH44). Interestingly GPA2/GPB5 and DH44 are involved in the regulation of water balance physiology. These results reveal neuroanatomical links through which tracheal sensory neurons could impact hormonal physiology, and provide a basis for future investigations into the functional td circuitry.

Identification of GPA2/GPB5 neurons as candidate downstream targets in the VNC

To identify post-synaptic targets of td sensory neurons, we screened through the InSITE GAL4 (Gohl et al., 2011) and Janelia GAL4/LexA (Jenett et al., 2012) collections for lines that sparsely label neuronal populations with processes that could overlap with td axons in the CNS. From this screen, we identified a population of VNC neurons labelled by the *0003-Gal4* InSITE line (Figure 4.1A). *0003-Gal4* labelled bilateral pairs of neurons in A1-A4 neuromeres of the VNC. These neurons extended processes in the VNC that appeared to take similar trajectories as td axons, and also extended processes out of the CNS to the periphery. We also identified a LexA line, *74C06-LexA*, that labels the same population of neurons, as demonstrated by overlap of expression in *0003-Gal4>mCherry, 74C06-LexA>GFP* animals (Figure 4.1B). We further investigated this population of neurons.

The location and morphology of the neurons labelled by *0003-Gal4* resembled neuroendocrine cells that produce GPA2/GPB5 dimer hormones (Sellami et al., 2011). These neuroendocrine cells are labelled by GPB5-Gal4. Dual labelling through *76C06-LexA>GFP, GPB5-Gal4>mCherry* showed that *74C06-LexA* and *GPB5-Gal4* label the same population of neurons (Figure 4.1C), demonstrating that the candidate target neurons are GPA2/GPB5 neuroendocrine neurons. The *Drosophila* larval and adult GPA2/GPB5 neurons had recently

been characterized morphologically, however their connectivity is unknown. Having identified the candidate targets as GPA/GPB5 neurons, we next assessed whether they are downstream of td sensory neurons.

Anatomical evidence for connectivity between td and GPA2/GPB5 neurons

To visualize the relationship between td sensory axons and GPA2/GPB5 neuron processes, we dually labelled the two populations using the td reporter, *0260-Gal4*>mCherry and *74C06-LexA>GFP*. GPA2/GPB5 neurons were closely associated with td axons for the entirety of their longitudinal projection, and they remained closely associated as they made similar dorsomedial and anterior turns (Figure 4.2A). These results show that td axons are located in close proximity with GPA2/GPB5 neuron processes, providing conditions for potential synaptic connections.

To investigate whether td neurons synapse with GPA2/GPB5 neurons, we used GRASP, a fluorescent labelling technique that detects potential synaptic connections. In this technique two complementary non-fluorescent fragments of the GFP protein (called spGFP1-10 and spGFP11) are differentially expressed in pre- and post-synaptic neurons. Specifically, we used a modified version of GRASP (Syb-GRASP) where spGFP1-10 is attached to the presynaptic protein synaptobrevin (SybSpGFP1-10), which is localized to presynaptic zones (Macpherson et al., 2015). If the neurons form an active synaptic pairing the GFP is reconstituted, giving rise to a fluorescent signal. We drove expression of SybSpGFP1-10 under the control of *0260-Gal4*, which expresses in both VNC- and a subset of SEZ-projecting td neurons; we drove expression of the complementary SpGFP11 fragment under the control of *74C06-LexA*. We observed reconstituted GRASP signal in the VNC resembling the pattern of

anatomical overlap between the two populations (Figure 4.2B), suggesting td sensory neurons synapse onto GPA2/GPB5 neuroendocrine neurons.

Further characterization of GPA2/GPB5 neurons

We used the stochastic cell labelling technique MCFO (Nern et al., 2015) to visualize individual GPA2/GPB5 neurons. Each GPA2/GPB5 neuron sends a process anteriorly in the ventrolateral neuropil tract (Figure 4.3A). Single-cell labeling indicted that not all GPA2/GPB5 processes extend anteriorly to the thoracic neuromeres. Those arising from more posterior neuromeres appear to terminate early, sometimes overlapping with the GPA2/GPB5 processes from more anterior neuromeres. These morphological characteristics enabled us to later identify these neurons in electron miscroscopy reconstructions.

GPA2/GPB5 neurons project axons to the periphery where the axons run over the surface of muscles (Sellami et al., 2011). There, GPA2/GPB5 hormones are thought to be secreted into the hemolymph. Because of the close association with muscles, we considered the possibility that GPA2/GPB5 neurons function as motor neurons, perhaps through the co-release of a classical neurotransmitter. All *Drosophila* motor neurons are glutamatergic (Daniels et al., 2008). We did not observe expression of the *Drosophila* vesicular glutamate transporter (Vglut) at GPA2/GPB5 terminals (Figure 4.3B). This result argues against a motor neuron function for GPA2/GPB5 neurons, and supports the idea that GPA2/GPB5 neurons serve primarily or solely neuroendocrine roles.

Td neurons do not connect to LK neurons

We identified another population of neuroendocrine neurons, the leukokinin (LK) cells, that extend longitudinal processes into the same tract as td axons and GPA2/GPB5 processes

(Sellami et al., 2011). LK neurons are single bilateral neurons present in A1-A7 VNC neuromeres, and are labelled by *LK-Gal4* (de Haro et al., 2010). Since their processes extend in the td axon tract, we wondered whether they might also be downstream targets. To perform dual-labelling and GRASP experiments, we converted the *0260-Gal4* enhancer trap into a LexA line (Gohl et al., 2011). The resultant *260-LexA* line gained expression in additional cells (class IV nociceptive sensory neurons and CNS neurons) but still labelled td neurons. Dual-color *260-LexA>GFP, LK-Gal4>mCherry* labelling showed that LK processes associate with td axons (Figure 4.4A). To determine if td neurons synapse onto LK neurons, we expressed the SybSpGFP1-10 fragment in td neurons under the control of *260-LexA*, and expressed the spGFP11 fragment under the control of *LK-Gal4*. We did not observe reconstituted GFP fluorescence (Figure 4.4B), suggesting that td neurons do not strongly synapse onto LK neurons. In contrast, when we used another variant of GRASP in which the both fragments are tethered to a membrane protein (CD4-SpGFP1-10), we observed reconstituted GFP resembling the pattern of anatomical overlap between the two populations (Figure 4.4C). Together, these results show that td neurons and LK neurons are close enough for cell-to-cell contact to be detected by non-synaptic GRASP methods, but that synapses appear not to form between these cell populations. However, because *260-LexA* does not label a subset of SEZ-projecting td neurons, we cannot rule out the possibility some td neurons could form *en passant* synapses with LK neurons. The labeling observed with the non-synaptic GRASP also supports the specificity of synapse specific GRASP, providing more confidence for the synapse-specific GRASP signal seen between td sensory axons and GPA2/GPB5 hormone-producing neurons.

DH44 dendrites innervate the SEZ and are in close proximity to td axons

To identify additional downstream targets of td neurons in the SEZ, we reviewed the literature in search of neurons that innervate the SEZ, where most td neurons ultimately target. In *Drosophila* adults, the SEZ is heavily innervated by DH44-hormone producing neurons (Dus et al., 2015). DH44 has been shown to regulate water balance, circadian rhythm and feeding (Cannell et al., 2016; Dus et al., 2015; King et al., 2017). We used *DH44-Gal4>GFP* to mark DH44 neurons and asked whether they similarly innervated the SEZ in larval stages. Similar to adults, larval brains also contained bilateral clusters of three DH44 neurons (Figure 4.5A). DH44 neurons extended processes to the SEZ in the brain and also out of the CNS to the ring gland, a major endocrine system (Schlegel et al., 2016). To determine whether DH44 processes in the SEZ are dendrites or axons, we expressed the dendritic marker DenMark (Nicolai et al., 2010) and the presynaptic marker BrpShort (Schmid et al., 2008) in DH44 neurons. DenMark was enriched in DH44 processes in the SEZ (Figure 4.5B), while BrpShort labelled DH44 processes target the ring gland (Figure 4.5C). Next, we co-labelled a subset of SEZ-projecting td neurons (using *31D10-LexA>GFP*) and the DH44 neurons (using *DH44-Gal4>mCherry*) to ask whether their SEZ processes overlap. We observed close association of td axons and DH44 dendrites (Figure 4.5D), hinting that DH44 may be downstream elements in the td circuitry.

Altogether, the results of our GAL4 screen and literature review led us to the conclusion that td sensory axons closely associate with the processes of two populations of hormone-producing neurons: GPA2/GPB5 neurons in the VNC, and DH44 neurons in the SEZ. We have provided GRASP evidence suggesting synaptic connectivity between td neurons and GPA2/GPB5 neurons. We lacked reagents to assess GRASP between all SEZ-targeting td axons and DH44 neurons (e.g. *31D10-LexA* only labels 3/9 of SEZ-projecting td neurons). Likewise, this candidate-based approach was unlikely to reveal all elements of td circuitry, so

we next used electron microscopy reconstructions to further assess connectivity downstream of td neurons.

Electron microscopy reconstruction of td neurons and downstream circuitry

To validate our findings and to elucidate the downstream circuitry more comprehensively, we collaborated with Albert Cardona's lab (Janelia Research Campus) to reconstruct td neurons and downstream targets using an electron microscopic (EM) volume of an entire 1st instar larval CNS (Figure 4.6) (Helmstaedter et al., 2011; Schneider-Mizell et al., 2016). The remotely-accessible neural circuit reconstruction software, CATMAID, allows a consortium of labs to participate in reconstruction simultaneously (Saalfeld et al., 2009). SEZ-targeting td axons in the CNS were previously reconstructed as part of an effort to reconstruct all the neurons upstream of Hugin neurons in the SEZ, but their identities were not known (Schlegel et al., 2016). Our anatomical characterization of all td neurons (Chapter 2) permitted annotation of these axon reconstructions as td neurons (Figure 4.7A). The remaining VNC-targeting td axons had not been reconstructed in the CNS. Therefore, we first focused on identifying and reconstructing the VNC-targeting td axons in the EM volume.

To find VNC-td axons in the EM volume, we began by reconstructing randomly chosen fragments in the ventrolateral bundle of processes in the VNC neuropil. From a subset of these fragments, we identified and reconstructed to completion the bilateral A4-A7 VNC-projecting td neurons (Figure 4.7B). The morphology EM-reconstructed td axons in the 1st instar largely match those seen in the 3rd instar stage (Qian et al., 2018). Consistent with our previous observation at the confocal microscopy level, td neuron presynaptic sites were distributed in an *en passant* manner along most of the length of the axon in the CNS (Figure 4.7).

We used the presynaptic sites of td axons as starting points for reconstructing the downstream post-synaptic connectome. Due to the collaborative nature of circuit reconstruction, most circuits were at least already partially reconstructed, particularly in the SEZ. Thus, we focused our efforts on reconstructing post-synaptic td targets in the VNC. We have partially reconstructed the VNC td connectome. To date, 84% of synapses of VNC-targeting td neurons and 57% of synapses of SEZ-targeting td neurons have been connected to a moderately completed downstream neuron (see Methods). We focused our connectivity analysis on downstream neurons with the highest number of synapses with td axons and present data on a subset of those targets here (Figure 4.8). Among the top hit targets are GPA2/GPB5 neurons, which receive direct and relayed input from both VNC- and SEZ-targeting td axons. SEZ-targeting td neurons provide strong input to a group of interneurons ("Thoracic to Brain", or TB neurons) that synapse onto to DH44 neurons. Thus, we have confirmed with EM that td neurons synapse directly (and via relays) onto GPA2/GPB5 neurons. We also show that td neuron provides relayed input to DH44 neurons.

The three different interneuron populations that relay td input to DH44 and GPA2/GPB5 output neurons are interconnected (Figure 4.8A). TB neurons receive input from the MP (Midline Projection) neurons and the NPF+pCC neurons, linking VNC td input to DH44 neurons in the SEZ. MP neurons provide input onto NPF+pCC neurons, and also provide feedback onto SEZ-projecting td neurons. Overall, this circuitry suggests the potential for additional modulation between td sensory input and DH44 or GPA2/GPB5 output.

Discussion

We investigated the td downstream circuitry using complementary confocal and EM reconstruction methods. We identified GPA2/GPB5 and DH44 neurohormone-producing

neurons downstream of td sensory neurons, providing a neuroanatomical basis for internal sensory neuron regulation of hormonal physiology.

We found td neurons provide strong sensory input to GPA2/GPB5-producing output neurons. The *Drosophila* GPA2/GPB5 dimer hormone was recently characterized and found to be expressed in a small number of CNS neurons that project axons out to the periphery (Sellami et al., 2011). GPA2/GPB5 function is physiologically important, as ablation of GPA2/GPB5 neurons or RNAi knockdown of GPB5 within these neurons caused embryonic/larval lethality (Sellami et al., 2011). The GPA2/GPB5 receptor Lgr1 is expressed mainly in water-transporting epithelia such as the hindgut, salivary gland, and Malpighian tubules (fly kidneys) (Vandersmissen et al., 2014). The axon terminals of GPA2/GPB5-producing neurons project peripherally over muscles and are positioned far from tissues where Lgr1 is expressed, suggesting that GPA2/GPB5 function is endocrine in nature (Sellami et al., 2011). GPA2/GPB5 has been suggested to function as an anti-diuretic, as inferred from loss-of-function phenotypes of its receptor. RNAi knockdown of Lgr1 in adult flies caused lethality in desiccated conditions, but not in wet conditions (Vandersmissen et al., 2014). Lgr1 knockdown also led to increased water intake (Rocco et al., 2017). These results are consistent with the idea Lgr1 activation normally increases water reuptake from the hindgut to prevent desiccation. The regulation of GPA2/GPB5 hormone release is not known. Here, we show that td axons synapse directly onto GPA2/GPB5-producing neurons, suggesting a hormonal reflex arc in which sensory input directly controls the release of hormones involved in fluid balance.

We also found that td neurons provide strong relayed input onto Diuretic Hormone 44 (DH44) neurons. As the name implies, DH44 is a diuretic that induces fluid secretion by the Malpighian tubules (Cannell et al., 2016; Zandawala et al., 2018). Interestingly, DH44 and GPA2/GPB5 hormones have opposing effects on fluid balance, promoting and limiting water loss respectively. Given that td input is relayed by TB interneurons to DH44 neurons, it is

unclear if the ultimate effect of td neurons on DH44 neurons is excitatory or inhibitory. In either case, td sensory input appears to be able to regulate two separate populations of output neurons in the VNC and the SEZ that controls fluid balance. In addition to fluid balance, DH44 have been reported to have a number of other functions in adult flies, including circadian rhythm and feeding (Dus et al., 2015; King et al., 2017). Furthermore, larval DH44 neurons project axon to the ring gland, the major larval endocrine organ analogous to the mammalian pituitary gland (De Velasco et al., 2004). Thus, in addition to endocrine functions of DH44 itself, DH44 neurons may also initiate hormone cascades in the ring gland, potentially leading to the release of hormones that regulate growth and moulting (Liu et al., 2018).

In mammals, internal sensory signals are first sent to the nucleus of the solitary tract (NTS) by the vagus nerve. From the NTS, information is relayed via direct and indirect pathways to the endocrine hypothalamus, which controls the release of hormones from the pituitary gland. (Rinaman, 2007; Ter Horst et al., 1989). The ability of vagal sensory neurons to affect pituitary hormone release has been functionally demonstrated through electrical or pharmacological stimulation of the vagus nerve (Rinaman, 2007). Here, we show that *Drosophila* td downstream circuitry similarly feeds into a major neuroendocrine center in the CNS (the median neurosecretory cells, to which DH44 belongs) neurons that target an endocrine organ. Furthermore, we observed a direct connection between td sensory neurons and hormone-producing output neurons (GPA2/GPB5 neurons). Thus, some aspects of the circuitry downstream of internal sensory neurons appear to be similar between mammals and *Drosophila*.

In Chapters 2 and 3 we identified GR expression and gas-sensing functions for a subset of td neurons. How these chemosensory inputs are processed in downstream circuits is unknown. Specifically, we found that v′td2 neurons in A1-A2 responded to low O_2 and v′td2 neurons in A1-A3 responded to high CO_2. We were not able to distinguish between v′td1 and

v′td2 axons in A1-A3 in EM, precluding analysis of downstream targets specific to this subset of gas-sensitive td neurons. The gas-responsive td neurons are SEZ-projecting, and SEZ-projecting td neurons as a group target GPA2/GPB5 neurons and DH44 neurons directly and indirectly. Assuming td neuron input onto GPA2/GPB5 and DH44 neuron are ultimately excitatory, why would td neurons induce both diuretic and anti-diuretic effectors? The co-release of diuretic and anti-diuretic hormones make physiological sense if the goal were not to eliminate water but to increase hemolymph filtration (Sellami et al., 2011). Diuretic hormones operate on the Malpighian tubule to increase urine production, while anti-diuretic hormones operate on the hindgut downstream of urine flow to reabsorb water and prevent desiccation (Johnson et al., 2005; Luan et al., 2015). In circumstances of internal chemical imbalances, td neurons may function to filter hemolymph contents to restore homeostasis (Denholm and Skaer, 2009). Excess CO_2 leads to high proton concentration, which lowers hemolymph pH (acidosis) (Tresguerres et al., 2010). One potential way to restore acid-base balance may be to excrete protons from the hemolymph into urine (Bertram and Wessing, 1994). In this scenario, td neurons may sense either high CO_2 or low pH itself, and elicit downstream physiological responses to increase hemolymph filtration to excrete protons in order to restore homeostasis. Although it is not known if td neurons detect other types of aversive stimuli, this td circuitry could in principle detect and promote the excretion of other excess harmful compounds present in the hemolymph. Currently, it is unclear how the sensing of low O_2 relates to a potential hemolymph filtration function. One possibility is that detection of low O_2 is a proxy for high CO_2 due to their inverse correlation (i.e. via cellular respiration). Future experiments that manipulate td activity and measure responses of the neurohormone populations and physiological responses should yield functional insights into this circuitry.

Figure 4.1: A population of candidate targets in the VNC are GPA2/GPB5 neurons

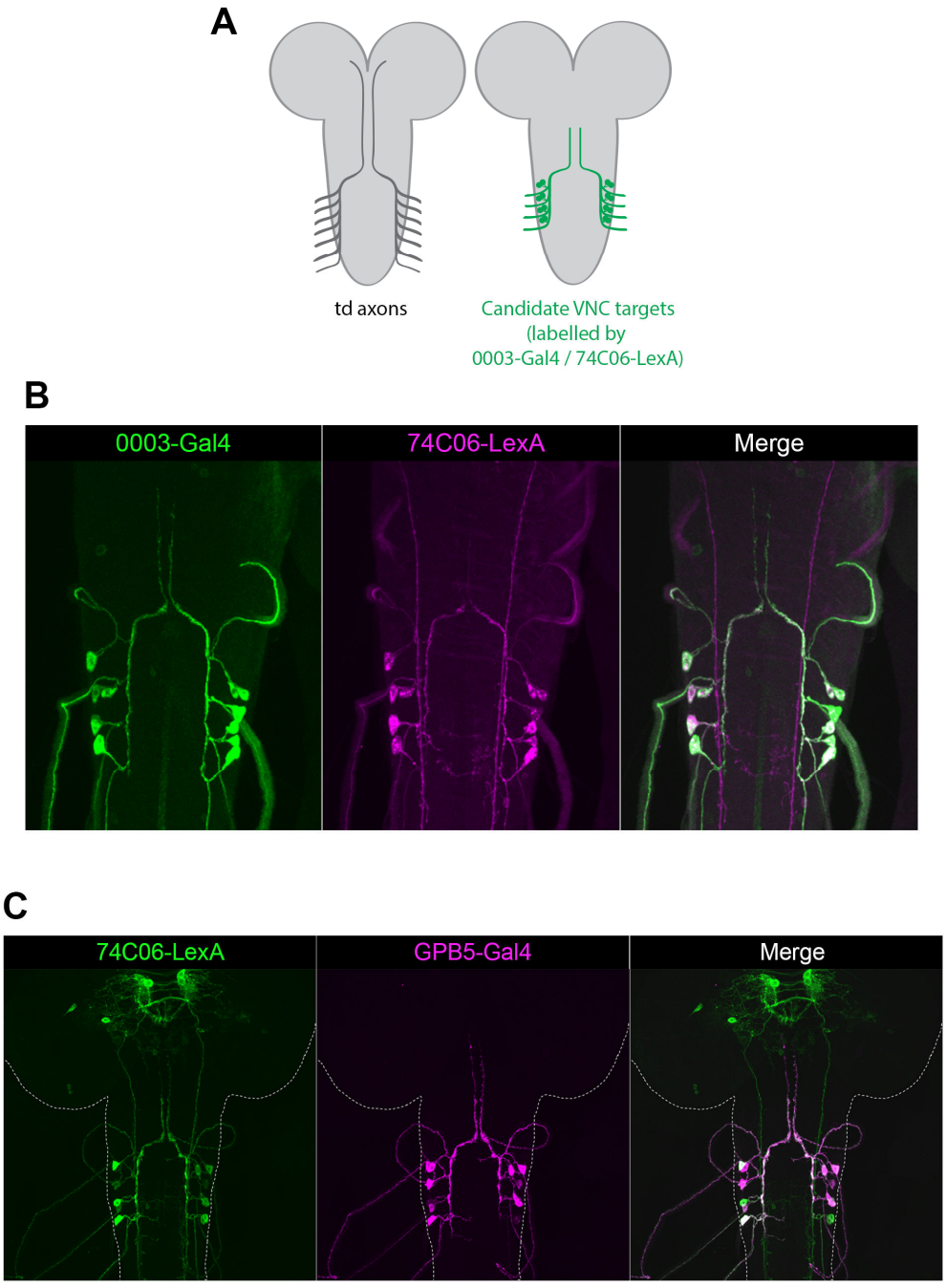

A, Schematic of CNS showing td axons (left) and candidate targets labelled by *0003-Gal4* and *74C06-LexA* (right).

B, Dual colour labelling of *0003-Gal4* and *74C06-LexA* show that they are expressed in the same bilateral pairs of neurons in A1-A4 neuromeres of the VNC. *74C06-LexA* labels additional cells in the brain (out of field of view) that extend processes down the VNC.

C, Dual-colour labelling shows candidate targets in VNC (labelled by *74C06-LexA*) are GPA2/GPB5 neurons (as labelled by *GPB5-Gal4*). Dashed lines outline the CNS.

Figure 4.2: Anatomical evidence for connectivity between td and GPA2/B5 neurons

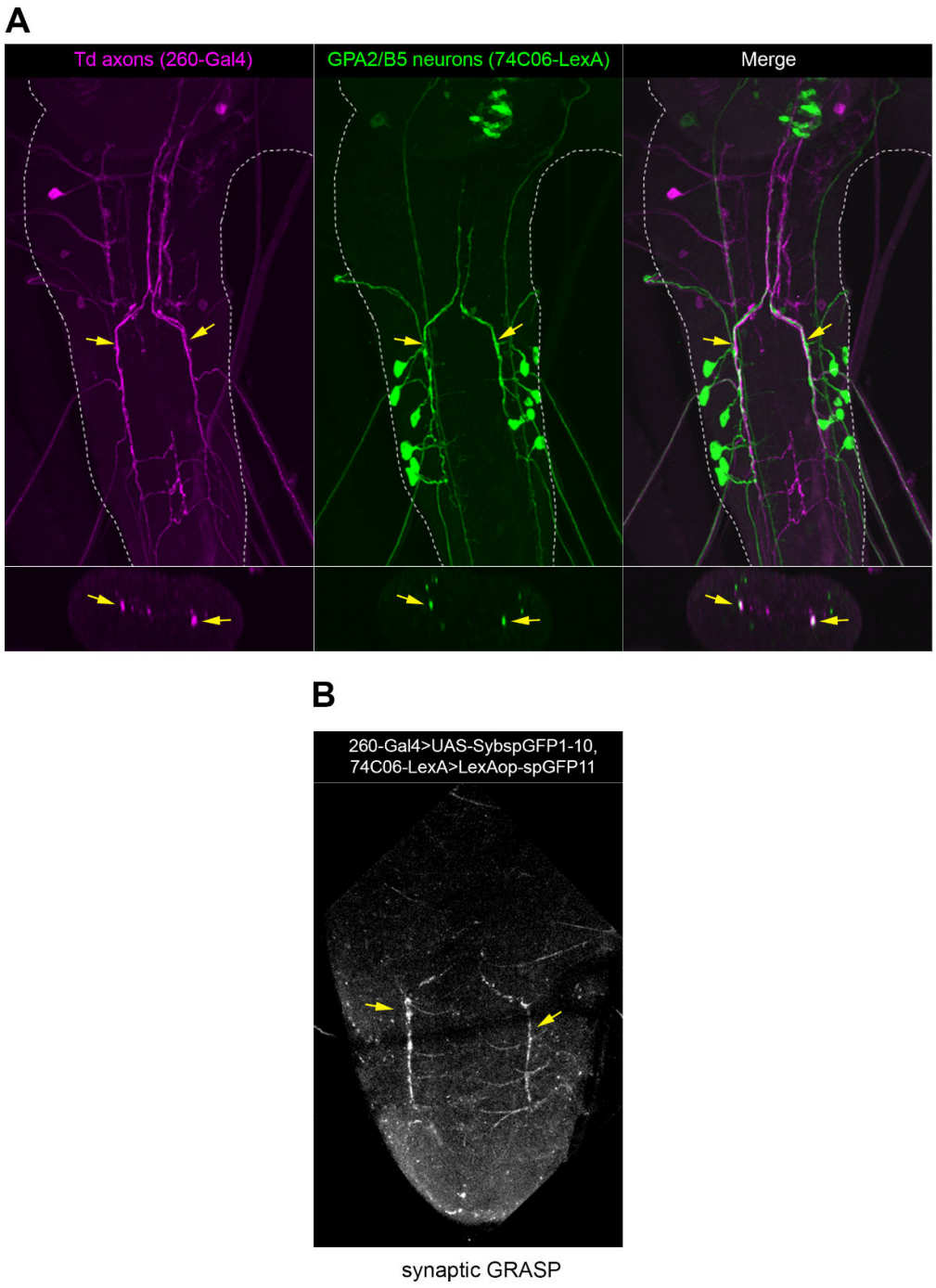

A, Td axons are closely associated with GPA2/GPB5 neuron processes, as shown by co-labelling of *260-Gal4>mCherry, 74C06-LexA>GFP*. Bottom panel shows orthogonal view. Arrows point to an example of an area where td axons and GPA2/GPB5 neuron processes overlap, in the same location for top and bottom panels.

B, Synaptic GRASP signal between td neurons (expressing the SybspGFP1-10 fragment) and GPA2/GPB5 neurons (expressing the spGFP11 fragment) in the VNC.

Figure 4.3: Further characterization of GPA2/GPB5 neurons

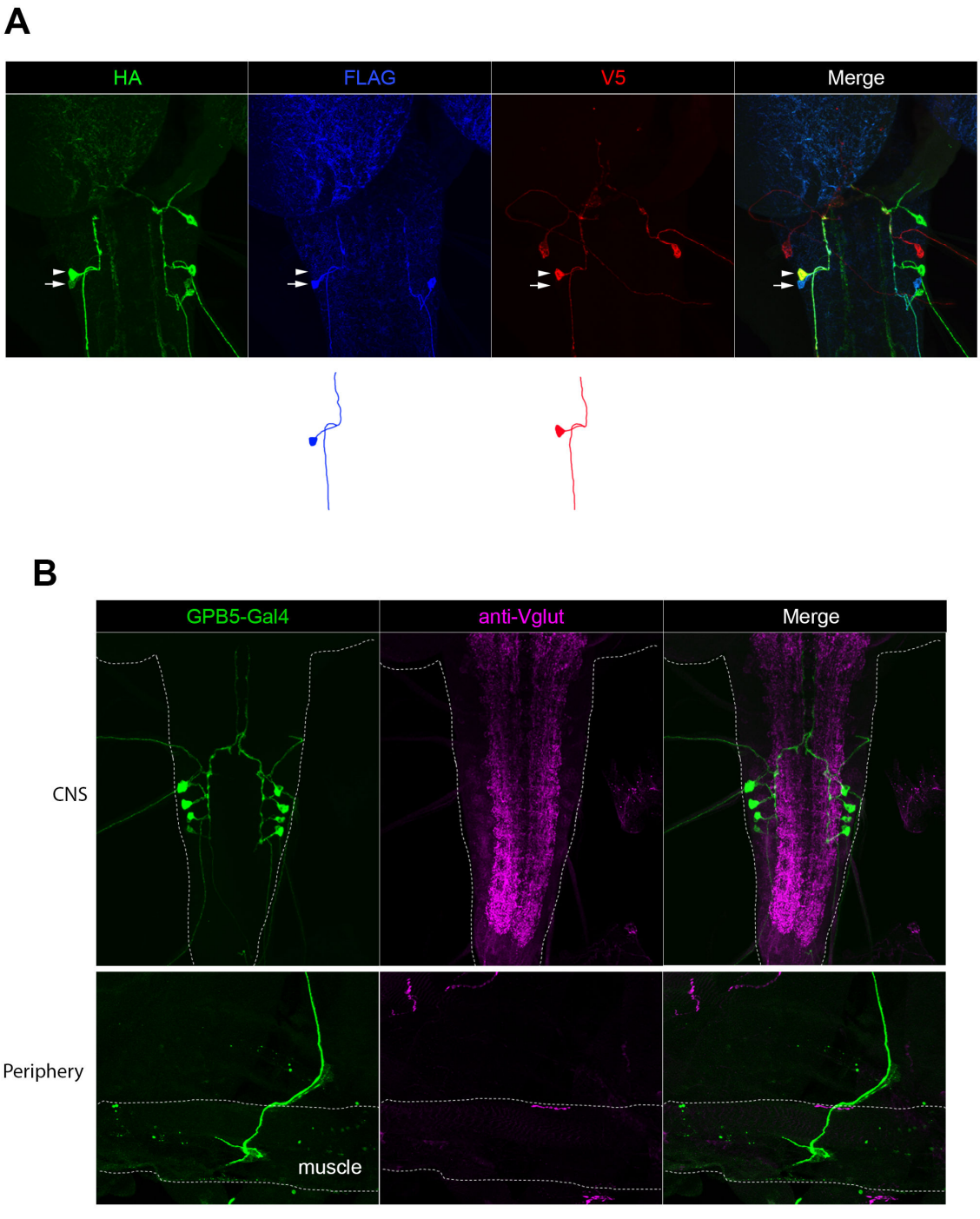

A, MCFO labelling of GPA2/GPB5 neurons with separated channels showing the HA, VLAG, and V5 epitope tags and merged image. Arrowhead and arrow show a pair of differentially labelled neurons. Tracings are shown below. *GPB5-Gal4>UAS-MCFO* animals were used.

B, Images of GPA2/GPB5 neurons in the CNS (top) and axon terminals in the periphery (bottom). GPA2/GPB5 neurons do not express Vglut, suggesting they are not glutamatergic motor neurons.

Figure 4.4: Lack of synaptic GRASP signal between td neurons and LK neurons

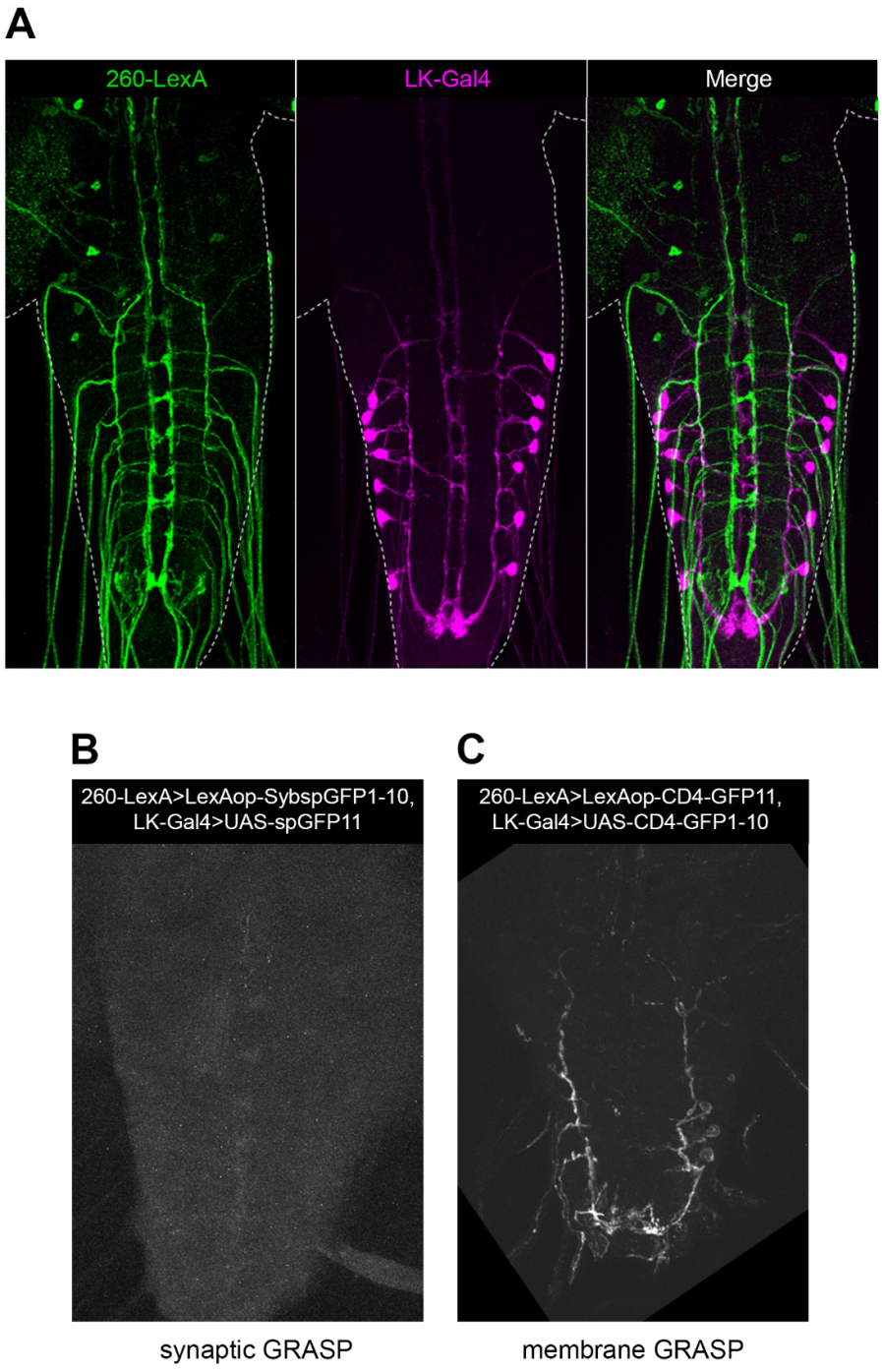

A, Td axons are closely associated with LK neuron processes, as shown by co-labelling of *260-LexA>GFP, LK-Gal4>mCherry*.

B, Lack of synaptic GRASP signal between *260-LexA*$^{+}$ td neurons (expressing the SybspGFP1-10 fragment) and LK neurons (expressing the spGFP11 fragment) in the VNC.

C, Membrane GRASP signal between *260-LexA*$^{+}$ td neurons (expressing the CD4-spGFP11 fragment) and LK neurons (expressing the CD4-spGFP1-10 fragment) in the VNC.

Figure 4.5: DH44 dendrites innervate the SEZ and are in close proximity to td axons

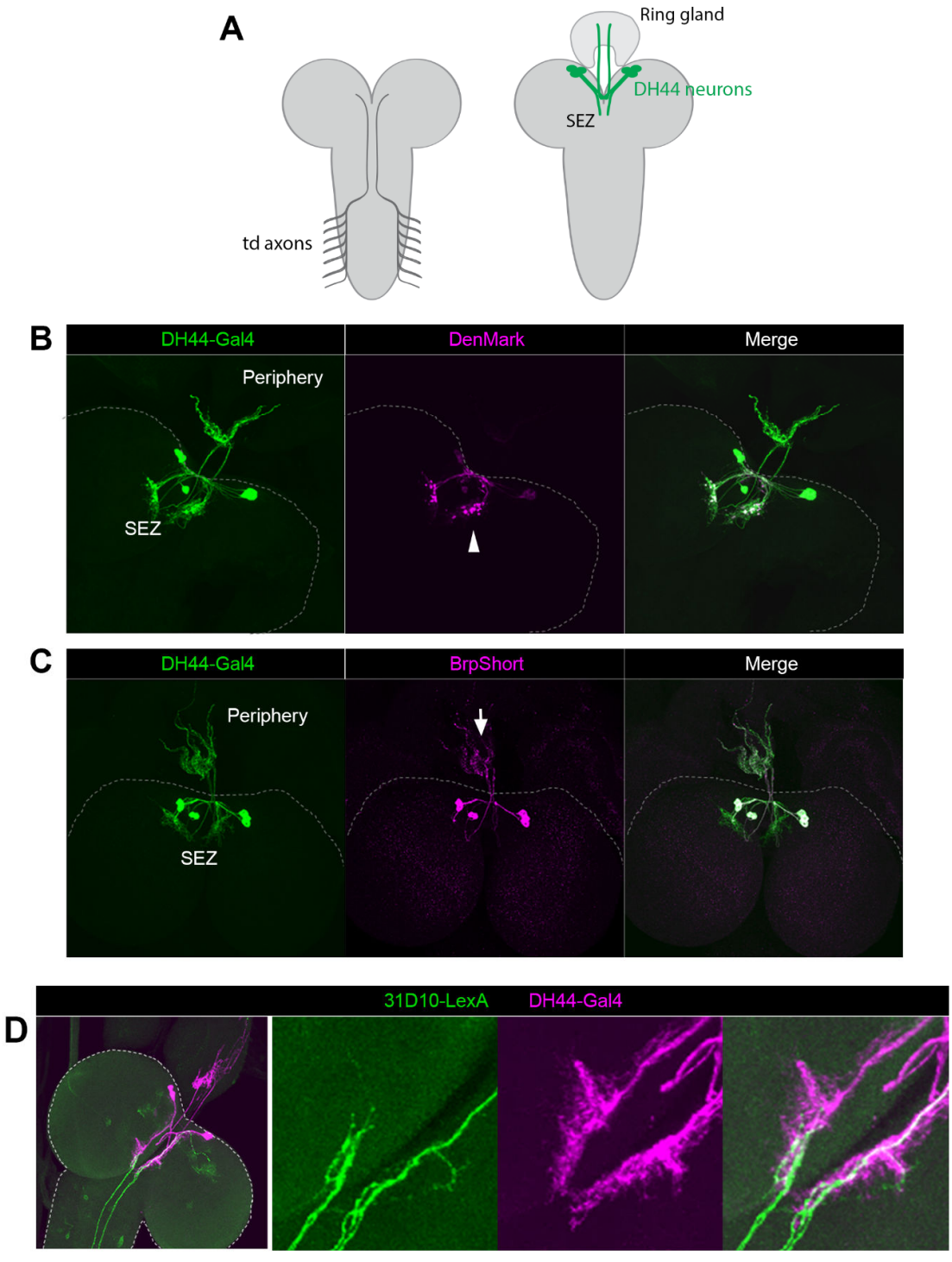

A, Schematic of CNS showing td axons (left) and DH44 neurons (right).

B, The dendritic marker DenMark in DH44 neurons are localized to processes in the SEZ.

C, The presynaptic marker BrpShort in DH44 neurons are localized to processes in the periphery.

D, Td axons are closely associated with DH44 dendrites, as shown by co-labelling of *31D10-LexA>GFP, DH44-Gal4>mCherry*.

Figure 4.6: EM reconstruction of neural circuits

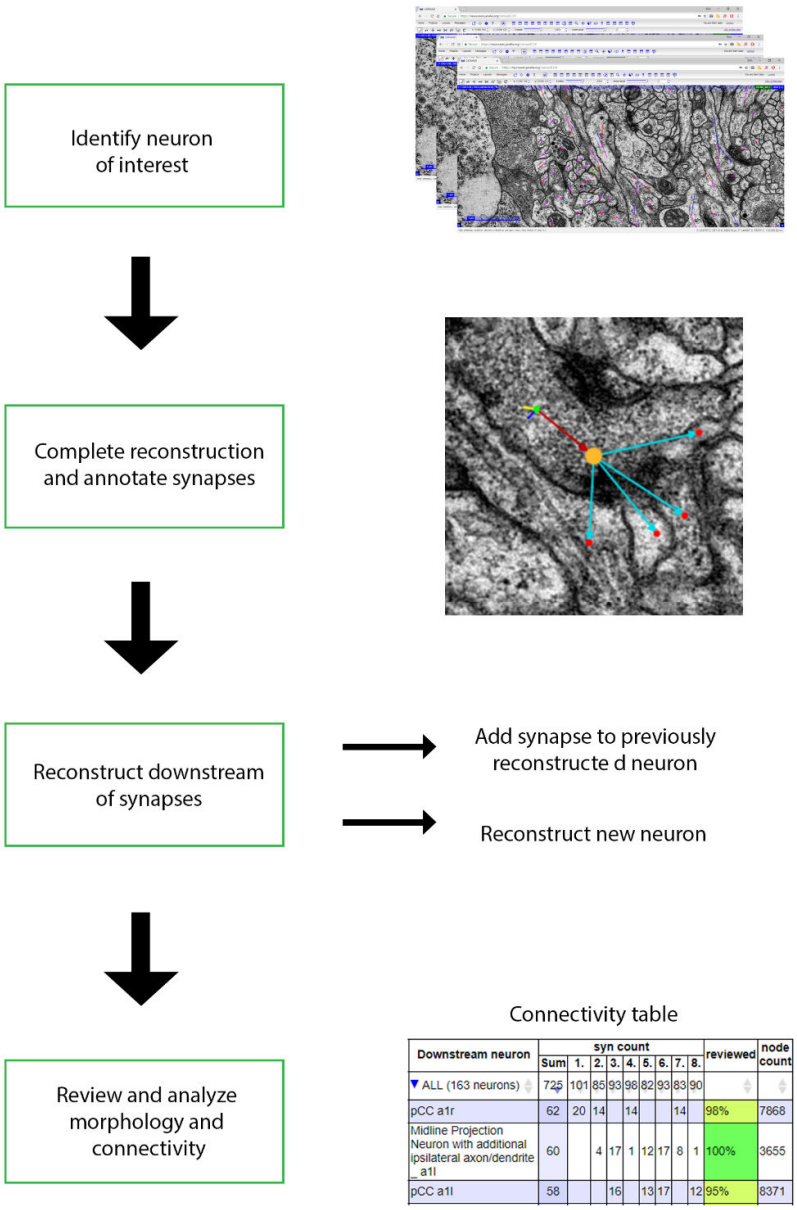

Workflow of neural reconstruction using the CATMAID software

Figure 4.7: EM reconstruction of td axons

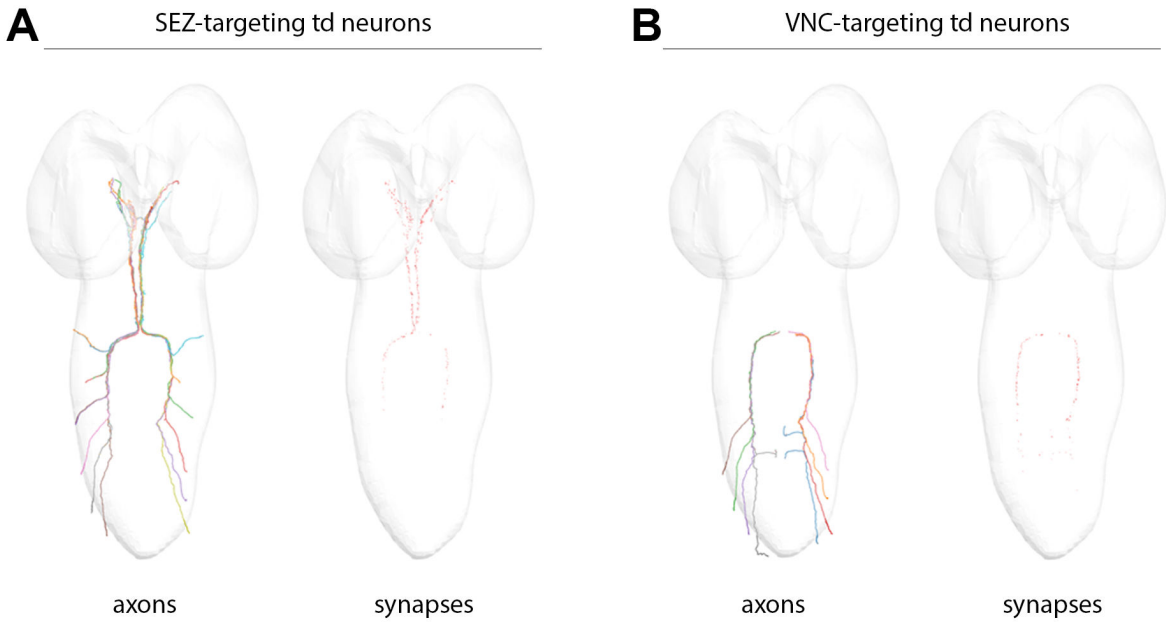

A, Axons and presynaptic sites of all SEZ-projecting td neurons (except for the right side A2 and A3 td).

B, Axons and presynaptic sites of all VNC-projecting td neurons.

Figure 4 8: EM reconstruction of td downstream targets

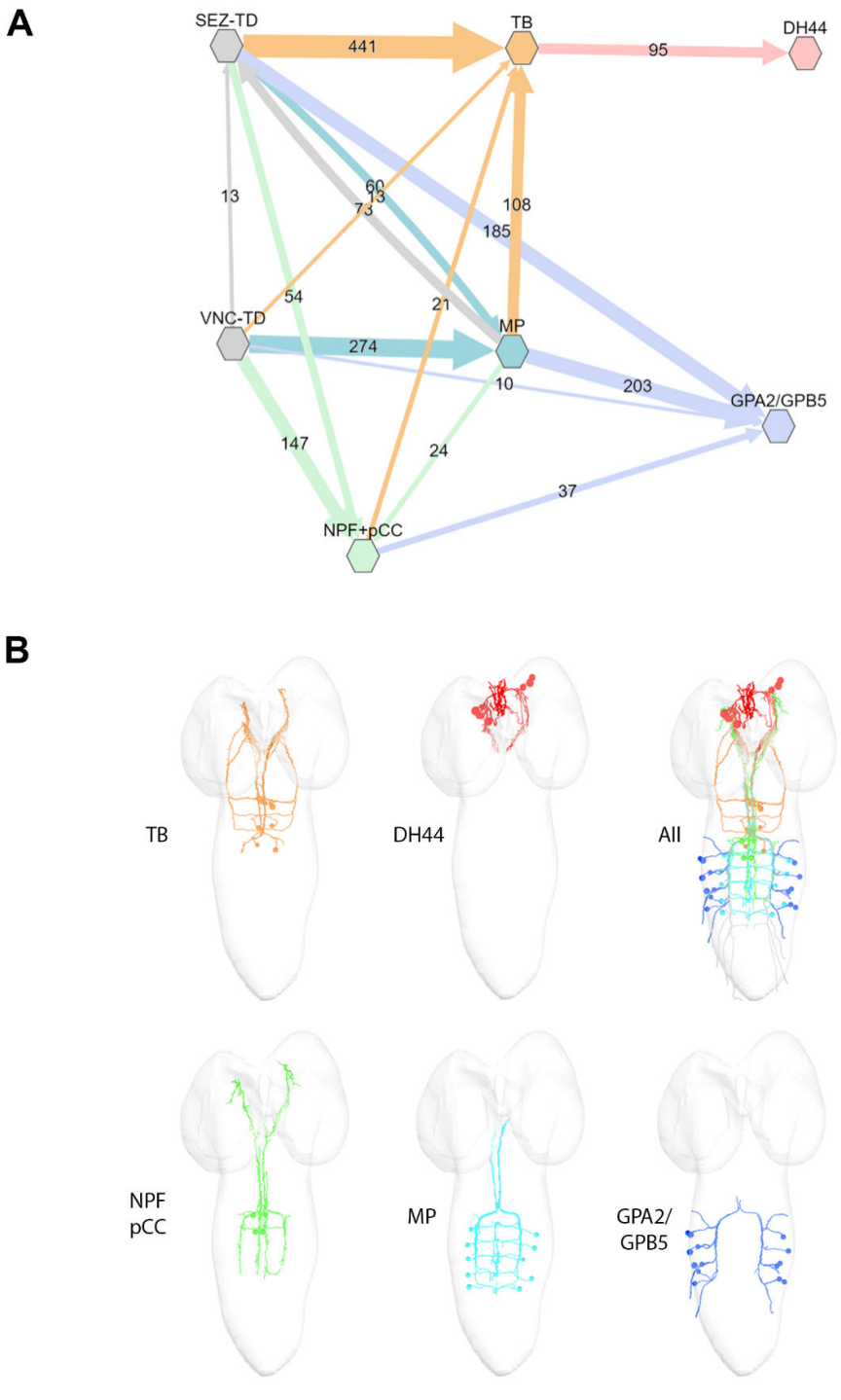

A, Connectivity between td and downstream targets. Each node presents a population of neurons with similar cell body location and morphology. Arrows represent synaptic connections, with size of arrow reflecting the number of synapses (numbers are also shown on top of arrows). Arrows are coloured by the postsynaptic target. Intragroup synapses are omitted. Arrows with less than 10 synapses are omitted.

B, EM reconstruction of downstream target neurons. Top right: overlay of all downstream targets with td axons in grey.

Chapter 5: Conclusions and future directions

The finding presented in this thesis represent my efforts to characterize the cellular and molecular organization, sensory functions, and downstream circuitry of internal tracheal sensory neurons in *Drosophila*. As an entry point, I characterized larval tracheal dendrite (td) neurons to reveal distinct subtypes of td neurons with different chemosensory receptor expression and central axon projections. I found that td neurons comprise two classes with similar dendrite morphologies but divergent axon projections to the VNC or the SEZ. Using a candidate gene approach that built on enhancer trap expression, I show that td axon projections to the SEZ are regulated by the POU-homeodomain transcription factor Pdm3. The projection of td axons to the SEZ (the primary gustatory brain region) and the expression of chemosensory receptors led us to investigate potential chemosensory functions for td neurons. As a result, I found that overlapping subsets of td neurons are activated by decrease in O_2 and increase in CO_2 levels. I assessed the roles of chemosensory receptor genes that are expressed in td neurons in mediating responses to O_2 and CO_2. From this work, I identified Gr28b as a putative mediator of td responses to CO_2, thus uncovering a molecular mediator for novel chemosensory functions in td neurons. To provide insights into the neural circuitry downstream of td neurons, I used complementary confocal microscopy and EM methods and identified neurohormone populations as direct and indirect central targets of td neurons, providing a neuroanatomical basis for internal sensory neuron regulation of neurohormone release. These circuit mapping findings may help guide future experiments for studying the physiological and behavioral functions of the td circuitry.

The findings in this thesis open up a number of new avenues for further investigations. Here, I will discuss some of the immediate questions raised by our studies.

Development

I demonstrated that td axon projection and chemosensory receptor expression is regulated by Pdm3. Ectopic Pdm3 expression in VNC-projecting td neurons suppressed VNC-specific gustatory receptor expression and promoted axon projection to the SEZ. However, loss of Pdm3 function did not cause SEZ-projecting td neurons to show altered chemosensory receptor expression or to revert to VNC-projecting td type. These results suggest that there are redundant factors that determine SEZ versus VNC axon projection identity. Based on expression pattern, I ruled out the remaining *Drosophila* POU proteins as possible factors, suggesting that other unrelated proteins help to generate subtype diversity within td neurons. My strategy for identifying candidate regulators of td diversity involved screening expression patterns of enhancer trap lines. I was thus limited by the availability and accuracy of enhancer trap lines. Now that td subtypes and GAL4 lines to label td subsets have been identified, it may be useful to perform single cell RNA sequencing (Iyer and Cox, 2010; Li et al., 2017) to profile the transcriptome of individual or subsets of td neurons in order to identify additional molecules that mediate td development and sensory function. For example, the td neuron transcriptomes would be useful for identifying differentially expressed transcriptional regulators that determine axon or chemoreceptor subtype identity, cell-surface molecules (perhaps including those downstream of Pdm3) that control axon growth to the SEZ versus the VNC, and new chemosensory receptor genes that may mediate td sensory functions.

Sensory functions

I showed that a defined subset of td neurons responds to changes in respiratory gas levels. Specifically, three SEZ-projecting td neurons responded to high CO_2 levels, and two of these neurons also responded to low O_2 levels. My results do not differentiate between detection of molecular CO_2 versus detection of dissociated ions of carbonic acid (i.e.

bicarbonate and protons), as is the case for mammalian CO_2 sensors. Future experiments that inhibit the function of carbonic anhydrase enzymes (Francis et al., 2016) to block the interconversion between aqueous CO_2 and carbonic acid may be able to provide insight into the exact nature of sensory detection. Furthermore, the CaMPARI2 imaging method was used so that I could apply gaseous stimuli to larvae and image recorded neural activity post-hoc without movement artefacts. However, CaMPARI2 imaging results do not provide temporal information about the td neural activity during gas stimuli application. Furthermore, CaMPARI2 may be less sensitive than other neural activity imaging methods such as GCaMP6, which can detect single action potentials (Chen et al., 2013). This may partly explain why a very high level of CO_2 was needed to elicit responses from td neurons. To improve on these aspects, it may be advantageous to use recently developed SCAPE imaging (Bouchard et al., 2015), which may allow fast volumetric imaging of moving larvae that express GCaMP6 in neurons, in order to better understand td neural activity dynamics.

My results show that response to high CO_2 is mediated by Gr28b, as demonstrated by loss-of-function manipulations. Some ambiguities remain in interpreting how Gr28b functions. Based on GAL4 reporter lines, only the Gr28b.c isoform is expressed in td neurons. However, Gr28b.c is apparently expressed in td neurons that did not show response to CO_2. Thus, either Gr28b.c function requires other co-factors that are expressed in the gas-sensitive subset of td neurons, or the GAL4 reporter lines do not accurately report expression (e.g. if in fact Gr28b.c is only expressed in the CO_2-responsive td neurons there would be no discrepancy). One way to address the latter possibility would be to explicitly misexpress Gr28b.c in non-gas responsive td neurons and assess whether this confers responsiveness to CO_2. I have tested one combination of apparently co-expressed GRs (Gr28a, Gr28b.c, and Gr89a) and found that this combination did not confer td neurons with the ability to respond to CO_2. However, I cannot rule out the possibility that Gr33a expression in these neurons inhibit CO_2 response. As

mentioned above, profiling of td neurons may help identify the full complement of genes that are expressed in subsets of td neurons and that are required for the response to CO_2.

The sensory function of the majority of td neurons remains unknown. Each td neuron expresses at least one GR or IR, hinting they could all have chemosensory functions. An important next step is to identify the sensory stimuli for the other td neurons. Aside from the tracheal lumen, from which respiratory gases may be detected, td dendrites are surrounded by hemolymph, the equivalent to blood in insects. Thus, in addition to gaseous stimuli, td neurons may also be sensitive to circulating compounds in the hemolymph. In particular, recent studies in gustatory neurons have demonstrated sensory functions for certain chemosensory receptors that are also found in td neurons. For example, Ir76b mediates salt sensing (Ganguly et al., 2017) and Gr28 genes mediate sensing of ribose, ribonucleosides, and RNA (Mishra et al., 2018). It will be of great interest to test if these stimuli are also detected internally by td neurons and whether td neurons use shared molecular mechanisms for internal chemosensation.

Behavioral and physiological functions

The results of this thesis have established a foundation for studying the td sensory system. A major next step will be to investigate the behavioral or physiological functions of td neurons by interrogating the consequences of td neuron activation and inactivation. The findings that td neurons respond to low O_2 and high CO_2, as well as connectivity to diuretic and suggested anti-diuretic hormone-producing neurons, help to prioritize specific hypotheses about the role of td neurons in affecting behavior and physiology. Regarding behavior, hypoxic conditions have been known to cause an escape response in which feeding larvae withdraws from food (Vermehren-Schmaedick et al., 2010). The precise cellular basis for this behavior has not been definitively shown and td neurons may play a partial role. More recently, it has been shown that under normal conditions, feeding larvae will occasionally dive deeply into the

food and resurface within minutes to reoxygenate (Kim et al., 2017). The cellular basis for this behavior has also not been identified. Here, the td neurons may play a role in monitoring internal gas levels and alerting the animal to surface once internal O_2 level decreases and CO_2 level increases to a harmful level. In terms of physiological responses, my circuit mapping results show that td input feeds into neurohormone populations that release diuretic and suggested anti-diuretic hormones (which taken together may be interpreted as regulation of hemolymph filtration). Thus, future experiments may address how activity of td neurons regulate the activity of central neurohormone-producing populations, and whether td activity affects water balance. One important methodological consideration for future behavioral or physiological experiments is that unambiguous interpretation of the results depends on the ability to selectively manipulate td neuron activity. Thus, the generation of reagents that allow more specific labelling and manipulation of subsets of td neurons will also be a priority. My studies have provided an experimental entry point into studying internal tracheal sensory neurons in *Drosophila* larvae. Future studies may provide further insights into this sensory system by elucidating additional molecular mechanisms that underlie development and function, and by linking internal sensory input to behavior and physiology.

Methods

Drosophila stocks

Animals were reared using standard methods. The following stocks were used, and were obtained from Bloomington Drosophila Stock Center unless otherwise indicated: *R31D10-LexA*, *R22C07-Gal4*, *R35B01-Gal4*, *R35B01-LexA*, *R73B01-Gal4*, *OK282-Gal4* (generated by Cahir.J.O'Kane (unpublished), gift from Brian McCabe), *260-Gal4* (InSITE GAL4 collection), *Gr28a-Gal4*, *Gr28a-QF2*^{G4H} (generated using the HACK method) (Lin and Potter, 2016), *Gr28b.c-Gal4*, *Gr32a-Gal4*, *Gr33a-Gal4*, *Gr33a*^{GAL4}, *Gr33a-QF* (gift from Dr. Jae Young Kwon), *Gr89a-Gal4*, *Ir56a-Gal4*, *Ir76b-Gal4, Ir76b-QF*, *ppk-Gal4*, *tsh-Gal80* (gift from Julie Simpson, Janelia Research Campus, Virginia), *UAS-mCD8-GFP*, *13XLexAop2-mCD8-GFP*, *20XUAS-IVS-mCD8-GFP*, *UAS-mCD8-cherry*, *QUAS-mCD8-GFP*, *QUAS-mtdTomato* (gift from Dr. Jae Young Kwon), *UAS-MCFO-1*, *UAS-pdm3.long* (gift from John Carlson, Yale University), *pdm3*^{f00828}, *Elav-Gal4*, *P(TRiP.HMJ21205)attP40*, *Pdm1-Gal4* (*Nub-Gal4*; gift from Stephen Cohen), *Drifter-Gal4* (gift from Makoto Sato), *UAS-Brp.short.mCherry* ((Schmid et al., 2008), provided by Dr. Richard Mann, Columbia University), *LexAop-Brp.short.cherry* (gift from Takashi Suzuki, Tokyo Institute of Technology), *UAS-CaMPARI2LT* (unpublished reagent, courtesy of Benjamien Moeyaert, Schreiter lab, Janelia Research campus), *Gr28a*^{1} (gift from Seok Jun Moon, Yonsei University), *Gr28b TRiP.HMJ30111*, *Gr28b KK105653* (Vienna Drosophila Resource Center, or VDRC), *ΔGr28 30i* (gift from Huber Amrein, Texas A&M University), *Gr89a TRiP.HMS05359*, *UAS-Gr28a* (gift from John Carlson, Yale University), *Gyc88E GD11230* (VDRC), *Gyc89Db TRiP.HM05207*, *0003-Gal4* (InSITE Gal4 collection), *R74C06-LexA*, *GPB5-Gal4(51)* (courtesy of Benjamin White, NIMH), *13XLexAop2-6XmCherry-HA*, *UAS-syb:spGFP*$^{1-10}$ (gift from Lindsey Macpherson, Columbia University), *13X-LexAop-spGFP*^{11} (generated by our lab), *LexAop-nSyb-spGFP*$^{1-10}$, *UAS-CD4-spGFP*^{11}, *UAS-CD4::spGFP*$^{1-10}$

(Gordon and Scott, 2009), *LexAop-CD4::spGFP*^{11} (Gordon and Scott, 2009), *DH44-Gal4*, *UAS-DenMark*. Animals of either sex were analyzed at the third instar larval stage.

Generation of clones

Multicolor Flpout (MCFO) clones were generated essentially as previously described (Nern et al., 2015). GAL4 lines driving expression in td neurons were crossed to *UAS-MCFO-1*. Early larval progeny were heat-shocked at 38°C for 10 to 15 minutes to sparsely label td neurons.

Immunohistochemistry

Immunohistochemistry was performed as previously described (Matthews et al., 2007). Third instar larvae were dissected in 1X PBS, fixed in 4% paraformaldehyde (Electron Microscopy Sciences) in PBS for 15 minutes, rinsed three times in PBS-TX (0.3% Triton X-100 in PBS), and blocked for 1 hour at 4°C in normal donkey serum (Jackson Immunoresearch). Primary antibodies used were chicken anti-GFP (1:1000; Abcam), rabbit anti-DsRed (1:200; Clontech), mouse anti-FasII (1:10, Developmental Studies Hybridoma Bank, DSHB), mouse anti-Coracle (1:10, DSHB), mouse anti-HA (1:1200, Cell Signaling Technology), rat anti-FLAG (1:100, Novus), mouse anti-Elav (1:10, DSHB), rat anti-pdm3 (1:100; gift from Carlson lab; RRID:AB_2569865), guinea pig anti-pdm3 (1:100; gift from Chien lab; RRID:AB_2567243), rat anti-pdm2 (1:10; gift from Mann lab), mouse anti-acj6 (1:10; DSHB), rabbit anti-V5 epitope, DyLight 549 conjugated (1:200, Rockland Inc.), rabbit anti-dvglut (1:1000, gift from Aaron DiAntonio).

For GRASP experiments, third instar larval brains were dissected in PBS and fixed in 4% paraformaldehyde (Electron Microscopy Sciences) for 15 minutes. Brains were mounted in Vectashield (Vector lab) on poly-L-lysine coated coverslips and imaged for native reconstituted GFP signal.

Electron microscopy

To identify td neurons for TEM, *pdm3^{OK282}-Gal4, UAS-mCD8::GFP* third instar larvae were dissected in PBS and fixed in 3% glutaraldehyde. Larvae were then stained with chicken anti-GFP (1:1000, Abcam) primary antibody followed by goat anti-mouse HRP secondary antibody at a 1:200 dilution. For chromogenic detection, larvae were incubated in 1:20 diaminobenzidine, with 0.3% $NiCl_2$ and 3% hydrogen peroxide solution. Larvae were postfixed with 1% osmium tetroxide in 0.1M phosphate buffer and processed for TEM as previously described (Kim et al., 2012a). Similar to the procedure published by Kim et al., 2012, td neurons were identified after larvae were mounted on epon between two plastic slides. Blocks were trimmed according to the area of interest and longitudinal serial sections were made prior to viewing grids on a JEOL electron microscope (Kim et al., 2012a).

CaMPARI imaging

For CaMPARI imaging of neuronal responses to gaseous stimuli, individual late third-instar larvae were first washed in PBS buffer, dried on a Kimwipe, transferred onto a detached centrifuge tube lid which was then placed inside the gas-delivery apparatus. The apparatus consists of a FlyPad (Genesee Scientific) on the bottom, a spacer ring above the pad and around the larva, and a 395nm UV LED (LEDwholesalers, 7202UV395) positioned on top of the space

ring. The UV LED was used at 3.5V, supplied by a bench power supply (TENMA, 72-7245). Customized gas mixtures (Tech Air) were delivered to the FlyPad at 5L/min through a benchtop Flowbuddy (Genesee Scientific). Following coincident application of gaseous stimuli and UV light for the specified duration, the larva was immediately dissected. Larvae were immersed in PBS with 10mM EGTA and dissected in a fillet larval preparation. The buffer was replaced with 2mL of fresh PBS with 10mM EGTA and the larva was immediately imaged using a Zeiss LSM 700 with a 40x water-immersion Plan-Apochromat objective lens (N.A.=1.0). Green CaMPARI2 fluorescence was imaged using the both the 488nm and low power 405nm (at 5% power for improved signal, see (Fosque et al., 2015)) laser lines. Similarly, the red CaMPARI2 fluorescence was imaged using both the 555 nm and 405 nm laser lines. Single 5μM thick sections were acquired. Unless the preparation was obscured or damaged, one pair of td neurons per segment was acquired for each animal. Images were analysed in Fiji (Schindelin et al., 2012). Green and red fluorescence were measured in the region of interest (cell body).

For CaMPARI imaging of neuronal responses to submersion, individual late third-instar larvae were placed in 35 x 10 mm petri dishes (Falcon) filled completely with ddH2O. Larvae were gently pushed to the bottom of the dish. UV light was applied from above for 1 min either starting immediately or after the specified submersion duration. Larvae were dissected in PBS and immediately imaged in PBS with 10mM EGTA, as described above.

EM reconstruction of td circuit

EM reconstruction was performed in CATMAID as previously described (Burgos et al., 2018; Ohyama et al., 2015; Schneider-Mizell et al., 2016). Previous work had reconstructed sensory axons that originate from abdominal segments and project to the SEZ (Schlegel et al.,

2016); we identified these to be the SEZ-td axons. VNC-td axons were identified by tracing longitudinal processes in the ventrolateral neuronal fiber tracts in the VNC. We annotated synapses in td neurons and used these as starting points to reconstruct the post-synaptic neurons downstream. For estimation of reconstruction progress, we considered reconstructed neurons with >600 nodes as "moderately completed neuron", because almost all reconstructions downstream of VNC-targeting td neurons with >600 nodes include processes and a cell body (which allows for inference of neuronal identity).

Statistical analyses

Axon lengths and VNC lengths were measured in Fiji and statistically analyzed using the Kruskal-Wallis test, followed by Bonferroni post-hoc pairwise comparisons. Axon midline contact frequencies were analyzed using the Chi-squared tests with Bonferroni correction. Dendritic arbors were traced in Neurolucida (Microbrightfield, Natick, MA) and analyzed in Neurolucida Explorer. Dendrite lengths and node counts were statistically analyzed with Mann–Whitney U test with Bonferroni correction. Statistical analyses were conducted using IBM SPSS Statistics v20. Mann-Whitney U test was performed on red/green CaMPARI2 ratios to test for statistical significance between control and experimental conditions (*$p<0.05$, **$p<0.01$, ***$p<0.001$). See figure legends for sample sizes.

References

Adler, E., Hoon, M.A., Mueller, K.L., Chandrashekar, J., Ryba, N.J.P., and Zuker, C.S. (2000). A novel family of mammalian taste receptors. Cell *100*, 693-702.

Andrews, P.L.R. (1986). Vagal Afferent Innervation of the Gastrointestinal-Tract. Prog Brain Res *67*, 65-86.

Bauke, A.C., Sasse, S., Matzat, T., and Klambt, C. (2015). A transcriptional network controlling glial development in the Drosophila visual system. Development *142*, 2184-2193.

Bellen, H.J., Tong, C., and Tsuda, H. (2010). 100 years of Drosophila research and its impact on vertebrate neuroscience: a history lesson for the future. Nat Rev Neurosci *11*, 514-522.

Berthoud, H.R., and Neuhuber, W.L. (2000). Functional and chemical anatomy of the afferent vagal system. Auton Neurosci-Basic *85*, 1-17.

Bertram, G., and Wessing, A. (1994). Intracellular pH regulation by the plasma membrane V-ATPase in Malpighian tubules of Drosophila larvae. J Comp Physiol B *164*, 238-246.

Black, A.M., McCloskey, D.I., and Torrance, R.W. (1971). The responses of carotid body chemoreceptors in the cat to sudden changes of hypercapnic and hypoxic stimuli. Respir Physiol *13*, 36-49.

Bodmer, R., and Jan, Y.N. (1987). Morphological differentiation of the embryonic peripheral neurons in *Drosophila*. Roux's Arch Dev Biol *196*, 69-77.

Bonaz, B., Bazin, T., and Pellissier, S. (2018). The Vagus Nerve at the Interface of the Microbiota-Gut-Brain Axis. Front Neurosci-Switz *12*.

Bouchard, M.B., Voleti, V., Mendes, C.S., Lacefield, C., Grueber, W.B., Mann, R.S., Bruno, R.M., and Hillman, E.M. (2015). Swept confocally-aligned planar excitation (SCAPE) microscopy for high speed volumetric imaging of behaving organisms. Nat Photonics *9*, 113-119.

Brand, A.H., and Perrimon, N. (1993). Targeted Gene-Expression as a Means of Altering Cell Fates and Generating Dominant Phenotypes. Development *118*, 401-415.

Bray, S., and Amrein, H. (2003). A putative Drosophila pheromone receptor expressed in male-specific taste neurons is required for efficient courtship. Neuron *39*, 1019-1029.

Buck, L., and Axel, R. (1991). A Novel Multigene Family May Encode Odorant Receptors - a Molecular-Basis for Odor Recognition. Cell *65*, 175-187.

Burgos, A., Honjo, K., Ohyama, T., Qian, C.S., Shin, G.J., Gohl, D.M., Silies, M., Tracey, W.D., Zlatic, M., Cardona, A.*, et al.* (2018). Nociceptive interneurons control modular motor pathways to promote escape behavior in Drosophila. Elife *7*.

Callier, V., Hand, S.C., Campbell, J.B., Biddulph, T., and Harrison, J.F. (2015). Developmental changes in hypoxic exposure and responses to anoxia in Drosophila melanogaster. J Exp Biol *218*, 2927-2934.

Cannell, E., Dornan, A.J., Halberg, K.A., Terhzaz, S., Dow, J.A.T., and Davies, S.A. (2016). The corticotropin-releasing factor-like diuretic hormone 44 (DH44) and kinin neuropeptides modulate desiccation and starvation tolerance in Drosophila melanogaster. Peptides *80*, 96-107.

Certel, S.J., Clyne, P.J., Carlson, J.R., and Johnson, W.A. (2000). Regulation of central neuron synaptic targeting by the Drosophila POU protein, Acj6. Development *127*, 2395-2405.

Chandrashekar, J., Yarmolinsky, D., von Buchholtz, L., Oka, Y., Sly, W., Ryba, N.J., and Zuker, C.S. (2009). The taste of carbonation. Science *326*, 443-445.

Chang, H.Y., Mashimo, H., and Goyal, R.K. (2003). Musings on the wanderer: what's new in our understanding of vago-vagal reflex? IV. Current concepts of vagal efferent projections to the gut. Am J Physiol Gastrointest Liver Physiol *284*, G357-366.

Chang, R.B., Strochlic, D.E., Williams, E.K., Umans, B.D., and Liberles, S.D. (2015). Vagal Sensory Neuron Subtypes that Differentially Control Breathing. Cell *161*, 622-633.

Chen, C.K., Chen, W.Y., and Chien, C.T. (2012). The POU-domain protein Pdm3 regulates axonal targeting of R neurons in the Drosophila ellipsoid body. Dev Neurobiol *72*, 1422-1432.

Chen, T.W., Wardill, T.J., Sun, Y., Pulver, S.R., Renninger, S.L., Baohan, A., Schreiter, E.R., Kerr, R.A., Orger, M.B., Jayaraman, V.*, et al.* (2013). Ultrasensitive fluorescent proteins for imaging neuronal activity. Nature *499*, 295-+.

Cheung, B.H., Arellano-Carbajal, F., Rybicki, I., and de Bono, M. (2004). Soluble guanylate cyclases act in neurons exposed to the body fluid to promote C. elegans aggregation behavior. Curr Biol *14*, 1105-1111.

Choi, J., van Giesen, L., Choi, M.S., Kang, K., Sprecher, S.G., and Kwon, J.Y. (2016). A Pair of Pharyngeal Gustatory Receptor Neurons Regulates Caffeine-Dependent Ingestion in Drosophila Larvae. Front Cell Neurosci *10*.

Chyb, S. (2004). Drosophila gustatory receptors: from gene identification to functional expression. J Insect Physiol *50*, 469-477.

Clancy, J.A., Deuchars, S.A., and Deuchars, J. (2013). The wonders of the Wanderer. Exp Physiol *98*, 38-45.

Clandinin, T.R., and Zipursky, S.L. (2002). Making connections in the fly visual system. Neuron *35*, 827-841.

Clyne, P.J., Certel, S.J., de Bruyne, M., Zaslavsky, L., Johnson, W.A., and Carlson, J.R. (1999a). The odor specificities of a subset of olfactory receptor neurons are governed by Acj6, a POU-domain transcription factor. Neuron *22*, 339-347.

Clyne, P.J., Warr, C.G., and Carlson, J.R. (2000). Candidate taste receptors in Drosophila. Science *287*, 1830-1834.

Clyne, P.J., Warr, C.G., Freeman, M.R., Lessing, D., Kim, J.H., and Carlson, J.R. (1999b). A novel family of divergent seven-transmembrane proteins: Candidate odorant receptors in Drosophila. Neuron *22*, 327-338.

Cognigni, P., Bailey, A.P., and Miguel-Aliaga, I. (2011). Enteric neurons and systemic signals couple nutritional and reproductive status with intestinal homeostasis. Cell Metab *13*, 92-104.

Coleridge, H.M., Coleridge, J.C., and Roberts, A.M. (1983). Rapid shallow breathing evoked by selective stimulation of airway C fibres in dogs. J Physiol *340*, 415-433.

Coleridge, J.C., and Coleridge, H.M. (1984). Afferent vagal C fibre innervation of the lungs and airways and its functional significance. Rev Physiol Biochem Pharmacol *99*, 1-110.

Coll, A.P., Farooqi, I.S., and O'Rahilly, S. (2007). The hormonal control of food intake. Cell *129*, 251-262.

Corty, M.M., Matthews, B.J., and Grueber, W.B. (2009). Molecules and mechanisms of dendrite development in Drosophila. Development *136*, 1049-1061.

Corty, M.M., Tam, J., and Grueber, W.B. (2016). Dendritic diversification through transcription factor-mediated suppression of alternative morphologies. Development *143*, 1351-1362.

Craig, A.D. (2003). Interoception: the sense of the physiological condition of the body. Curr Opin Neurobiol *13*, 500-505.

Critchley, H.D., and Harrison, N.A. (2013). Visceral influences on brain and behavior. Neuron *77*, 624-638.

Dahanukar, A., Lei, Y.T., Kwon, J.Y., and Carlson, J.R. (2007). Two Gr genes underlie sugar reception in Drosophila. Neuron *56*, 503-516.

Daniels, R.W., Gelfand, M.V., Collins, C.A., and DiAntonio, A. (2008). Visualizing glutamatergic cell bodies and synapses in Drosophila larval and adult CNS. J Comp Neurol *508*, 131-152.

de Haro, M., Al-Ramahi, I., Benito-Sipos, J., Lopez-Arias, B., Dorado, B., Veenstra, J.A., and Herrero, P. (2010). Detailed analysis of leucokinin-expressing neurons and their candidate functions in the Drosophila nervous system. Cell Tissue Res *339*, 321-336.

De Velasco, B., Shen, J., Go, S., and Hartenstein, V. (2004). Embryonic development of the Drosophila corpus cardiacum, a neuroendocrine gland with similarity to the vertebrate pituitary, is controlled by sine oculis and glass. Dev Biol *274*, 280-294.

Delventhal, R., and Carlson, J.R. (2016). Bitter taste receptors confer diverse functions to neurons. Elife *5*.

Denholm, B., and Skaer, H. (2009). Bringing together components of the fly renal system. Curr Opin Genet Dev *19*, 526-532.

Depoortere, I. (2014). Taste receptors of the gut: emerging roles in health and disease. Gut *63*, 179-190.

Docherty, R.J., Charlesworth, G., Farrag, K., Bhattacharjee, A., and Costa, S. (2005). The use of the rat isolated vagus nerve for functional measurements of the effect of drugs in vitro. J Pharmacol Toxicol Methods *51*, 235-242.

Dus, M., Lai, J.S., Gunapala, K.M., Min, S., Tayler, T.D., Hergarden, A.C., Geraud, E., Joseph, C.M., and Suh, G.S. (2015). Nutrient Sensor in the Brain Directs the Action of the Brain-Gut Axis in Drosophila. Neuron *87*, 139-151.

Egerod, K.L., Petersen, N., Timshel, P.N., Rekling, J.C., Wang, Y., Liu, Q., Schwartz, T.W., and Gautron, L. (2018). Profiling of G protein-coupled receptors in vagal afferents reveals novel gut-to-brain sensing mechanisms. Mol Metab *12*, 62-75.

El Ouazzani, T., and Mei, N. (1982). Electrophysiologic properties and role of the vagal thermoreceptors of lower esophagus and stomach of cat. Gastroenterology *83*, 995-1001.

Erkman, L., McEvilly, R.J., Luo, L., Ryan, A.K., Hooshmand, F., OConnell, S.M., Keithley, E.M., Rapaport, D.H., Ryan, A.F., and Rosenfeld, M.G. (1996). Role of transcription factors Brn-3.1 and Brn-3.2 in auditory and visual system development. Nature *381*, 603-606.

Fajardo, O., Meseguer, V., Belmonte, C., and Viana, F. (2008). TRPA1 channels mediate cold temperature sensing in mammalian vagal sensory neurons: pharmacological and genetic evidence. J Neurosci *28*, 7863-7875.

Faucher, C., Forstreuter, M., Hilker, M., and de Bruyne, M. (2006). Behavioral responses of Drosophila to biogenic levels of carbon dioxide depend on life-stage, sex and olfactory context. J Exp Biol *209*, 2739-2748.

Finger, J.H., Bronson, R.T., Harris, B., Johnson, K., Przyborski, S.A., and Ackerman, S.L. (2002). The netrin 1 receptors Unc5h3 and Dcc are necessary at multiple choice points for the guidance of corticospinal tract axons. J Neurosci *22*, 10346-10356.

Fischler, W., Kong, P., Marella, S., and Scott, K. (2007). The detection of carbonation by the Drosophila gustatory system. Nature *448*, 1054-1057.

Fosque, B.F., Sun, Y., Dana, H., Yang, C.T., Ohyama, T., Tadross, M.R., Patel, R., Zlatic, M., Kim, D.S., Ahrens, M.B.*, et al.* (2015). Labeling of active neural circuits in vivo with designed calcium integrators. Science *347*, 755-760.

Francis, S.A., Taylor-Wells, J., Gross, A.D., and Bloomquist, J.R. (2016). Toxicity and Physiological Actions of Carbonic Anhydrase Inhibitors to Aedes aegypti and Drosophila melanogaster. Insects *8*.

Ganguly, A., Pang, L., Duong, V.K., Lee, A., Schoniger, H., Varady, E., and Dahanukar, A. (2017). A Molecular and Cellular Context-Dependent Role for Ir76b in Detection of Amino Acid Taste. Cell Reports *18*, 737-750.

Gerhard, S., Andrade, I., Fetter, R.D., Cardona, A., and Schneider-Mizell, C.M. (2017). Conserved neural circuit structure across Drosophila larval development revealed by comparative connectomics. Elife *6*.

Gohl, D.M., Silies, M.A., Gao, X.J.J., Bhalerao, S., Luongo, F.J., Lin, C.C., Potter, C.J., and Clandinin, T.R. (2011). A versatile in vivo system for directed dissection of gene expression patterns. Nat Methods *8*, 231-U271.

Gordon, M.D., and Scott, K. (2009). Motor control in a Drosophila taste circuit. Neuron *61*, 373-384.

Grabauskas, G., Song, I., Zhou, S., and Owyang, C. (2010). Electrophysiological identification of glucose-sensing neurons in rat nodose ganglia. J Physiol *588*, 617-632.

Gray, J.M., Karow, D.S., Lu, H., Chang, A.J., Chang, J.S., Ellis, R.E., Marletta, M.A., and Bargmann, C.I. (2004). Oxygen sensation and social feeding mediated by a C. elegans guanylate cyclase homologue. Nature *430*, 317-322.

Grosskortenhaus, R., Robinson, K.J., and Doe, C.Q. (2006). Pdm and Castor specify late-born motor neuron identity in the NB7-1 lineage. Gene Dev *20*, 2618-2627.

Grueber, W.B., Jan, L.Y., and Jan, Y.N. (2002). Tiling of the Drosophila epidermis by multidendritic sensory neurons. Development *129*, 2867-2878.

Grueber, W.B., Jan, L.Y., and Jan, Y.N. (2003). Different levels of the homeodomain protein cut regulate distinct dendrite branching patterns of Drosophila multidendritic neurons. Cell *112*, 805-818.

Grueber, W.B., Ye, B., Yang, C.H., Younger, S., Borden, K., Jan, L.Y., and Jan, Y.N. (2007). Projections of Drosophila multidendritic neurons in the central nervous system: links with peripheral dendrite morphology. Development *134*, 55-64.

Guyenet, P.G., and Bayliss, D.A. (2015). Neural Control of Breathing and CO2 Homeostasis. Neuron *87*, 946-961.

Hadjieconomou, D., Rotkopf, S., Alexandre, C., Bell, D.M., Dickson, B.J., and Salecker, I. (2011). Flybow: genetic multicolor cell labeling for neural circuit analysis in Drosophila melanogaster. Nat Methods *8*, 260-266.

Han, L., Limjunyawong, N., Ru, F., Li, Z., Hall, O.J., Steele, H., Zhu, Y., Wilson, J., Mitzner, W., Kollarik, M*., et al.* (2018). Mrgprs on vagal sensory neurons contribute to bronchoconstriction and airway hyper-responsiveness. Nat Neurosci *21*, 324-328.

Hasegawa, E., Kitada, Y., Kaido, M., Takayama, R., Awasaki, T., Tabata, T., and Sato, M. (2011). Concentric zones, cell migration and neuronal circuits in the Drosophila visual center. Development *138*, 983-993.

Hasemeyer, M., Yapici, N., Heberlein, U., and Dickson, B.J. (2009). Sensory neurons in the Drosophila genital tract regulate female reproductive behavior. Neuron *61*, 511-518.

Helmstaedter, M., Briggman, K.L., and Denk, W. (2011). High-accuracy neurite reconstruction for high-throughput neuroanatomy. Nat Neurosci *14*, 1081-1088.

Hibbard, T., and Killard, A.J. (2011). Breath Ammonia Analysis: Clinical Application and Measurement. Crit Rev Anal Chem *41*, 21-35.

Hillsley, K., and Grundy, D. (1998). Serotonin and cholecystokinin activate different populations of rat mesenteric vagal afferents. Neurosci Lett *255*, 63-66.

Hobert, O. (2008). Regulatory logic of neuronal diversity: Terminal selector genes and selector motifs. P Natl Acad Sci USA *105*, 20067-20071.

Hobert, O., Carrera, I., and Stefanakis, N. (2010). The molecular and gene regulatory signature of a neuron. Trends Neurosci *33*, 435-445.

Hu, N., and Castelli-Gair, J. (1999). Study of the posterior spiracles of Drosophila as a model to understand the genetic and cellular mechanisms controlling morphogenesis. Dev Biol *214*, 197-210.

Huckesfeld, S., Peters, M., and Pankratz, M.J. (2016). Central relay of bitter taste to the protocerebrum by peptidergic interneurons in the Drosophila brain. Nature Communications *7*.

Hughes, C.L., and Thomas, J.B. (2007). A sensory feedback circuit coordinates muscle activity in Drosophila. Mol Cell Neurosci *35*, 383-396.

Hwang, R.Y., Zhong, L.X., Xu, Y.F., Johnson, T., Zhang, F., Deisseroth, K., and Tracey, W.D. (2007). Nociceptive neurons protect Drosophila larvae from parasitoid wasps. Current Biology *17*, 2105-2116.

Iyer, E.P., and Cox, D.N. (2010). Laser capture microdissection of Drosophila peripheral neurons. J Vis Exp.

Jan, Y.N., and Jan, L.Y. (1994). Neuronal cell fate specification in Drosophila. Curr Opin Neurobiol *4*, 8-13.

Jang, H.J., Kokrashvili, Z., Theodorakis, M.J., Carlson, O.D., Kim, B.J., Zhou, J., Kim, H.H., Xu, X., Chan, S.L., Juhaszova, M.*, et al.* (2007). Gut-expressed gustducin and taste receptors regulate secretion of glucagon-like peptide-1. P Natl Acad Sci USA *104*, 15069-15074.

Jeanningros, R. (1982). Vagal unitary responses to intestinal amino acid infusions in the anesthetized cat: a putative signal for protein induced satiety. Physiol Behav *28*, 9-21.

Jenett, A., Rubin, G.M., Ngo, T.T., Shepherd, D., Murphy, C., Dionne, H., Pfeiffer, B.D., Cavallaro, A., Hall, D., Jeter, J.*, et al.* (2012). A GAL4-driver line resource for Drosophila neurobiology. Cell Rep *2*, 991-1001.

Johnson, E.C., Shafer, O.T., Trigg, J.S., Park, J., Schooley, D.A., Dow, J.A., and Taghert, P.H. (2005). A novel diuretic hormone receptor in Drosophila: evidence for conservation of CGRP signaling. J Exp Biol *208*, 1239-1246.

Jones, W.D., Cayirlioglu, P., Kadow, I.G., and Vosshall, L.B. (2007). Two chemosensory receptors together mediate carbon dioxide detection in Drosophila. Nature *445*, 86-90.

Joseph, R.M., and Carlson, J.R. (2015). Drosophila Chemoreceptors: A Molecular Interface Between the Chemical World and the Brain. Trends Genet *31*, 683-695.

Kang, N., and Koo, J. (2012). Olfactory receptors in non-chemosensory tissues. BMB Rep *45*, 612-622.

Kim, D., Alvarez, M., Lechuga, L.M., and Louis, M. (2017). Species-specific modulation of food-search behavior by respiration and chemosensation in Drosophila larvae. Elife *6*.

Kim, M.E., Shrestha, B.R., Blazeski, R., Mason, C.A., and Grueber, W.B. (2012a). Integrins establish dendrite-substrate relationships that promote dendritic self-avoidance and patterning in drosophila sensory neurons. Neuron *73*, 79-91.

Kim, S.E., Coste, B., Chadha, A., Cook, B., and Patapoutian, A. (2012b). The role of Drosophila Piezo in mechanical nociception. Nature *483*, 209-212.

King, A.N., Barber, A.F., Smith, A.E., Dreyer, A.P., Sitaraman, D., Nitabach, M.N., Cavanaugh, D.J., and Sehgal, A. (2017). A Peptidergic Circuit Links the Circadian Clock to Locomotor Activity. Curr Biol *27*, 1915-1927 e1915.

Koh, T.W., He, Z., Gorur-Shandilya, S., Menuz, K., Larter, N.K., Stewart, S., and Carlson, J.R. (2014). The Drosophila IR20a Clade of Ionotropic Receptors Are Candidate Taste and Pheromone Receptors. Neuron *83*, 850-865.

Kohsaka, H., Guertin, P.A., and Nose, A. (2017). Neural Circuits Underlying Fly Larval Locomotion. Curr Pharm Design *23*, 1722-1733.

Komiyama, T., Johnson, W.A., Luo, L., and Jefferis, G.S. (2003). From lineage to wiring specificity. POU domain transcription factors control precise connections of Drosophila olfactory projection neurons. Cell *112*, 157-167.

Kong, J., Fang, J., Park, J., Li, S., and Rong, P. (2018). Treating Depression with Transcutaneous Auricular Vagus Nerve Stimulation: State of the Art and Future Perspectives. Front Psychiatry *9*, 20.

Kuraishi, T., Kenmoku, H., and Kurata, S. (2015). From mouth to anus: Functional and structural relevance of enteric neurons in the Drosophila melanogaster gut. Insect Biochem Molec *67*, 21-26.

Kwon, J.Y., Dahanukar, A., Weiss, L.A., and Carlson, J.R. (2007). The molecular basis of CO2 reception in Drosophila. Proc Natl Acad Sci U S A *104*, 3574-3578.

Kwon, J.Y., Dahanukar, A., Weiss, L.A., and Carlson, J.R. (2011). Molecular and cellular organization of the taste system in the Drosophila larva. J Neurosci *31*, 15300-15309.

Kwon, J.Y., Dahanukar, A., Weiss, L.A., and Carlson, J.R. (2014). A map of taste neuron projections in the Drosophila CNS. J Biosci *39*, 565-574.

Lai, S.L., and Lee, T. (2006). Genetic mosaic with dual binary transcriptional systems in Drosophila. Nature Neuroscience *9*, 703-709.

Lal, S., Kirkup, A.J., Brunsden, A.M., Thompson, D.G., and Grundy, D. (2001). Vagal afferent responses to fatty acids of different chain length in the rat. Am J Physiol Gastrointest Liver Physiol *281*, G907-915.

Landgraf, M., Sanchez-Soriano, N., Technau, G.M., Urban, J., and Prokop, A. (2003). Charting the Drosophila neuropile: a strategy for the standardised characterisation of genetically amenable neurites. Dev Biol *260*, 207-225.

Langlais, K.K., Stewart, J.A., and Morton, D.B. (2004). Preliminary characterization of two atypical soluble guanylyl cyclases in the central and peripheral nervous system of Drosophila melanogaster. J Exp Biol *207*, 2323-2338.

Lee, L.Y. (2009). Respiratory sensations evoked by activation of bronchopulmonary C-fibers. Respir Physiol Neurobiol *167*, 26-35.

Lee, R.J., and Cohen, N.A. (2014). Bitter and sweet taste receptors in the respiratory epithelium in health and disease. J Mol Med (Berl) *92*, 1235-1244.

Lee, Y., Moon, S.J., and Montell, C. (2009). Multiple gustatory receptors required for the caffeine response in Drosophila. Proc Natl Acad Sci U S A *106*, 4495-4500.

Li, H., Horns, F., Wu, B., Xie, Q., Li, J., Li, T., Luginbuhl, D.J., Quake, S.R., and Luo, L. (2017). Classifying Drosophila Olfactory Projection Neuron Subtypes by Single-Cell RNA Sequencing. Cell *171*, 1206-1220 e1222.

Lin, C.C., and Potter, C.J. (2016). Editing Transgenic DNA Components by Inducible Gene Replacement in Drosophila melanogaster. Genetics *203*, 1613-+.

Liu, S., Li, K., Gao, Y., Liu, X., Chen, W., Ge, W., Feng, Q., Palli, S.R., and Li, S. (2018). Antagonistic actions of juvenile hormone and 20-hydroxyecdysone within the ring gland determine developmental transitions in Drosophila. Proc Natl Acad Sci U S A *115*, 139-144.

Luan, Z., Quigley, C., and Li, H.S. (2015). The putative Na+/Cl--dependent neurotransmitter/osmolyte transporter inebriated in the Drosophila hindgut is essential for the maintenance of systemic water homeostasis. Sci Rep-Uk *5*.

Macpherson, L.J., Zaharieva, E.E., Kearney, P.J., Alpert, M.H., Lin, T.Y., Turan, Z., Lee, C.H., and Gallio, M. (2015). Dynamic labelling of neural connections in multiple colours by trans-synaptic fluorescence complementation. Nat Commun *6*, 10024.

Manning, G., and Krasnow, M.A. (1993). Development of the Drosophila tracheal system, pp. 609-685.

Matthews, B.J., Kim, M.E., Flanagan, J.J., Hattori, D., Clemens, J.C., Zipursky, S.L., and Grueber, W.B. (2007). Dendrite self-avoidance is controlled by Dscam. Cell *129*, 593-604.

Mazzone, S.B., and Undem, B.J. (2016). Vagal Afferent Innervation of the Airways in Health and Disease. Physiol Rev *96*, 975-1024.

McEvilly, R.J., Erkman, L., Luo, L., Sawchenko, P.E., Ryan, A.F., and Rosenfeld, M.G. (1996). Requirement for Brn-3.0 In differentiation and survival of sensory and motor neurons. Nature *384*, 574-577.

McGovern, A.E., Davis-Poynter, N., Farrell, M.J., and Mazzone, S.B. (2012). Transneuronal tracing of airways-related sensory circuitry using herpes simplex virus 1, strain H129. Neuroscience *207*, 148-166.

McGovern, A.E., Driessen, A.K., Simmons, D.G., Powell, J., Davis-Poynter, N., Farrell, M.J., and Mazzone, S.B. (2015). Distinct Brainstem and Forebrain Circuits Receiving Tracheal Sensory Neuron Inputs Revealed Using a Novel Conditional Anterograde Transsynaptic Viral Tracing System. Journal of Neuroscience *35*, 7041-7055.

Mei, N. (1978). Vagal glucoreceptors in the small intestine of the cat. J Physiol *282*, 485-506.

Mei, N., and Garnier, L. (1986). Osmosensitive Vagal Receptors in the Small-Intestine of the Cat. J Autonom Nerv Syst *16*, 159-170.

Merritt, D.J., and Whitington, P.M. (1995). Central projections of sensory neurons in the *Drosophila* embryo correlate with sensory modality, soma position, and proneural gene function. J Neurosci *15*, 1755-1767.

Merritt, D.J., and Whitington, P.M. (2002). Homeotic genes influence the axonal pathway of a Drosophila embryonic sensory neuron. Int J Dev Biol *46*, 633-638.

Milby, A.H., Halpern, C.H., and Baltuch, G.H. (2008). Vagus nerve stimulation for epilepsy and depression. Neurotherapeutics *5*, 75-85.

Minokoshi, Y., Alquier, T., Furukawa, N., Kim, Y.B., Lee, A., Xue, B., Mu, J., Foufelle, F., Ferre, P., Birnbaum, M.J.*, et al.* (2004). AMP-kinase regulates food intake by responding to hormonal and nutrient signals in the hypothalamus. Nature *428*, 569-574.

Mishra, D., Miyamoto, T., Rezenom, Y.H., Broussard, A., Yavuz, A., Slone, J., Russell, D.H., and Amrein, H. (2013). The molecular basis of sugar sensing in Drosophila larvae. Curr Biol *23*, 1466-1471.

Mishra, D., Thorne, N., Miyamoto, C., Jagge, C., and Amrein, H. (2018). The taste of ribonucleosides: Novel macronutrients essential for larval growth are sensed by Drosophila gustatory receptor proteins. Plos Biol *16*, e2005570.

Miyamoto, T., and Amrein, H. (2008). Suppression of male courtship by a Drosophila pheromone receptor. Nature Neuroscience *11*, 874-876.

Miyamoto, T., Slone, J., Song, X.Y., and Amrein, H. (2012). A Fructose Receptor Functions as a Nutrient Sensor in the Drosophila Brain. Cell *151*, 1113-1125.

Montell, C. (2009). A taste of the Drosophila gustatory receptors. Curr Opin Neurobiol *19*, 345-353.

Montell, C. (2013). Gustatory receptors: not just for good taste. Curr Biol *23*, R929-932.

Moon, S.J., Kottgen, M., Jiao, Y., Xu, H., and Montell, C. (2006). A taste receptor required for the caffeine response in vivo. Curr Biol *16*, 1812-1817.

Moon, S.J., Lee, Y., Jiao, Y., and Montell, C. (2009). A Drosophila gustatory receptor essential for aversive taste and inhibiting male-to-male courtship. Curr Biol *19*, 1623-1627.

Morton, D.B. (2004). Atypical soluble guanylyl cyclases in Drosophila can function as molecular oxygen sensors. J Biol Chem *279*, 50651-50653.

Morton, D.B., Stewart, J.A., Langlais, K.K., Clemens-Grisham, R.A., and Vermehren, A. (2008). Synaptic transmission in neurons that express the Drosophila atypical soluble guanylyl cyclases, Gyc-89Da and Gyc-89Db, is necessary for the successful completion of larval and adult ecdysis. J Exp Biol *211*, 1645-1656.

Murphey, R.K., Possidente, D., Pollack, G., and Merritt, D.J. (1989). Modality-specific axonal projections in the CNS of the flies Phormia and Drosophila. J Comp Neurol *290*, 185-200.

Nern, A., Pfeiffer, B.D., and Rubin, G.M. (2015). Optimized tools for multicolor stochastic labeling reveal diverse stereotyped cell arrangements in the fly visual system. Proc Natl Acad Sci U S A *112*, E2967-2976.

Ni, L., Bronk, P., Chang, E.C., Lowell, A.M., Flam, J.O., Panzano, V.C., Theobald, D.L., Griffith, L.C., and Garrity, P.A. (2013). A gustatory receptor paralogue controls rapid warmth avoidance in Drosophila. Nature *500*, 580-584.

Nicolai, L.J., Ramaekers, A., Raemaekers, T., Drozdzecki, A., Mauss, A.S., Yan, J., Landgraf, M., Annaert, W., and Hassan, B.A. (2010). Genetically encoded dendritic marker sheds light on neuronal connectivity in Drosophila. Proc Natl Acad Sci U S A *107*, 20553-20558.

Nonomura, K., Woo, S.H., Chang, R.B., Gillich, A., Qiu, Z., Francisco, A.G., Ranade, S.S., Liberles, S.D., and Patapoutian, A. (2017). Piezo2 senses airway stretch and mediates lung inflation-induced apnoea. Nature *541*, 176-181.

Ogbonnaya, S., and Kaliaperumal, C. (2013). Vagal nerve stimulator: Evolving trends. J Nat Sci Biol Med *4*, 8-13.

Ohyama, T., Schneider-Mizell, C.M., Fetter, R.D., Aleman, J.V., Franconville, R., Rivera-Alba, M., Mensh, B.D., Branson, K.M., Simpson, J.H., Truman, J.W*., et al.* (2015). A multilevel multimodal circuit enhances action selection in Drosophila. Nature *520*, 633-639.

Paintal, A.S. (1973). Vagal Sensory Receptors and Their Reflex Effects. Physiol Rev *53*, 159-227.

Park, J.H., and Kwon, J.Y. (2011a). Heterogeneous expression of Drosophila gustatory receptors in enteroendocrine cells. Plos One *6*, e29022.

Park, J.H., and Kwon, J.Y. (2011b). A Systematic Analysis of Drosophila Gustatory Receptor Gene Expression in Abdominal Neurons which Project to the Central Nervous System. Mol Cells *32*, 375-381.

Pavlov, V.A., and Tracey, K.J. (2012). The vagus nerve and the inflammatory reflex--linking immunity and metabolism. Nat Rev Endocrinol *8*, 743-754.

Pfluger, H.J., Braunig, P., and Hustert, R. (1988). The Organization of Mechanosensory Neuropiles in Locust Thoracic Ganglia. Philos T Roy Soc B *321*, 1-&.

Potter, C.J., and Luo, L. (2010). Splinkerette PCR for mapping transposable elements in Drosophila. Plos One *5*, e10168.

Potter, C.J., Tasic, B., Russler, E.V., Liang, L., and Luo, L.Q. (2010). The Q System: A Repressible Binary System for Transgene Expression, Lineage Tracing, and Mosaic Analysis. Cell *141*, 536-548.

Prabhakar, N.R. (2016). Chapter 18 - O2 and CO2 Detection by the Carotid and Aortic Bodies. In Chemosensory Transduction, F. Zufall, and S.D. Munger, eds. (Academic Press), pp. 321-338.

Python, F., and Stocker, R.F. (2002). Adult-like complexity of the larval antennal lobe of D. melanogaster despite markedly low numbers of odorant receptor neurons. J Comp Neurol *445*, 374-387.

Qian, C.S., Kaplow, M., Lee, J.K., and Grueber, W.B. (2018). Diversity of Internal Sensory Neuron Axon Projection Patterns Is Controlled by the POU-Domain Protein Pdm3 in Drosophila Larvae. J Neurosci *38*, 2081-2093.

Rinaman, L. (2007). Visceral sensory inputs to the endocrine hypothalamus. Front Neuroendocrinol *28*, 50-60.

Rinaman, L., Card, J.P., Schwaber, J.S., and Miselis, R.R. (1989). Ultrastructural demonstration of a gastric monosynaptic vagal circuit in the nucleus of the solitary tract in rat. J Neurosci *9*, 1985-1996.

Rocco, D.A., Kim, D.H., and Paluzzi, J.V. (2017). Immunohistochemical mapping and transcript expression of the GPA2/GPB5 receptor in tissues of the adult mosquito, Aedes aegypti. Cell Tissue Res *369*, 313-330.

Roman, C.W., Derkach, V.A., and Palmiter, R.D. (2016). Genetically and functionally defined NTS to PBN brain circuits mediating anorexia. Nat Commun *7*, 11905.

Saalfeld, S., Cardona, A., Hartenstein, V., and Tomancak, P. (2009). CATMAID: collaborative annotation toolkit for massive amounts of image data. Bioinformatics *25*, 1984-1986.

Sanes, J.R., and Zipursky, S.L. (2010). Design principles of insect and vertebrate visual systems. Neuron *66*, 15-36.

Sant'Ambrogio, G., Mathew, O.P., and Sant'Ambrogio, F.B. (1988). Characteristics of laryngeal cold receptors. Respir Physiol *71*, 287-297.

Santos, J.G., Vomel, M., Struck, R., Homberg, U., Nassel, D.R., and Wegener, C. (2007). Neuroarchitecture of Peptidergic Systems in the Larval Ventral Ganglion of Drosophila melanogaster. Plos One *2*.

Sawchenko, P.E. (1983). Central connections of the sensory and motor nuclei of the vagus nerve. J Auton Nerv Syst *9*, 13-26.

Schindelin, J., Arganda-Carreras, I., Frise, E., Kaynig, V., Longair, M., Pietzsch, T., Preibisch, S., Rueden, C., Saalfeld, S., Schmid, B.*, et al.* (2012). Fiji: an open-source platform for biological-image analysis. Nat Methods *9*, 676-682.

Schlegel, P., Texada, M.J., Miroschnikow, A., Schoofs, A., Huckesfeld, S., Peters, M., Schneider-Mizell, C.M., Lacin, H., Li, F., Fetter, R.D.*, et al.* (2016). Synaptic transmission parallels neuromodulation in a central food-intake circuit. Elife *5*.

Schmid, A., Hallermann, S., Kittel, R.J., Khorramshahi, O., Frolich, A.M., Quentin, C., Rasse, T.M., Mertel, S., Heckmann, M., and Sigrist, S.J. (2008). Activity-dependent site-specific changes of glutamate receptor composition in vivo. Nat Neurosci *11*, 659-666.

Schneider-Mizell, C.M., Gerhard, S., Longair, M., Kazimiers, T., Li, F., Zwart, M.F., Champion, A., Midgley, F.M., Fetter, R.D., Saalfeld, S.*, et al.* (2016). Quantitative neuroanatomy for connectomics in Drosophila. Elife *5*.

Schoofs, A., Huckesfeld, S., Schlegel, P., Miroschnikow, A., Peters, M., Zeymer, M., Spiess, R., Chiang, A.S., and Pankratz, M.J. (2014). Selection of Motor Programs for Suppressing Food Intake and Inducing Locomotion in the Drosophila Brain. Plos Biol *12*.

Sellami, A., Agricola, H.J., and Veenstra, J.A. (2011). Neuroendocrine cells in Drosophila melanogaster producing GPA2/GPB5, a hormone with homology to LH, FSH and TSH. Gen Comp Endocrinol *170*, 582-588.

Sengupta, P., Chou, J.H., and Bargmann, C.I. (1996). odr-10 encodes a seven transmembrane domain olfactory receptor required for responses to the odorant diacetyl. Cell *84*, 899-909.

Shim, J., Lee, Y., Jeong, Y.T., Kim, Y., Lee, M.G., Montell, C., and Moon, S.J. (2015). The full repertoire of Drosophila gustatory receptors for detecting an aversive compound. Nat Commun *6*, 8867.

Singhania, A., and Grueber, W.B. (2014). Development of the embryonic and larval peripheral nervous system of Drosophila. Wiley Interdiscip Rev Dev Biol *3*, 193-210.

Sotillos, S., Espinosa-Vazquez, J.M., Foglia, F., Hu, N., and Hombria, J.C.G. (2010). An efficient approach to isolate STAT regulated enhancers uncovers STAT92E fundamental role in Drosophila tracheal development. Developmental Biology *340*, 571-582.

Spitz, F., and Furlong, E.E. (2012). Transcription factors: from enhancer binding to developmental control. Nat Rev Genet *13*, 613-626.

Stewart, S., Koh, T.W., Ghosh, A.C., and Carlson, J.R. (2015). Candidate ionotropic taste receptors in the Drosophila larva. Proc Natl Acad Sci U S A *112*, 4195-4201.

Strochlic, D.E. (2015). Molecular and genetic analysis of the vagus nerve (Harvard University).

Sturm, R.A., and Herr, W. (1988). The Pou Domain Is a Bipartite DNA-Binding Structure. Nature *336*, 601-604.

Sun, L.M., Wang, H.Y., Hua, J., Han, J.L., Matsunamic, H., and Luo, M.M. (2009). Guanylyl cyclase-D in the olfactory CO2 neurons is activated by bicarbonate. P Natl Acad Sci USA *106*, 2041-2046.

Sung, H.Y., Jeong, Y.T., Lim, J.Y., Kim, H., Oh, S.M., Hwang, S.W., Kwon, J.Y., and Moon, S.J. (2017). Heterogeneity in the Drosophila gustatory receptor complexes that detect aversive compounds. Nature Communications *8*.

Suslak, T.J., Watson, S., Thompson, K.J., Shenton, F.C., Bewick, G.S., Armstrong, J.D., and Jarman, A.P. (2015). Piezo Is Essential for Amiloride-Sensitive Stretch-Activated Mechanotransduction in Larval Drosophila Dorsal Bipolar Dendritic Sensory Neurons. Plos One *10*.

Suster, M.L., Seugnet, L., Bate, M., and Sokolowski, M.B. (2004). Refining GAL4-driven transgene expression in Drosophila with a GAL80 enhancer-trap. Genesis *39*, 240-245.

Syrjanen, L., Tolvanen, M.E., Hilvo, M., Vullo, D., Carta, F., Supuran, C.T., and Parkkila, S. (2013). Characterization, bioinformatic analysis and dithiocarbamate inhibition studies of two new alpha-carbonic anhydrases, CAH1 and CAH2, from the fruit fly Drosophila melanogaster. Bioorg Med Chem *21*, 1516-1521.

Syrjanen, L., Valanne, S., Kuuslahti, M., Tuomela, T., Sriram, A., Sanz, A., Jacobs, H.T., Ramet, M., and Parkkila, S. (2015). beta carbonic anhydrase is required for female fertility in Drosophila melanogaster. Front Zool *12*.

Takahashi, T., and Owyang, C. (1997). Characterization of vagal pathways mediating gastric accommodation reflex in rats. J Physiol *504 (Pt 2)*, 479-488.

Ter Horst, G.J., de Boer, P., Luiten, P.G., and van Willigen, J.D. (1989). Ascending projections from the solitary tract nucleus to the hypothalamus. A Phaseolus vulgaris lectin tracing study in the rat. Neuroscience *31*, 785-797.

Thompson, B.J., and Cohen, S.M. (2006). The hippo pathway regulates the bantam microRNA to control cell proliferation and apoptosis in Drosophila. Cell *126*, 767-774.

Thorne, N., and Amrein, H. (2008). Atypical expression of Drosophila gustatory receptor genes in sensory and central neurons. J Comp Neurol *506*, 548-568.

Tichy, A.L., Ray, A., and Carlson, J.R. (2008). A new Drosophila POU gene, pdm3, acts in odor receptor expression and axon targeting of olfactory neurons. J Neurosci *28*, 7121-7129.

Tresguerres, M., Buck, J., and Levin, L.R. (2010). Physiological carbon dioxide, bicarbonate, and pH sensing. Pflugers Arch *460*, 953-964.

Vandersmissen, H.P., Van Hiel, M.B., Van Loy, T., Vleugels, R., and Vanden Broeck, J. (2014). Silencing D. melanogaster lgr1 impairs transition from larval to pupal stage. Gen Comp Endocrinol *209*, 135-147.

Venken, K.J.T., Simpson, J.H., and Bellen, H.J. (2011). Genetic Manipulation of Genes and Cells in the Nervous System of the Fruit Fly. Neuron *72*, 202-230.

Vermehren-Schmaedick, A., Ainsley, J.A., Johnson, W.A., Davies, S.A., and Morton, D.B. (2010). Behavioral responses to hypoxia in Drosophila larvae are mediated by atypical soluble guanylyl cyclases. Genetics *186*, 183-196.

Vosshall, L.B. (2001). The molecular logic of olfaction in Drosophila. Chem Senses *26*, 207-213.

Vosshall, L.B., Amrein, H., Morozov, P.S., Rzhetsky, A., and Axel, R. (1999). A spatial map of olfactory receptor expression in the Drosophila antenna. Cell *96*, 725-736.

Vosshall, L.B., and Stocker, R.E. (2007). Molecular architecture of smell and taste in Drosophila. Annu Rev Neurosci *30*, 505-533.

Vosshall, L.B., Wong, A.M., and Axel, R. (2000). An olfactory sensory map in the fly brain. Cell *102*, 147-159.

Weiss, L.A., Dahanukar, A., Kwon, J.Y., Banerjee, D., and Carlson, J.R. (2011). The Molecular and Cellular Basis of Bitter Taste in Drosophila. Neuron *69*, 258-272.

Williams, E.K., Chang, R.B., Strochlic, D.E., Umans, B.D., Lowell, B.B., and Liberles, S.D. (2016). Sensory Neurons that Detect Stretch and Nutrients in the Digestive System. Cell *166*, 209-221.

Witham, E., Comunian, C., Ratanpal, H., Skora, S., Zimmer, M., and Srinivasan, S. (2016). C. elegans Body Cavity Neurons Are Homeostatic Sensors that Integrate Fluctuations in Oxygen Availability and Internal Nutrient Reserves. Cell Rep *14*, 1641-1654.

Xiang, Y., Yuan, Q., Vogt, N., Looger, L.L., Jan, L.Y., and Jan, Y.N. (2010). Light-avoidance-mediating photoreceptors tile the Drosophila larval body wall. Nature *468*, 921-926.

Yan, Z.Q., Zhang, W., He, Y., Gorczyca, D., Xiang, Y., Cheng, L.E., Meltzer, S., Jan, L.Y., and Jan, Y.N. (2013). Drosophila NOMPC is a mechanotransduction channel subunit for gentle-touch sensation. Nature *493*, 221-225.

Yang, C.H., Rumpf, S., Xiang, Y., Gordon, M.D., Song, W., Jan, L.Y., and Jan, Y.N. (2009). Control of the postmating behavioral switch in Drosophila females by internal sensory neurons. Neuron *61*, 519-526.

Zandawala, M., Marley, R., Davies, S.A., and Nassel, D.R. (2018). Characterization of a set of abdominal neuroendocrine cells that regulate stress physiology using colocalized diuretic peptides in Drosophila. Cell Mol Life Sci *75*, 1099-1115.

Zhang, Y.L.V., Ni, J.F., and Montell, C. (2013). The Molecular Basis for Attractive Salt-Taste Coding in Drosophila. Science *340*, 1334-1338.

Zhivotovsky, B., and Orrenius, S. (2011). Calcium and cell death mechanisms: a perspective from the cell death community. Cell Calcium *50*, 211-221.

Zlatic, M., Landgraf, M., and Bate, M. (2003). Genetic specification of axonal arbors: atonal regulates robo3 to position terminal branches in the Drosophila nervous system. Neuron *37*, 41-51.

Zlatic, M., Li, F., Strigini, M., Grueber, W., and Bate, M. (2009). Positional Cues in the Drosophila Nerve Cord: Semaphorins Pattern the Dorso-Ventral Axis. Plos Biol *7*.